JOURNAL OF CAVE AND KARST STUDIES

April 2011
Volume 73, Number 1
ISSN 1090-6924
A Publication of the National Speleological Society

Published By
The National Speleological Society

The *Journal of Cave and Karst Studies* (ISSN 1090-6924, CPM Number #40065056) is a multi-disciplinary, refereed journal published three times a year by the National Speleological Society, 2813 Cave Avenue, Huntsville, Alabama 35810-4431 USA; Phone (256) 852-1300; Fax (256) 851-9241, email: nss@caves.org; World Wide Web: http://www.caves.org/pub/journal/.
Check the *Journal* website for subscripion rates. Back issues and cumulative indices are available from the NSS office.

POSTMASTER: send address changes to the *Journal of Cave and Karst Studies*, 2813 Cave Avenue, Huntsville, Alabama 35810-4431 USA.

The *Journal of Cave and Karst Studies* is covered by the following ISI Thomson Services Science Citation Index Expanded, ISI Alerting Services, and Current Contents/Physical, Chemical, and Earth Sciences.

Front cover: Passages of Nonshauggrotta, Norway with distinct guiding fractures. See Skoglund and Lauritzen in this issue.

S. C. Frontana-Uribe, and V. SolÍs-Weiss – First records of polychaetous annelids from Cenote Aerolito (sinkhole and anchialine cave) in Cozumel Island, Mexico. *Journal of Cave and Karst Studies,* v. 73, no. 1, p. 1–10. DOI: 10.4311/jcks2009lsc0107

FIRST RECORDS OF POLYCHAETOUS ANNELIDS FROM CENOTE AEROLITO (SINKHOLE AND ANCHIALINE CAVE) IN COZUMEL ISLAND, MEXICO

Sarita C. Frontana-Uribe and Vivianne Solís-Weiss
Lab. de Ecología y Biodiversidad de Invertebrados Marinos, Instituto de Ciencias del Mar y Limnología, Universidad Nacional Autónoma de México, México, solisw@cmarl.unam.mx

Abstract: In this study, polychaetous annelids are recorded for the first time in Mexican cenotes and anchialine caves. These organisms were collected in the Cenote Aerolito (Cozumel Island, on the Caribbean coast of Quintana Roo) during three sampling events from February 2006 to April 2008, among algae, roots of mangroves, and in karst sediments. A total of 1518 specimens belonging to five families (Paraonidae, Capitellidae, Nereididae, Dorvilleidae, and Syllidae), ten genera, and eleven species were collected. In the cave system, two specimens of the amphinomid *Hermodice carunculata* were found. This cenote and its biota are now in danger of disappearing because of a marina construction project in its western shore.

Introduction

Polychaetes constitute the largest class of the phylum Annelida, with about 12,000 species described to date in more than 80 recognized families (Rouse and Pleijel, 2006). They are ubiquitous in marine habitats from intertidal to abyssal depths, where they are often the most diverse or dominant group. However, they are also found in some freshwater habitats and in karst systems like cenotes (or sinkholes) and even in the associated caves. Cave records are scarce, but the most important can be found in Augener, 1932; Remy, 1937; Hartmann-Schröder, 1977 and 1986; Sket and Iliffe, 1980; Culver and Sket, 2000; Wilson and Humphreys, 2001; and Martínez-García et al., 2009.

In 2002, Schmitter-Soto et al. made an exhaustive list of organisms collected in Yucatán cenotes, from bacteria and protozoa to algae and small invertebrates, such as copepods, amphipods, and isopods, but these authors did not report polychaetes; larger animals, such as fishes, amphibians, iguanas or crocodiles are better known in these habitats. Previously, Suárez-Morales and Rivera-Arriaga (1998) mentioned that no published references exist about free living nematodes, annelids, or mollusks in the Yucatán cenotes. Mejía-Ortíz et al. (2007b) studied some of the cenotes' macrofauna of Cozumel Island and mentioned the presence of worms in the cave system of Cenote Aerolito, but they did not specify if they were indeed polychaetes. In this study, we focused solely on the polychaetous annelids in this cenote and its cave system.

Cenotes are sinkholes found almost everywhere in the Yucatán Peninsula, which comprises the Mexican states of Yucatán, Campeche, and Quintana Roo, as well as northern Belize and the Guatemalan department of El Petén. They are a product of the geological characteristics of that region: in the whole peninsula, no rivers are found because its calcareous landscape is characterized, among other factors, by its high permeability. Thus, the abundant rainfall (average 1300 mm per year) sinks down to the phreatic level, where a complex web of subterranean rivers, mostly unknown, are formed and flow towards the sea at different levels (Schmitter-Soto et al., 2002). In places where the underground flow has produced caves, occasionally their ceiling collapses, uncovering the subterranean waters, and a cenote is born (Aguilar, 2003).

Cozumel Island is formed from reef sediments with an average thickness of 100 m or more from the Oligocene to the Quaternary; in these limestone beds, a karst aquifer is present and 18 cenotes are known (Wurl and Giese, 2005).

Site Description

With dimensions of 52 km by 14 km and a surface area of about 650 km^2, Cozumel is the largest island in Mexico. It is located in the northeastern region of the Yucatán Peninsula, in the northern Mexican Caribbean, about 18 km from the mainland (Pacheco and Vega, 2008). Its soil is mainly karstic, composed of limestone (Wurl and Giese, 2005), with four kinds of cenotes represented: those with surface connection narrower than the diameter of the water body (*cenotes cántaro*), those with vertical walls (*cenotes cilíndricos*), those degraded to shallow water basins (*cenotes aguadas*), and those with horizontal entrances to dry sections (*grutas*). The island's freshwater supply comes mainly from the cenotes and associated subterranean water systems (Mejía-Ortíz et al., 2007b). It has approximately 70,000 inhabitants and is totally devoted to tourism, which nowadays is expanding at a rate of more than 100% per year (Solís-Weiss et al., 2007).

Cenote Aerolito, one of the 18 cenotes known in Cozumel Island, is located close to the western coast of Cozumel, at 240 m from shore (20°28′00″ N and 86°58′45″ W). It is approximately 68 m long, 25 m wide, and 8 m deep. It is connected to the sea through an underwater cave system (Mejía-Ortíz et al., 2007a). At its northwestern end,

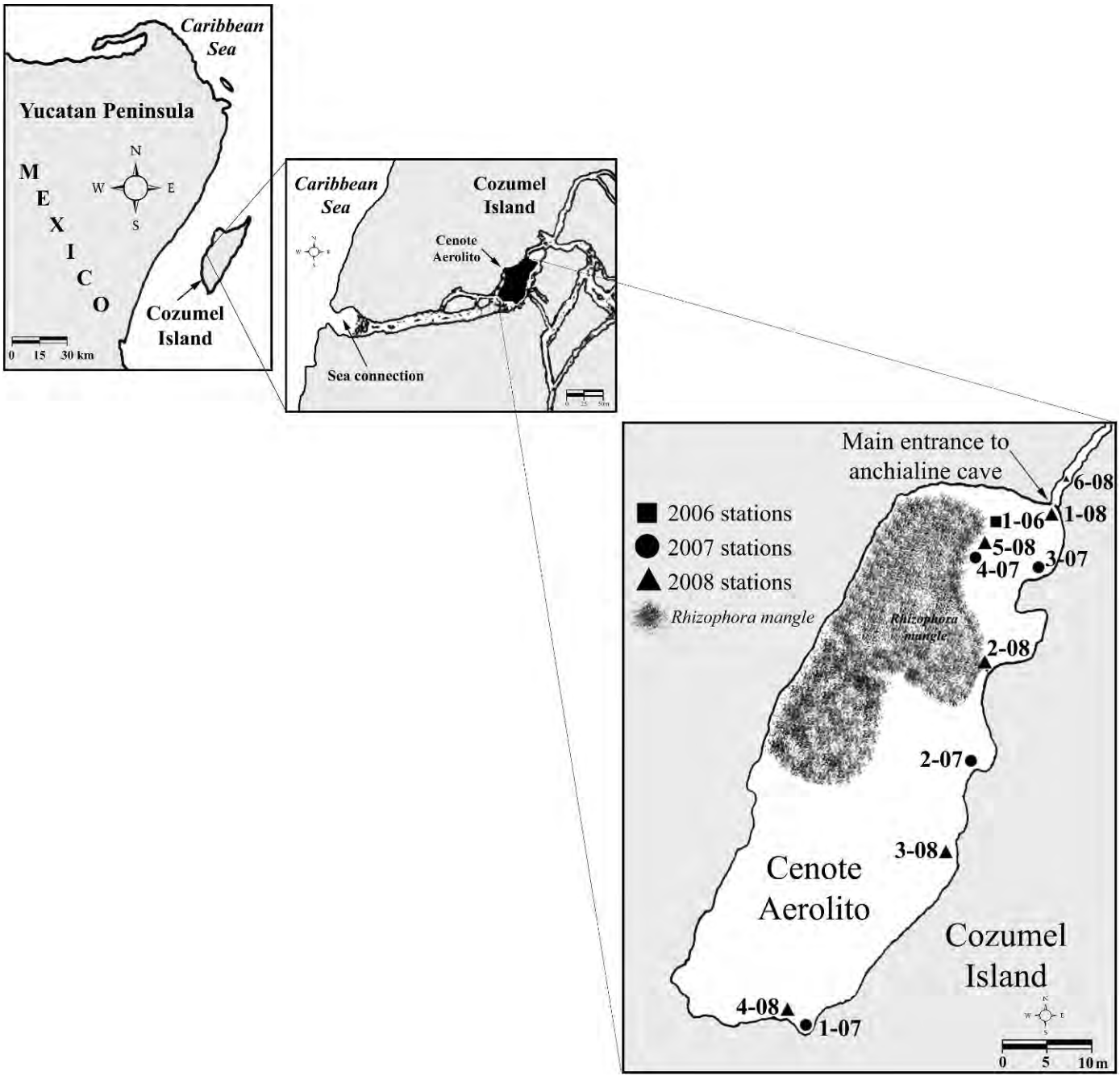

Figure 1. Study Area. Cenote Aerolito on Cozumel Island.

a relict of mangrove vegetation is present (*Rhizophora mangle* Linnaeus, 1753) (Fig. 1), and large aggregations of algae are found all around its edges.

Methods

Samples were collected by hand in February 2006 as part of the project Echinoderms from Cozumel Anchialine Caves. Each sample consisted of 200 ml of algae or karst sediment taken among mangrove roots in an area close to the main cave entrance of the Cenote Aerolito (station 1-06). In June 2007, as part of the project Benthic Fauna of the Mexican Caribbean Shores, further sampling was carried out at four stations (1-07, 2-07, 3-07, and 4-07); approximately 1000 ml of algae were collected, as well as karst sediment along the eastern edge of the cenote. A third sampling occurred in April 2008 at five stations (1-08, 2-08, 3-08, 4-08, and 5-08), and an additional station (6-08) was sampled using scuba diving in its cave system (Fig. 1, Table 1). Physical and chemical parameters were measured during each visit with a Hydrolab Data Sonde (HDS3) multiparameter probe.

Table 1. Sampling stations at Cenote Aerolito.

Sample No.	Latitude (N)	Longitude (W)	Depth (m)	Salinity (ppt)	Water Temp. (°C)	pH	Substrate
1-06[a]	20° 27′ 58.64″	86° 58′ 41.43″	0.5	18.1	25.08	7.25	algae and sediment
1-07[b]	20° 27′ 56.76″	86° 58′ 42.21″	0.3	15.1	27.02	7.30	algae and sediment
2-07[b]	20° 27′ 57.74″	86° 58′ 41.55″	0.5	15.8	27.08	7.42	algae
3-07[b]	20° 27′ 58.48″	86° 58′ 41.27″	0.5	15.8	27.04	7.37	algae
4-07[b]	20° 27′ 58.54″	86° 58′ 41.54″	0.5	15.8	26.89	4.44	algae
1-08[c]	20° 27′ 58.70″	86° 58′ 41.20″	1.0	19.68	24.67	7.35	algae
2-08[c]	20° 27′ 58.11″	86° 58′ 41.49″	0.3	20.33	24.61	7.34	algae and sediment
3-08[c]	20° 27′ 57.40″	86° 58′ 41.70″	1.0	20.41	24.88	7.40	algae
4-08[c]	20° 27′ 56.80″	86° 58′ 42.30″	0.5	20.30	25.07	7.45	algae and sediment
5-08[c]	20° 27′ 58.55″	86° 58′ 41.51″	0.3	19.68	24.67	7.37	algae
6-08[c]	Anchialine cave		8.0	34.71	26.03	7.74	sediment

[a] Collected February 15, 2006.
[b] Collected July 5, 2007.
[c] Collected April 19, 2008.

All the biological material was fixed in 7% formalin in the field, later rinsed with water, sieved through a 0.5 mm sieve, preserved in 70% alcohol, and identified to species level. The taxonomic arrangement follows Rouse and Fauchald (1997). In the faunal list, the syllids listed as sp. 1 are incomplete specimens, so their identification could only be carried out to the genus level. The dorvilleids identified as *Ophryotrocha* sp. A could not be referred to a known species and are now under study as potentially new to science. All the specimens are deposited in the National Polychaete Collection of the Laboratorio de Ecología y Biodiversidad de Invertebrados Marinos, Instituto de Ciencias del Mar y Limnología, UNAM (CPICML-UNAM, DFE.IN.061.0598).

The sediment was classified following Folk's (1974) method for size classes, while mineralogical and organic composition was done with the method of Gaudette et al. (1974).

Results

A total of 1518 specimens belonging to five families (Paraonidae, Capitellidae, Nereididae, Dorvilleidae, and Syllidae), ten genera, and eleven species are reported for Cenote Aerolito, while in its cave system two specimens of *Hermodice carunculata* were found. All the polychaete species collected during this study represent first records for the location in which they were found.

Species Account

Capitellidae Grube, 1862

Capitella cf. *capitata* (Fabricius, 1780) species complex

Material examined. Cenote Aerolito, Cozumel Island, Quintana Roo, February 15, 2006 (25 specimens), July 5, 2007 (66 specimens), April 19, 2008 (21 specimens) in soft bottoms associated with mangrove roots, algae, and karst sediments (CPICML-UNAM-PO-17-015).

Description. Largest specimen complete with 36 chaetigers, 11-mm long and 0.9-mm wide including parapodia, smaller specimen complete with 12 chaetigers, 5-mm long and 0.5-mm wide including parapodia. Prostomium broad and triangular; eyes absent. Body elongate, thoracic region broadest, partially inflated, with narrow segments; thoracic chaetigers with reduced podial lobes and capillary chaetae in both rami from chaetigers 1–6; chaetiger 7 with capillaries or mixed fascicles of capillary and hooded hooks; parapodia of chaetigers 8–9 with only hooks and, in most of the specimens, with enlarged opposing notopodial genital spines. Abdominal region narrower and segments longer with tori of hooded hooks. Pygidium without appendixes.

Habitat. In intertidal and subtidal mud and sand, especially in organically enriched sediments (Blake, 2000), dead coral (Ochoa-Rivera et al., 2000).

Distribution remarks. The species *C. capitata* has been considered cosmopolitan but is composed by several sibling species found to be genetically distinct, but morphologically similar (Grassle and Grassle, 1976; Grassle, 1980). Following the recent publication by Blake (2009) on this subject, we believe, as he does, that the true *C. capitata* will ultimately be confined to arctic and sub-arctic environments and that all other records of the species will ultimately be recognized as different species, some of them new to science. His important study of the taxonomic problems surrounding the so-called *C. capitata* complex will result in further studies of these species, so that, in this case, the species previously reported from Cozumel Island by Ochoa-Rivera et al. (2000) as *C. capitata* will probably have to be corrected, and that record, as well as the present one from Cenote Aerolito, will have to be re-evaluated.

Capitella aciculatus (Hartman, 1959)

Material examined. Cenote Aerolito, Cozumel Island, Quintana Roo, April 19, 2008 (2 specimens) in karst sediments (CPICML-UNAM-PO-17-034).

Description. Both specimens incomplete, males, largest with 20 chaetigers, 11-mm long and 1-mm wide including parapodia, smaller specimen with 17 chaetigers, 9-mm long and 1.2-mm wide including parapodia. Body elongate, thoracic region barrel-shaped, partially inflated, with narrow segments, abdominal region narrower, segments longer. Prostomium broadly triangular; eyes absent. Thorax with 9 chaetigers, the first and second are unique in bearing heavy acicular spines, 2 or 3 in a fascicle, they are known to occur in both notopodia and neuropodia in the males, 3–7 with capillary chaetae. On chaetigers 8–9 (sometimes 6–8), enlarged opposing notopodial genital spines are present. Abdominal segments with tori of hooded hooks in slightly elevated ridges located closer to the posterior end of the segment; single series of few uncini numbering 5 to 10 in a row. Hooded hooks with long shafts and distally end in recurved fangs surmounted by five smaller teeth in two rows.

Habitat. Subtidal mud (Tagatz et al., 1982)

Distribution. Atlantic Ocean in Florida (Hartman, 1959), Costa Rica (Dean, 2004). This species is newly recorded for Mexican waters.

Heteromastus filiformis (Claparède, 1864)

Material examined. Cenote Aerolito, Cozumel Island, Quintana Roo, April 19, 2008 (2 specimens) in karst sediment (CPICML-UNAM-PO-17-029).

Description. Both specimens incomplete, largest with 30 chaetigers, 7.5-mm long and 0.25-mm wide including parapodia, smaller specimen with 20 chaetigers, 4.1-mm long and 0.25-mm wide including parapodia. Prostomium thin and conical; eyes absent. Eversible proboscis inflated, with papillae, peristomium a single achaetous ring. Thorax with 12 segments, first achaetous. Chaetigers 1–5 with capillary chaetae, chaetigers 6–11 with hooded hooks. Thoracic-abdominal junction indistinct, but anterior abdominal segments larger in cross-section, especially dorsally. Posterior chaetigers campanulate, trapezoid in section, widest ventrally. Parapodial dorsal branchiae (located posteriorly) and pygidium could not be observed.

Habitat. Intertidal muds, anaerobic and estuarine habitats (Blake, 2000). Muddy sands and sands (Dean, 2004).

Distribution. Mediterranean Sea (Hutchings and Rainer, 1981) Atlantic and Pacific Oceans, Australia (Blake, 2000), Southern California (Cadien and Lovell, 2008).

Paraonidae Cerruti, 1909

Paradoneis lyra (Southern, 1914)

Material examined. Cenote Aerolito, Cozumel Island, Quintana Roo, February 15, 2006 (154 specimens) in soft bottoms associated with mangrove roots (CPICML-UNAM-PO-02-004).

Description. Largest specimen complete with 105 chaetigers, 18.5-mm long and 0.2-mm wide; smaller specimen complete with 51 chaetigers, 6.8-mm long and 0.2-mm wide. Body elongate, prostomium short, bluntly conical, fused to achaetigerous peristomium. Antennae and subdermal eyes absent. Prebranchial chaetigers from 1–3, branchiae from segments 4 to 12 to14, long, slender and blunt, first few pairs generally shorter. Notochaetae lyrate, slender, from chaetigers 2–3 with two unequal tines with inner row of spines, acicular neurochaetae absent. Pygidium rounded, anal cirri short.

Habitat. Sandy muds, sands, gravels (Mackie, 1991).

Distribution. Northeastern Atlantic (Mackie, 1991), Indo-Pacific, Mediterranean, Panama (Aguado and López, 2003), Southern California (Cadien and Lovell, 2008).

Amphinomidae Lamarck, 1818

Hermodice carunculata (Pallas, 1766)

Material examined. Anchialine cave of the Cenote Aerolito, Cozumel Island, Quintana Roo, April 19, 2008 (2 specimens) (CPICML-UNAM-PO-49-008).

Description. Specimens complete with 45 to 48 chaetigers, 45- to 65-mm long and 8-to 10-mm wide including parapodia. Body elongate, intensely red in color, the largest specimen with intersegmental transverse black lines from chaetigers 5–6. Prostomium covered by an elaborate caruncle covering the first 3 chaetigers and formed by two series of 7 or 8 transverse folds; two pairs of eyes and 3 antennae. Double dendritic branchiae present along whole body. Parapodia with abundant notochaetae and neurochaetae. Notochaetae very long capillaries and harpoon chaetae (stout pointed chaetae with recurved barbs near the tip) of smaller size; three types of acicular neurochaetae: subdistally flat, distally denticulate (3 to 5 teeth), subdistally with a tooth and denticulate until the apex, with up to 15 small teeth. Notopodial cirri biarticulated and larger than neuropodial cirri. Last segment encircling the anus.

Habitat. Associated to sessile organisms in rocky substrate (Salazar-Vallejo, 1996–1997); in dead coral (Ochoa-Rivera et al., 2000).

Distribution. Transatlantic and Mediterranean in tropical and subtropical waters (Salazar-Vallejo, 1996–1997); in the Mexican Caribbean previously reported from Cozumel Island by Ochoa-Rivera et al. (2000).

Dorvilleidae Chamberlin, 1919

Ophryotrocha sp. A.

Material examined. Cenote Aerolito, Cozumel Island, Quintana Roo, February 15, 2006 (10 specimens), July 5, 2007 (758 specimens), April 19, 2008 (227 specimens) in soft bottoms associated with mangrove roots, algae, and karst sediments (CPICML-UNAM-PO-53-012).

Description. Most of the specimens complete with 12 to 15 chaetigers, 0.5- to 0.8-mm long and 0.4- to 0.5-mm wide including parapodia. Body short, cylindrical, compressed dorsoventrally, tapering towards pygidium. Prostomium bluntly triangular with two lateral antennae and ciliary aggregations both in the frontal region and at the top. Peristomium with two apodous rings. Parapodia unirramous, with ventral retractile lobe and simple chaetae.

Supra-acicular fascicle with 2 to 3 simple chaetae, infra-acicular fascicle with 4 to 5 heterogomph falcigers and one inferior-most simple Chaeta. Both types of chaetae finely serrated subdistally, tapering to small distal tooth. Pygidium with one pair of minute ovate pygidial cirri. Jaw apparatus with elongate distally bifid mandibles with serrated cutting edge. Maxillary apparatus of P or K type; P type present in smallest specimens and K type in larger specimens. K-forceps distally falcate. D1–D7 denticles attached by ligament to forceps. With blue methyl dye a reduced ciliary distribution on each segment and pygidium is evident

Remarks. The maxillary apparatus known as P-type may have falcate or bidentate forceps and the number of free denticles ranging from five to seven pairs, while the maxillary apparatus known as K-type may have two unidentate, two bidentate, or one unidentate and one bidentate prong and the number of free denticles ranges from six to eight pairs; there may be one, two or three different kinds of denticles in one jaw apparatus. The remarkable feature here is that in these organisms, both types are found, depending on the size of the specimens, raising the question of the importance of this character to differentiate between species in this genus.

Other species of *Ophryotrocha* are opportunistic (Desbruyères et al., 2006) and therefore found in many different habitats, which could explain why this species is so abundant here. Its status as a new species is presently under study.

Nereididae Johnston, 1865

Stenoninereis martini Wesenberg-Lund, 1959

Material examined. Cenote Aerolito, Cozumel Island, Quintana Roo, February 15, 2006 (14 specimens), July 5, 2007 (203 specimens), April 19, 2008 (9 specimens) in soft bottoms associated with mangrove roots.

Comparative material examined. San Julián, Laguna de Términos, Campeche, México 1 March 1984 (18 specimens) (CPICML-UNAM-PO-39-039).

Description. Largest specimen complete with 33 chaetigers, 10.5-mm long and 1.5-mm wide including parapodia, smaller specimen complete with 21 chaetigers, 2.5-mm long and 0.6-mm wide. Prostomium pentagonal, slightly notched frontally. Two pairs of eyes. Frontal antennae cirriform and not longer than distal palps. Palps marginal, globular, biarticulate with elongate conical palpostyles. Peristomium slender with four pairs of tentacular cirri, anterior dorsal pair reaching posterior to chaetiger 6. Pharynx with paired jaws armed with 10 to 12 teeth, no paragnaths or papillae. First two parapodia subbiramous with notopodia reduced to small notoacicula; following parapodia biramous; anterior ones with long dorsal cirri consisting of elongate basal cirrophore and short pyriform cirrostyle, becoming longer towards end of the body. Notopodia trilobate, superior lobe short and digitiform, decreasing in size in posterior chaetigers; inferior lobes subulate, with small presetal lobe at base of upper lobe. Neuropodia with bluntly conical acicular lobe in anterior region, becoming more elongate in middle chaetigers and shorter, more pointed in posterior region. Supra-acicular notochaetae sesquigomph spinigers, infra-acicular notochaetae homogomph spinigers; both with slender appendix, serrated on the inner edge. Supracicular neurochaetae heterogomph and sesquigomph spinigers; one heterogomph spiniger with a strongly serrated short blade on at least three quarters of its length on its inner margin; heterogomph falcigers with spinulose distally hooked long blade. Pygidium with a pair of lateral flattened, wide lobes, and a pair of long anal cirri.

Habitat. Soft bottoms associated with mangrove roots (de León-González and Solís-Weiss, 1997).

Distribution. Laguna de Términos, Campeche, Mexico (de León-González and Solís-Weiss, 1997), greater Caribbean region, San Martín Island, Sarasota Florida, western Gulf of Mexico (Texas), Cuba, North Carolina (Wesenberg-Lund, 1958; Pettibone, 1971; Hartman-Schröeder, 1977).

Syllidae Grube, 1850

Erinaceusyllis centroamericana (Hartmann-Schröder, 1959)

Material examined. Cenote Aerolito, Cozumel Island, Quintana Roo, February 15, 2006 (1 specimen), July 5, 2007 (4 specimens), April 19, 2008 (1 specimen) (CPICML-UNAM-POH-076).

Description. One specimen complete with 21 chaetigers, 1.5-mm long and 0.2-mm wide including parapodia. Body small, covered with small, scattered papillae. Prostomium oval with 4 small eyes in rectangular arrangement and 2 anterior eyespots; antennae pyriform, median and lateral antennae similar in size. Palps short, fused along their length. Peristomium long, tentacular cirri similar to antennae. Dorsal cirri similar to antennae, with bulbous bases and short tips, absent on chaetiger 2. Ventral cirri digitiform. Compound chaetae heterogomph, similar throughout body; blades slender, elongate, unidentate, distally slightly hooked, provided with proportionally long marginal spines on bases of longer blades; parapodia each with one long bladed compound chaeta and 6 falcigers. From chaetiger 1, simple unidentate chaetae with short marginal spines dorsally. Simple chaetae ventrally. Aciculae acuminate, one per parapodium throughout the body. Pharynx extending from chaetigers 1 to 3 or even 4; pharyngeal tooth small and enlarged on anterior margin. Proventricle barrel-shaped, extending from chaetigers 3–6; with about 13 to 16 rows of transverse muscle bands. Pygidium small, with two anal cirri.

Habitat. In sand, algae and mangroves (San Martín, 2005).

Distribution. Circumtropical: El Salvador, Galápagos Islands, Caribbean Sea, Hawaii, Samoa, Angola, Mozambique, Tanzania, Australia (San Martín, 2005). New record for Mexican Caribbean.

Salvatoria sp. 1

Material examined. Cenote Aerolito, Cozumel Island, Quintana Roo, July 5, 2007 (4 specimens), in soft bottoms associated with mangrove roots, algae, and karst sediments (CPICML-UNAM-PO-37-077).

Description. All specimens incomplete, largest with 21 chaetigers, 1.8-mm long and 0.25-mm wide including parapodia. Body small. Prostomium with 3 antennae, 4 eyes and, usually, without 2 eyespots. Palps well developed, joined along their length by a dorsal membrane. Two pairs of tentacular cirri. Antennae tentacular, dorsal cirri long and slender, slightly bulbous at their base and with an elongate, acute tip; dorsal cirri present on all segments. Ventral cirri digitiform, shorter than parapodial lobes. Compound chaetae heterogomph with small indistinct subdistal tooth; dorsal simple chaetae bidentate, with short subdistal marginal spines, ventral simple chaetae not observed. Acicula distally rounded, one per parapodium throughout the body. Pharynx extending through chaetigers 1–3, surrounded by a crown of 12 soft pharyngeal papillae and a small tooth on anterior margin; proventricle of the same length through chaetigers 4–6, with about 19 rows of transverse muscle bands. Pygidium unknown.

Exogone (Paraexogone) sp. 1.

Material examined. Cenote Aerolito, Cozumel Island, Quintana Roo, July 5, 2007 (1 specimen), in soft bottoms associated with mangrove roots and algae (CPICML-UNAM-PO-37-077).

Description. Specimen incomplete with 15 chaetigers, 0.5-mm long and 0.2-mm wide. Body small and slender. Prostomium without antennae, four eyes with 2 eyespots. Palps slender, well developed, completely fused to each other. Tentacular cirri fragmented. Dorsal cirri small, ovoid, present on all segments. Compound chaetae falcigers, incomplete and no spinigers visible, dorsal bifid simple chaetae present from first chaetiger. Acicula distally truncate. Pharynx sinuous, extending through chaetigers 1 and 2, pharyngeal tooth small on anterior margin. Proventricle through chaetigers 2–4, with about 22 rows of transverse muscle bands. Pygidium unknown.

Syllis prolifera Krohn, 1852

Material examined. Cenote Aerolito, Cozumel Island, Quintana Roo, July 5, 2007 (15 specimens), in algae and karst sediments (CPICML-UNAM-PO-37-007).

Description. Largest specimen complete with 48 chaetigers, 9-mm long and 0.25-mm wide. Body thick. Prostomium oval with 4 small eyes in trapezoidal arrangement; median antennae longer than prostomium and palps together, with about 24 articles; lateral antennae with about 29 or 30 articles. Palps triangular, robust, larger than prostomium. Dorsal tentacular cirri long, with about 37 to 45 articles; ventral tentacular cirri with about 33 to 38 articles. Dorsal cirri long and slender, with about 45 to 52 articles. Ventral cirri digitiform. Compound chaetae falcigers, strongly bidentate with teeth of similar size. Aciculae rounded with hollow tips; their number changes depending on body region, four in anterior and median region and only one in posterior region; dorsal bifid simple chaetae present from chaetiger 18 and ventral simple chaetae only present in posterior chaetigers. Pharynx extending through chaetigers 1–7; pharyngeal tooth small on middle dorsal position. Proventricle through chaetigers 7–10, with about 25 rows of transverse muscle bands. Pygidium small, with two anal cirri with 28 to 30 articles.

Habitat. On *Rhizophora mangle* roots, coralline rocks (San Martín, 1992). Abundant in algae, sandy and hard substrate (San Martín, 2003).

Distribution. A cosmopolitan species in tropical and temperate seas (San Martín, 2003). The closest record to the study area is Cuba (San Martín, 1992).

Syllis maryae San Martín, 1992

Material examined. Cenote Aerolito, Cozumel Island, Quintana Roo, April 19, 2008 (1 specimen) (CPICML-UNAM-POH-37-045).

Description. Specimen complete with 61 chaetigers, 8.5-mm long and 0.5-mm wide. Body thick. Prostomium oval with 4 small eyes in trapezoidal arrangement; median antennae longer than prostomium and palps together, with about 25 articles; lateral antennae, with about 12 to 14 articles. Palps triangular, similar in length to prostomium. Dorsal tentacular cirri long, with about 13 to15 articles; ventral tentacular cirri with 10 to 12 articles. Dorsal cirri slender, alternating long (23 to 26 articles) and short (10 to 16 articles). Ventral cirri digitiform. Dorsal glands on segments 14–16. Compound chaetae including 1 or 2 bidentate pseudospinigers with teeth of similar size and about 6 bidentate falcigers with proximal tooth shorter than distal one, and with short spines on cutting margin with dorsoventral gradation. Aciculae distally truncate, forming a right angle, their number changing along the body, two in anterior and median region and only one in posterior region. Pharynx extending through chaetigers 1–7; pharyngeal tooth small on anterior margin. Proventricle through chaetigers 7–10, with about 29 rows of transverse muscle bands. Pygidium small, with two anal cirri with 16 to 18 articles.

Habitat. Shells (San Martín, 1992), dead coral (Granados-Barba et al., 2003).

Distribution. North Carolina, Cuba (San Martín, 1992), Gulf of Mexico (Granados-Barba et al., 2003).

Seasonal Species Occurrence

In this study, the family Dorvilleidae is dominant, with 995 specimens or 65.5% of the polychaetes collected, although it is represented by only one species, *Ophryotrocha* sp. A. Some differences in seasonal distribution were noted. In July 2007 and April 2008, *Paradoneis lyra* was absent, while in February 2006 it was by far the most abundant species (75% of the total). *Syllis prolifera* was present only in July 2007, *Capitella aciculatus* and

Heteromastus filiformis where present only in April 2008, and the specimens of *Salvatoria* sp.1 and *Exogone* sp.1 were present only in July 2007. In all samples and at almost all stations, except in the cave system, (February 2006, July 2007, and April 2008) the *Capitella capitata* species complex and *Ophryotrocha* sp. A, were present (Table 2). The differences observed in species composition and distribution are recorded here as part of this first study on the polychaete fauna of Mexican cenotes, but cannot be fully interpreted at this point until more sampling is carried out. Nevertheless, this study documents both the fact that polychaetes are present and diversified in this habitat, and that seasonal changes or species replacements might take place. It is interesting to note that, in the second sampling period, epitokes were collected from the families Nereididae and Syllidae, while none were present in the first and third sampling periods.

Bottom-water salinity and temperature were different in each sampling period. In February 2006, the salinity was 18.1 ppt with a temperature of 25 °C, in July 2007 the salinity was between 15 and 15.8 ppt and temperature 26.89 to 27.08 °C whereas in April 2008 the salinity was between 19.68 and 20.33 ppt and temperature 24.61 to 24.88 °C. In the cave system, the salinity was 34.71 ppt and temperature 26.03 °C. The sediment in the cave consists of sand of biogenic origin (very fine coral debris).

Discussion

Since this is the first study about polychaetes in cenotes in Mexico, all records are new for Cenote Aerolito itself and its cave system, but so far only the dominant species *Ophryotrocha* sp. A is potentially new to science.

The polychaete species already recorded for the Cozumel area include *Hermodice carunculata* and the so-called complex of species under the name *Capitella capitata*, both recorded from dead coral (Ochoa-Rivera et al., 2000). In this case, the presence of this species complex could be attributed to the abundance of organic matter (mangrove roots, algae) in which the species complex is known to thrive.

At the regional scale, *Stenoninereis martini* is known from Florida, down to the Gulf of Mexico (Términos lagoon) and the greater Caribbean (de León-González and Solís-Weiss, 1997), and the capitellids *Capitella aciculatus* and *Heteromastus filiformis* have also been recorded previously for the greater Caribbean. Although some species of Exogoninae of the Caribbean have been reported by Ruíz-Ramírez and Salazar-Vallejo (2000), the species *Erinaceusyllis centroamericana* is a new record for the Mexican Caribbean. This species had been previously recorded from the West Indies (San Martín, 2005). *Syllis prolifera* is considered cosmopolitan but, like *Syllis maryae*, the closest records to the study area are from Cuba and the Gulf of Mexico (San Martín 1992; 2003).

Conclusions

This first study on polychaetous annelids in Mexican cenotes revealed a relatively diversified (10 genera and 11 species) and interesting polychaete fauna in the best-known and most popular cenote on Cozumel Island. We believe that the underwater connection to the sea, in addition to the nearby mangrove habitat, create propitious conditions for Polychaeta, and many other species can be expected in these unique habitats.

Even though there are important differences between the cenote habitat and a truly marine one, no morphological differences could be observed in any of the species recorded, with the possible exception of the *Ophriotrocha* sp. 1.

Although the best-represented macrofaunal invertebrate animal group in caves and also cenotes is macrofaunal crustaceans (Schmitter-Soto et al., 2002; Mejía-Ortíz et al., 2007b), more recent studies are revealing new taxa. Mejía-Ortíz et al. (2007a) and Solís-Marín and Laguarda-Figueras (2008), for example, found species of all the echinoderm classes except the Crinoidea for the system of caves connected to Cenote Aerolito.

In addition, this study constitutes a baseline study that will be especially important because the cenote is on the verge of being severely transformed by the construction of a marina at its western end, which will include the destruction of the cave in creating a direct connection between the marina area of the cenote to the sea. This will certainly affect the local fauna as we know it now, not only because of the change in salinity, which will become like the surrounding sea, but because of the construction itself and subsequent maritime traffic. All this impact will change the environmental conditions and not only the polychaete composition but also the other fauna groups already recorded.

There is concern in the scientific community, because legislation concerning the cenotes in Mexico is not yet well defined. They are not differentiated from other freshwater bodies, so they cannot be properly protected. The Mexican government agency CONAGUA (Comisión Nacional del Agua) has only begun in 2009 to work on a legal framework to promote the sustainable use and conservation of these unique water bodies.

Acknowledgements

We are grateful to Alfredo Laguarda and Francisco Solís, from the Instituto de Ciencias del Mar y Limnología, UNAM, as well as to divers Germán Yánez, Adrian Medina, and Emmanuel Teysier, for their help in the field, and to Diego Trujillo and Efrain Chávez for their help in collecting the cave samples. Victor Ochoa, María Elena García, and Pablo Hernández are also thanked for their help in some identifications. Antonio Márquez, Laboratorio de Sedimen-

Table 2. Abundance of polychaetes collected in Cenote Aerolito and its anchialine cave in 2006–2008.

Taxa	Stations											Total Specimens
	1-06	1-07	2-07	3-07	4-07	1-08	2-08	3-08	4-08	5-08	6-08	
Family Capitellidae Grube, 1862												
Capitella capitata (Fabricius, 1780) *sensu lato*	25	9	16		41	3	2	2	6	8		112
Capitella aciculatus (Hartman, 1959)									2			2
Heteromastus filiformis (Claparède, 1864)							2					2
Family Paraonidae Cerruti, 1909												
Paradoneis lyra (Southern, 1914)	154											154
Family Amphinomidae Lamarck, 1818												
Hermodice carunculata (Pallas, 1766)											2	2
Family Dorvilleidae Chamberlin, 1919												
Ophryotroca sp. A	10	144	34	239	341	84	8	10	4	121		995
Family Nereididae Johnston, 1845												
Stenoninereis martini Wesenberg-Lund, 1959	14		91		112	1		8				226
Family Syllidae Grube, 1850												
Subfamily Exogoninae Langerhans, 1879												
Erinaceusyllis centroamericana (Hartmann-Schröder, 1959)	1	2	1		1					1		6
Salvatoria sp.1			3		1							4
Exogone sp.1					1							1
Subfamily Syllinae Grube, 1850												
Syllis prolifera Krohn, 1852		1	13	1								15
Syllis maryae San Martín, 1992										1		1

tología from Unidad de Oceanografía, ANIDE, Mexico, is deeply acknowledged for his analysis of the sediment.

References

Aguado, M.T., and López, E., 2003, Paraonidae (Annelida: Polychaeta) del Parque Nacional de Coiba (Pacífico, Panamá), con la descripción de una nueva especie de *Aricidea* Webster, 1879: Revista Chilena de Historia Natural, v. 76, p. 363–370.

Aguilar, V., 2003, Aguas continentales y diversidad biológica de México: Un recuento actual: Biodiversitas, v. 8, no. 48, p. 1–14.

Augener, H., 1932, Die Polychaeten und Hirudineen des Timavo-gebietes in der Adriatischen Karstregion: Abdruck aus Zoologische Jahrbucher, Abteilung fur Systematik, Okologie und Geographie der Tier, v. 63, no. 5–6, p. 657–680.

Blake, J.A., 2000, Family Capitellidae Grube, 1862, *in* Blake, J.A., Hilbig, B., and Scott, P.H., eds., Taxonomic Atlas of the Benthic Fauna of the Santa Maria Basin and Western Santa Barbara Channel, Volume 7. The Annelida, Part 4. California, Santa Barbara Museum of Natural History, p. 47–96.

Blake, J.A., 2009, Redescription of *Capitella capitata* (Fabricius) from West Greenland and designation of a neotype (Polychaeta, Capitellidae): Zoosymposia, v. 2, p. 55–80.

Cadien, D.B., and Lovell, L.L., eds., 2008, A Taxonomic Listing of Soft Bottom Macro-and Megainvertebrates from Infaunal & Epibenthic Monitoring Programs in the Southern California Bight, Fifth Edition: The Southern California Association of Marine Invertebrate Taxonomists, 210 p.

Chamberlin, R.V., 1919, Albatross Polychaeta (Rep. Sci. Res. Exp. Albatross): Memoirs of the Museum of Comparative Zoology, Harvard University, v. 48, 514 p.

Cerruti, A., 1909, Contributo all'anatomia, biologia e sistematica delle Paraonidae (Levinsenidae) con particolare riguardo alle specie del golfo di Napoli: Mitteilungen aus der Zoologischen Station zu Neapel, Berlin, v. 19, p. 459–512.

Claparède, E., 1864, Glanures zootomiques parmi les Annélides de Port-Vendres (Pyrénées Orientales): Mémoires de la Société de Physique et d'Histoire Naturelle de Genève, v. 17, no. 2, p. 463–600.

Culver, D.C., and Sket, B., 2000, Hotspots of subterranean biodiversity in caves and wells: Journal of Cave and Karst Studies, v. 62, no. 1, p. 11–17.

Dean, H.K., 2004, Marine biodiversity of Costa Rica: Class Polychaeta (Annelida): Revista de Biología Tropical, v. 52, supl. 2, p. 131–181.

de León-González, J.A., and Solís-Weiss, V., 1997, A new species of *Stenoninereis* (Polychaeta: Nereididae) from the Gulf of Mexico: Proceedings of the Biological Society of Washington, v. 110, no. 2, p. 198–202.

Desbruyères, D., Segonzac, M., and Bright, M., 2006, Handbook of deep-sea hydrotermal vent fauna. 2nd edition, Denisia 18, Linz-Dornach, Austria, Biologiezentrum, 544 p.

Fabricius, O., 1780. Fauna Groenlandica. Systematice sistens, Animalia Groenlandiae occidentalis hactenus indagata, quad nomen specificum, triviale, vernaculumque synonyma auctorum plurium, descriptionem, locum, victum, generationem, mores, usum, capturamque singuli; prout detegendi occasio fuit, maximaque parti secundum propias observationes, Hafniae et Lipsiae, J.G. Rothe, xvi, 452 p.

Folk, R.L., 1974, Petrology of Sedimentary Rocks: Austin, Texas, Hemphill, 170 p.

Gaudette, H.E., Flight, W.R., Toner, L., and Folger, D.W., 1974, An inexpensive titration method for determination of organic carbon in recent sediments: Journal of Sedimentology and Petrology, v. 44, no. 1, p. 249–253.

Grassle, J.P., and Grassle, J.F., 1976, Sibling species in the marine pollution indicator *Capitella* (Polychaeta): Science, v. 192, p. 567–569.

Grassle, J.P., 1980, Polychaete sibling species, *in* Brinkhurst, R.O., and Cook, D.G., eds., Aquatic Oligochaete Biology: New York, Plenum, p. 25–32.

Granados-Barba, A., Solís-Weiss, V., Tovar-Hernández, M.A., and Ochoa-Rivera, V., 2003, Distribution and diversity of the Syllidae (Annelida: Polychaeta) from the Mexican Gulf of Mexico and Caribbean, *in* Sigvaldadóttir, E., Mackie, A.S.Y., Helgason, G.V., Reish, D.J., Svavarsson, J., Steingrímsson, S.A., and Guomundsson, G., eds., Advances in Polychaete Research, Hydrobiologia, v. 496, no. 1–3, p. 337–345.

Grube, A.E., 1850, Die Familien der Anneliden: Archiv für Naturgeschichte, v. 16, p. 249–364.

Grube, A.E., 1862, Noch ein Wort ueber die Capitellen und ihre Stellung im Systeme der Anneliden: Bonn, Carl Georgi, p. 65–378.

Hartman, O., 1959, Capitellidae and Nereidae (Marine Annelids) from the Gulf side of Florida, with a review of freshwater Nereidae: Bulletin of Marine Science of the Gulf and Caribbean, v. 9, p. 153–168.

Hartmann-Schröder, G., 1977, Die Polychaeten der Kubanisch-Rumanischen Biospeologischen Expedition nach Kuba 1973, *in* Résultats des Expéditions Biospéologiques Cubano-Roumaines à Cuba, Volume 2: Bucharest, Academiei Rebublich Socialiste România 2, p. 51–63.

Hartmann-Schröder, G., 1986, Polychaeta (Incl. Archiannelida), *in* Botosaneanu, L., ed., Stygofauna Mundi: A Faunistic, Distributional, and Ecological Synthesis of the World Fauna inhabiting Subterranean Waters (including the Marine Interstitial: Leiden, E.J. Brill, p. 210–233.

Hutchings, P.A., and Rainer, S.F., 1981, Designation of a neotype of Capitella filiformis Claparede, 1864, type species of the genus *Heteromastus* (Polychaeta: Capitellidae): Records of the Australian Museum, v. 35, no. 4, p. 373–381.

Johnston, G., 1865, A Catalogue of the British Non-parasitical Worms in the Collection of the British Museum: London, British Museum (Natural History), 366 p.

Krohn, A., 1852, Ueber die Erscheinungen bei der Fortpflanzung von *Syllis prolifera* und *Autolytus prolifer*: Archiv für Naturgeschichte, Berlin, v. 18, no. 1, p. 66–76.

Lamarck, J.B.P., 1818, Histoire Naturelle des Animaux sans Vertèbres, Volume 5: Paris, Deterville and Verdiere, 612 p.

Linnaeus, C., 1753, Species Plantarum, Exhibentes Plantas Rite Cognitas, ad General Relatas, cum Differentiis Specificis, Nominibus Trivialibus, Synonymis Selectis, Locis Natalibus, Secundum Systema Sexuale Digestas: Holmiæ, Sweden, Impensis L. Salvii, two volumes 1200 p.

Mackie, A.S.Y., 1991, *Paradoneis eliasoni* sp. nov. (Polychaeta: Paraonidae) from northern European waters, with a redescription of *Paradoneis lyra* (Southern, 1914), *in* Petersen, M.E., and Kirkegaard, J.B., eds., Systematics, Biology and Morphology of World Polchaeta: Copenhagen, Ophelia Supplement 5, p. 147–155.

Martínez-García, A., Palmero, A.M., Brito, M.C., Núñez, J., and Worsaae, K., 2009, Anchialine fauna of the Corona lava tube (Lanzarote, Canary Islands): diversity, endemism and distribution: Marine Biodiversity, v. 39, p. 169–182.

Mejía-Ortíz, L.M., Yánez, G., and López-Mejía, M., 2007a, Echinoderms in an anchialine cave in Mexico: Marine Ecology, v. 28, no. 1, p. 31–34.

Mejía-Ortíz, L.M., Yánez, G., López-Mejía, M., and Zarza-González, E., 2007b, Cenotes (anchialine caves) on Cozumel Island, Quintana Roo, México. Journal of Cave and Karst Studies, v. 69, no. 2, p. 250–255.

Ochoa-Rivera, V., Granados-Barba, A., and Solís-Weiss, V., 2000, The Polychaete cryptofauna from Cozumel Island, Mexican Caribbean: Bulletin of Marine Science, v. 67, no. 1, p. 137–146.

Pacheco, M.A., and Vega, F.J., 2008, Reseña Geológica, *in* Mejía-Ortíz, L.M., ed., Biodiversidad Acuática de la Isla de Cozumel: Universidad de Quintana Roo, p. 33–42.

Pallas, P.S., 1766, Miscellanea Zoologica: Quibus novae imprimis atque obsurae animalium species describunter et observantionibus icomibusque illustrantur: The Hague. Comitum: Hague, v. 12, 224 p.

Pettibone, M.H., 1971, Revision of Some Species Referred to *Leptonereis*, *Nicon* and *Laeonereis* (Polychaeta: Nereididae): Washington, D.C., Smithsonian Institution, Contributions to Zoology No. 104, 53 p.

Remy, P., 1937, Sur *Marifugia cavatica* Absalom et Hrabe, serpulide des eaux douces sousterranees du Karst adriatique: Bulletin du Museum d'Histoire Naturelle, Paris, v. 9, p. 66–72.

Rouse, G.W., and Fauchald, K., 1997, Cladistics and polychaetes: Zoologica Scripta, v. 26, p. 139–204.

Rouse, G.W., and Pleijel, F., 2006, Annelid phylogeny and systematics, *in* Rouse, G.W., and Pleijel, F., eds., Reproductive Biology and Phylogeny of Annelida: Enfield, New Hampshire, Science Publishers, p. 3–21.

Ruíz-Ramírez, J.D., and Salazar-Vallejo, S.I., 2000, Exogoninae (Polychaeta:Syllidae) del Caribe mexicano con una clave para las especies del Gran Caribe: Revista de Biología Tropical, v. 49, no. 1, p. 117–140.

Salazar-Vallejo, S.I., 1996–1997Anfinómidos y eufrosínidos (Polychaeta) del Caribe Mexicano con claves para las especies reconocidas del Gran Caribe: Revista de Biología Tropical, v. 44–45, no. 3-1, p. 379–390.

San Martín, G., 1992, *Syllis* Savigny in Lamarck, 1818 (Polychaeta:Syllidae:Syllinae) from Cuba, the Gulf of Mexico, Florida and North Carolina, with a revision of several species described by Verrill: Bulletin of Marine Science, v. 51, no. 2, p. 167–196.

San Martín, G., 2003, Annelida, Polychaeta II: Syllidae, *in* Ramos, M.A., ed., Fauna Ibérica, Volume 21: Madrid, Museo Nacional de Ciencias Naturales, p. 336–447.

San Martín, G., 2005, Exogoninae (Polychaeta: Syllidae) from Australia with descriptions of a new genus and twenty-two new species: Records of the Australian Museum, v. 57, p. 39–159.

Schmitter-Soto, J.J., Escobar, E., Alcocer, J., Suárez-Morales, E., Elias-Gutierrez, M., Marin, L.E., and Steinich, B., 2002, Hydrobiology of cenotes of the Yucatán Peninsula: Hydrobiologia, v. 467, p. 215–228.

Sket, B., and Iliffe, T., 1980, Cave fauna of Bermuda: Internationale Revue der Gesamten Hydrobiologie, v. 65, p. 871–882.

Solís-Marín, F.A., and Laguarda-Figueras, A., 2008, Equinodermos, *in* Mejía-Ortíz, L.M., ed., Biodiversidad Acuática de la Isla de Cozumel: Universidad de Quintana Roo, p. 187–214.

Solís-Weiss, V., Granados-Barba, A., and Malpica-Martínez, J., 2007, Environmental evaluation of Cozumel Island Mexico, *in* Ozhah, E., ed., Land Coastal Interactions: Managing Coastal Ecosystems, Proceedings of the joint conference VIII MEDCOAST, Volume 2: p. 775–786.

Southern, R., 1914, Clare Island Survey: Part 47, Archiannelida and Polychaeta: Proceedings of the Royal Irish Academy, v. 31, p. 1–160.

Suárez-Morales, E., and Rivera-Arriaga, E., 1998, Hidrología y fauna acuática de los Cenotes de la Península de Yucatán: Revista de la Sociedad Mexicana de Historia Natural, v. 48, p. 37–47.

Tagatz, M.E., Ivey, J.M., Dalbo, C.E., and Oglesby, J.L., 1982, Responses of developing estuarine macrobenthic communities to drilling muds: Estuaries, v. 5, no. 2, p. 131–137.

Wesenberg-Lund, E., 1958, Lesser Antillean polychaetes, chiefly from brackish water, with a survey and a bibliography of fresh and brackish-water polychaetes: Studies on the Fauna of Curaçao and Other Caribbean Islands, v. 30, p. 1–41.

Wilson, R.S., and Humphreys, W.F., 2001, *Prionospio thalanji* sp. nov. (Polychaeta: Spionidae) from an anchialine cave, Cape Range, northwest Western Australia: Records of the Western Australian Museum Supplement, v. 64, p. 105–113.

Wurl, J., and Giese, S., 2005, Ground water quality research on Cozumel Island, State of Quintana Roo, Mexico, *in* Frausto Martínez, O., ed., Desarrollo Sustentable: Turismo, Costas y Educación: Universidad de Quintana Roo, p. 171–176.

M. Gambetta, E. Armadillo, C. Carmisciano, P. Stefanelli, L. Cocchi, and F. C. Tontini – Determining geophysical properties of a near-surface cave through integrated microgravity vertical gradient and electrical resistivity tomography measurements. *Journal of Cave and Karst Studies,* v. 73, no. 1, p. 11–15. DOI: 10.4311/jcks2009ex0091

DETERMINING GEOPHYSICAL PROPERTIES OF A NEAR-SURFACE CAVE THROUGH INTEGRATED MICROGRAVITY VERTICAL GRADIENT AND ELECTRICAL RESISTIVITY TOMOGRAPHY MEASUREMENTS

Marco Gambetta[1]*, Egidio Armadillo[2], Cosmo Carmisciano[1], Paolo Stefanelli[1], Luca Cocchi[1], and Fabio Caratori Tontini[3]

Abstract: Vertical-gradient microgravity and electrical-resistivity tomography geophysical surveys were performed over a shallow cave in the Italian Armetta Mountain karst area, close to the Liguria-Piedmont watershed. The aim of this study was to test the geophysical response of a known shallow cave. The shallowest portion of the cave exhibits narrow passages and, at about 30 meters below the entrance, a fossil meander linking two large chambers, the target of the geophysical survey. The integrated results of the two surveys show a clear geophysical response to the cave. The surveys exhibited high resistivity values and a negative gravity anomaly over the large cave passages. This work confirms the ability of these geophysical techniques to give the precise location of the voids, even in complex environments. The application of these techniques can be successful for site surveying where the presence of hollows may be expected.

Introduction

Geophysical techniques provide quick, low-cost imaging of voids, and can play a key role in understanding epikarst. This understanding is crucial because karst conduits may conduct pollutants toward groundwater reservoirs and contaminate vulnerable water resources (Field, 1993). Moreover, collapse of underground voids may result in extensive damage to property and danger to people (Waltham, 2005). In this paper we show the results of a geophysical survey conducted over a shallow cave developed under the Cartei da Colla plain in the Mount Armetta karst, which is located near the Ligurian-Piedmont watershed in northwestern Italy. The aim of this study is to contribute to the body of void-detection techniques. This geophysical survey consisted of a multi-electrode electrical-resistivity tomographic survey combined with a vertical-gradient gravity survey. The geophysical imaging of underground voids was verified by comparison with the authors' measurements of the cave dimensions. Among various geophysical methods, electrical-resistivity tomography (ERT) and microgravity vertical-gradient (MVG) were chosen because of their recognized ability to detect shallow features such as hollows and cave voids. In particular, the MVG technique emphasizes shallow gravity anomalies with a strong reduction in geologic noise to allow determination of the horizontal position of voids. The high resolution ERT, conversely, outlines the shape and vertical distribution of the hollows, which appear as high-resistivity volumes.

Area Geology

The geophysical survey was carried out in Cartei da Colla plain (Figs. 1 and 2), located at 1400 m above sea level and encompassing more than 9 km^2 in the Mount Armetta karst complex in Val Pennavair, Italy, close to the Liguria-Piedmont watershed. The karst aquifer feeds a spring used by local municipalities for drinking water supplies.

The karst terrane belongs to the Caprauna Armetta tectonic unit, which is a cover nappe emplaced during the Briançonnais orogeny on the external margin of the Ligurian Briançonnais terrane. The unit features four superimposed deformations that produced large recumbent isoclinal folds (phase 1 folds in Fig. 2) associated with a strong axial-plane cleavage and a southwest-trending lineation. These folds can be related to a southwest-directed overthrust shear. The second phase of deformation (phase 2 folds in Fig. 2) yielded open to moderately tight folds with subvertical axial planes that are overturned towards the northeast. The later deformations are long-wavelength open folds affecting only the large-scale setting of the nappe (Menardi-Noguera, 1988). Folds from the two phases constrained the cave's evolution. The large room located at the intersection of the phase 1 and 2 anticlines (Fig. 2) has been interpreted as the topmost part of a pit, now filled with collapse debris. This large pit appears to have evolved over a dome-like structure featuring a pervasive axial-plane cleavage. The cave, dropping from the entrance at 1395 m above sea level to approximately 1200 m, also seems to be guided both by the rocks' brittle deformations and the stratigraphy. The deepening conduits follow both the strata dip direction of 20° and a set of

* Corresponding author, marco.gambetta@ingv.it
[1] INGV —Via Pezzino Basso 2 Fezzano di Portovenere (SP) —Italy
[2] University of Genova, DIP.TE.RIS, V.le Benedetto XV, Genova —Italy
[3] GNS Science, 1 Fairway Dr, Avalon, Lower Hutt, New Zealand

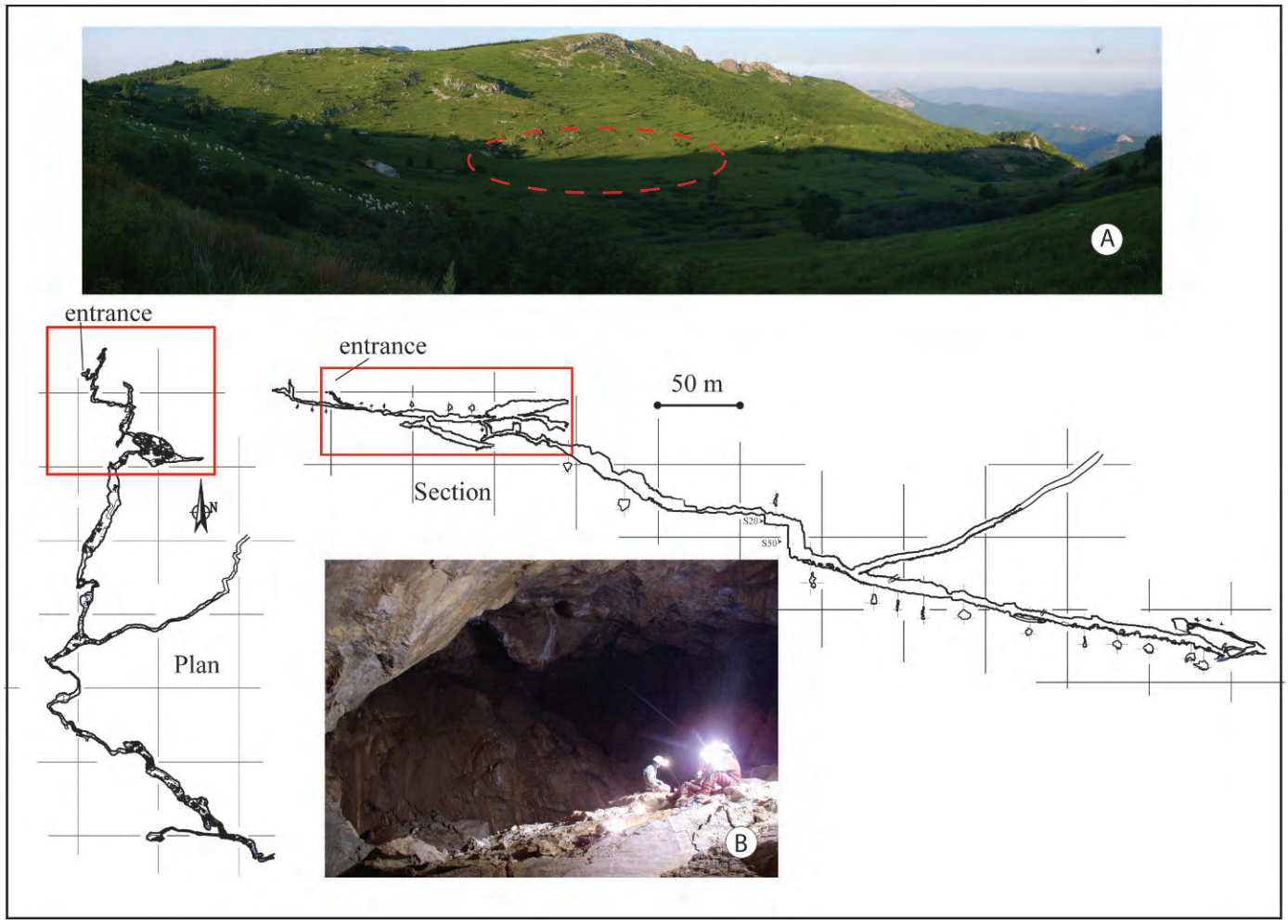

Figure 1. The survey area: (A) landscape of the Cartei da Colla plain; (B) picture of the largest room, which was the target of the geophysical experiment; partial plan and cross-section of the cave system. Cave survey performed with compass and tape.

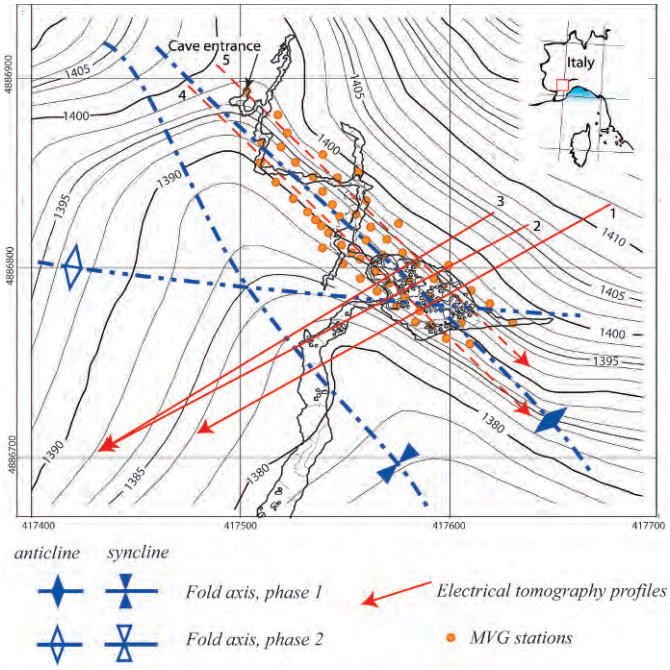

fractures trending 95°, with a prevailing drainage along the former. The deepest cave regions, conversely, exhibit an evolution along a fracture trending 135° that cannot be recognized by surface observations.

GEOPHYSICAL METHODS

Five two-dimensional, direct-current electrical-resistivity traverses were carried out. The ERT prospecting was performed using a Syscal R1 (Iris Instruments) multi-electrode system with a set of 48 electrodes evenly spaced every 5 m. A Wenner-Schlumberger array configuration was used with a geometrical factor, $k = \pi (n+1) a$, where a is the potential-electrode spacing and n is an integer. The Wenner-Schlumberger array combines the standard individual Wenner and Schlumberger arrays, but is adapted for

←

Figure 2. Topography of the survey area, with structural features and the outline of the cave.

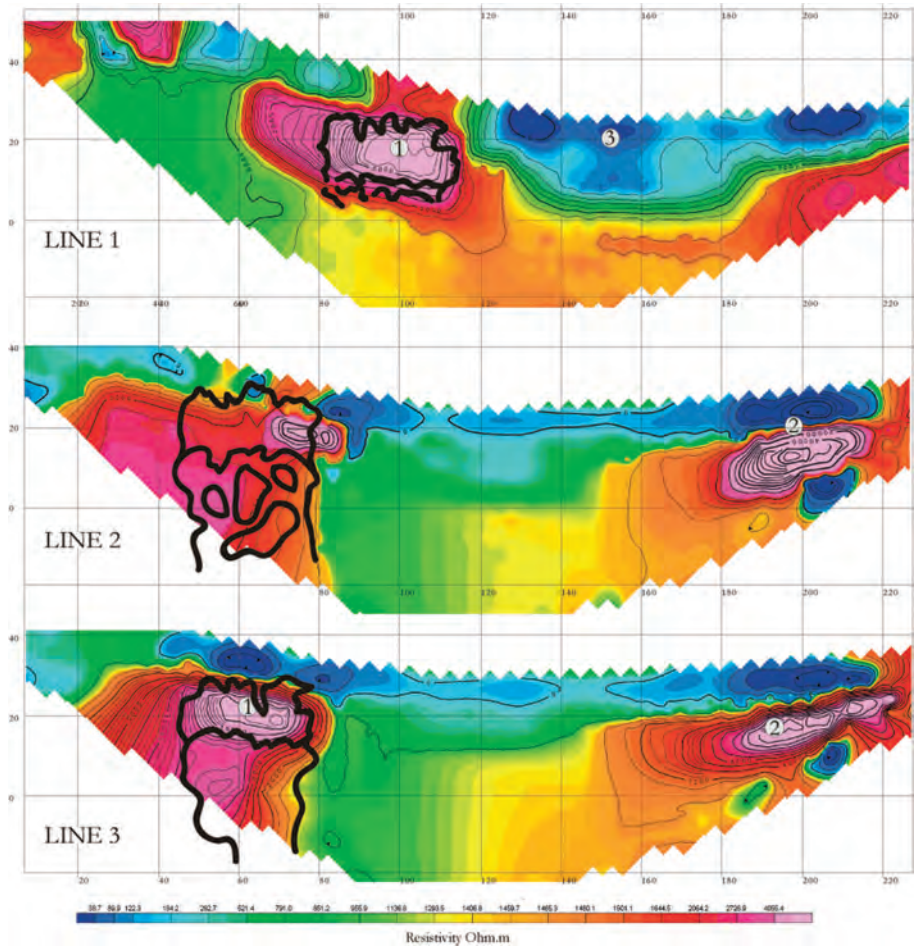

Figure 3. Electrical-resistivity tomography result for lines 1, 2, and 3 with the outline of the main room (see Fig. 2).

use with a line of electrodes with constant spacing, as normally used in 2-D imaging. Besides better horizontal coverage, the maximum depth of penetration of this array is about 1.5 times greater than the Wenner array (Loke and Barker, 1996). The measured resistance values are first reduced to apparent resistivity values and then inverted (Loke and Barker, 1996) to image the resistivity distribution below the traverse path (Fig. 3).

The MVG survey was performed using a LaCoste-Romberg model D gravity meter, equipped with digital data acquisition through the Aliod feedback system, GPS tracking, and automatic tide correction. The meter has a nominal resolution of one microgal (10 nm s^{-1}). The geographical positions of the 53 gravity stations (Fig. 2) were determined by using a differential GPS. The vertical gradient of the gravity field was measured as the ratio between the difference of two recordings at different heights and the height difference. Measurements were recorded for five minutes at the top and bottom of a 1.80-meter tower. The recording procedure included a tide correction. The recordings can be statistically averaged to give a best estimate of the gravity, reducing the noise inherent within a single measurement resulting from instrumental errors, vibrations of the support, and other related sources of uncertainty. The gravity data were processed to remove the instrument drift, determined by periodically reoccupying the gravity base station located near the survey area. The observed drift error was about 25 μgal d^{-1}. The overall error of the MVG data, including effects of nearby topography, tide, and drift was approximately 4 to 5 μgal m^{-1} (Stefanelli et al., 2008).

Results and Data Interpretation

Figure 3 shows the results of the inversion (Loke and Barker, 1996) of apparent resistivity data collected along profiles 1, 2, and, 3 that cross the main room. The cross-section of the room is superimposed on the plots. The results from traverses number 4 and 5 appear to be much noisier than the others, even though the cave outline is still recognizable. Because of the high noise, these results are not shown.

The resistivity values associated with the room range from 6,000 to 40,000 ohm-m (Fig. 3, line 1). The high variability of the void's electrical signature may be due to a micrometeorological effect inside the cave. A seasonal cave

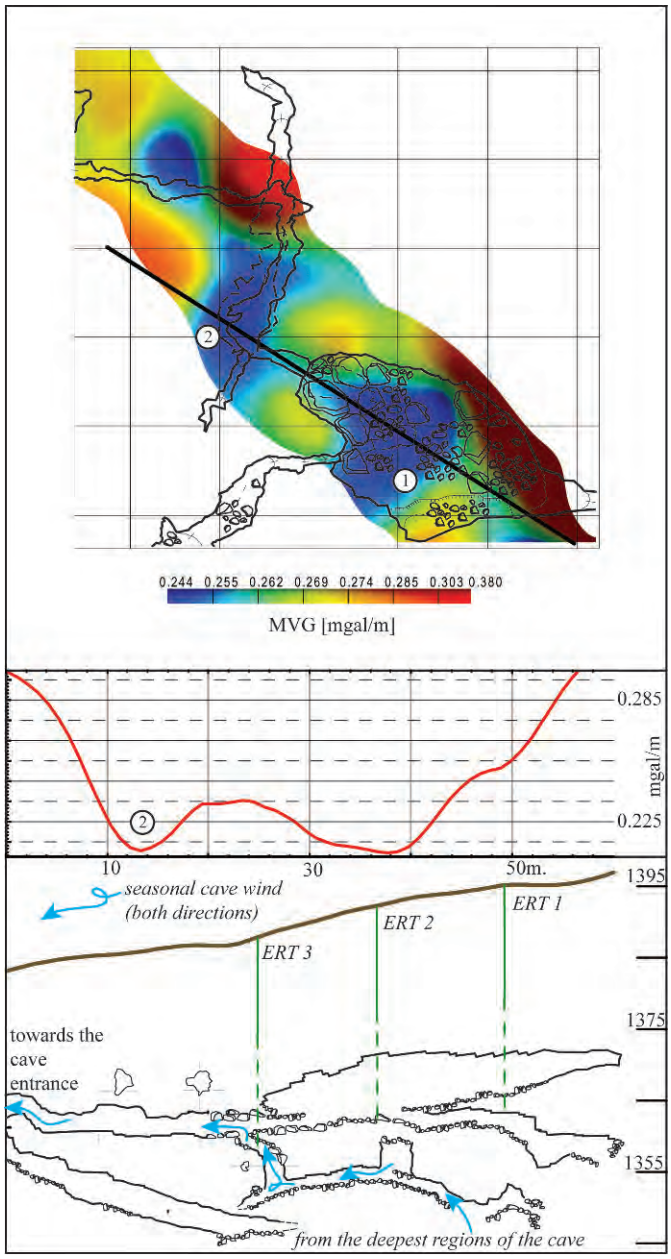

Figure 4. The microgravity vertical-gradient survey. Top panel, spatial distribution of the gradient; bottom panel, profile with the cave cross-section.

wind (Fig. 4) flows from the deepest regions towards the entrance, yielding a significant decrease in cave moisture. This air flow dries the cave walls, thus increasing their electrical resistivity; conversely, the parts of the cave far from the wind path are much more damp, and thus the resistivity drops. This effect is clearly shown in the sections for lines 1 and 3. Line 2, conversely, shows lower resistivity values than line 3. This may be due to the fact that the passages between the area of line 3 and the large room probed by line 1 are filled with large debris and blocks.

The ERT survey shows an unpredicted oval-shaped maximum of resistivity (labeled 2 in Fig. 3) and is interpreted as evidence of an unknown cave. The well-defined low-resistivity body (labeled 3 in Fig. 3) is interpreted as a sinkhole filled with residual clays.

The distribution of MVG data with the cave-plan outline are shown in the upper panel of Figure 4. The lower panel of Figure 4 shows a profile across the main hollow. There is a very good correlation between the horizontal geometry of the cave and the minima of the gradient map, as it is expected from the large negative density contrast between voids and rocks (-2400 kg m^{-3}). This shows that effects of local topography have been effectively filtered out in the gradient measurements. The gradient survey had a mean value of 0.268 mGal m^{-1}, in contrast with the standard vertical gradient value of approximately 0.3 mGal m^{-1}. This may result from the superposition of the localized negative anomaly that is well-correlated to the cave geometry and a more general regional feature coming from other large-scale geological effects. The amplitude of the gradient varies across the area by approximately 0.130 mGal m^{-1} because of the large underground voids. The gradient profile exhibits a negative anomaly approximately coincident with the known void geometry. The minimum above the largest room (Figure 4, labeled 1) is consistent with the presence of a large (about 20 × 20 × 80 m) collapsed pit partially filled by collapse debris. The minimum labeled 2 in Figure 4 is attributed to the two underlying levels of cave passage.

CONCLUSIONS

The combined application of microgravity vertical-gradient sounding and electrical resistivity tomography yields accurate imaging of underground hollows. The MVG shows minima coincident with the known void, showing a capability for void detection. The ERT results, combined with of the cave location and volume supplied by MVG, can give high-resolution images of underground voids. The low cost and the moderate logistics needs of both methods allow rapid noninvasive surveys, providing reliable results.

ACKNOWLEDGMENTS

The authors wish also to thank R. Castello and F. Poggi (Environment Department, Regione Liguria) for their confidence in the Speleology and Nature in Pennavaire High Valley (SNAP) Research Project, which has been funded by the department act n.1543 02/12/2005, granted to the Alassio Caving Club. Thanks are also due to the municipal authorities of Alassio and Alto for logistical support and permission to access the caves. The authors also acknowledge the assistance provided by the Alassio Caving Club and E. Massa and A. Maifredi in the underground survey.

References

Field, M., 1993, Karst hydrology and chemical contamination: Journal of Environmental Systems, v. 22, no. 1, p. 1–26.

Loke, M.H., and Barker, B.R., 1996, Rapid least squares inversion of apparent resistivity pseudosections by a quasi-Newton method: Geophysical Prospecting, v. 44, p. 131–152.

Menardi-Noguera, A., 1988, Structural evolution of a briançonnais cover nappe, the caprauna-armetta unit (Ligurian Alps, Italy): Journal of Structural Geology, v. 10, no. 6, p. 625–637.

Stefanelli, P., Carmisciano, C., Caratori Tontini, F., Cocchi, L., Beverini, N., Fidecaro, F., and Embriaco, D., 2008, Microgravity vertical gradient measurement in the site of Virgo interferometric antenna (Pisa Plain, Italy): Annals of Geophysics, v. 51, no. 5–6, p. 877–886.

Waltham, T., Bell, F.G., and Culshaw, M.G., 2005, Sinkholes and subsidence: Karst and cavernous rocks in engineering and construction, Chichester, U.K., Springer, 382 p.

M.S. Field and G. Li – Inversion for the input history of a dye tracing experiment. *Journal of Cave and Karst Studies,* v. 73, no. 1, p. 16–20.
DOI: 10.4311/jcks2010es0143

INVERSION FOR THE INPUT HISTORY OF A DYE TRACING EXPERIMENT

Malcolm S. Field[1] and Guangquan Li[2]*

Abstract: The advection-dispersion model (ADM) is a good tool for simulating transport of dye or solutes in a solution conduit. Because the general problem of transport can be decomposed into two problems, a boundary-value problem and an initial-value problem, the complete solution is a superposition of the solutions for these two problems. In this paper, the solution for the general problem is explained. A direct application of the solution for the boundary-value problem is dye-tracing experiments. The purpose is inclusion of the input history of a solute dye into the ADM. The measured breakthrough curve of a dye-tracing experiment is used to invert for the release history of the dye at the input point through the ADM. It is mathematically shown that the breakthrough curve can not be directly used to invert for the boundary condition at a tracer release point. Therefore, a conductance-fitting method is employed to obtain the input history. The inverted history for a simple example is then shown to be a step function with amplitude of 420 μg/L and a duration of 10 minutes. Simulations illustrate that the breakthrough curves at downstream springs provide a means for understanding the migration of dye. A discussion of the implication of the solution for an initial-value problem (e.g., simulating transport of preexisting solutes such as dissolved calcium carbonate in solution conduits) is also included.

Introduction

Solute-transport modeling, as part of a quantitative tracer-test conducted in karstic aquifers, is well established to be critical to developing an understanding of the nature of solute migration in solution conduits (e.g., Field and Pinsky 2000; Birk et al. 2005). The essential solute-transport parameters of velocity, dispersion, and retardation, to name just a few, are generally determined from groundwater tracing and solute-transport modeling processes. Unfortunately, the general complexity of a tracer-breakthrough curve (BTC) often leads to the development or use of models of ever increasing intricacies in attempts to obtain improved model fits to measured data. Although the improved model fits are usually preferred and valuable, there remain some concerns as to the overall applicability of models with very large numbers of parameters, especially those whose parameters may not be transferrable to other examples.

The advection-dispersion model (ADM), also known as the equilibrium model, may be regarded as the simplest of the various mathematical models used to describe solute transport in solution conduits. Although the ADM is theoretically reasonable, its application to measured BTCs is often disappointing because of excessively skewed BTC tails in the measured data that cannot be matched using the ADM. The skewness is often attributed to strong exchanges between mobile- and immobile-flow regions (Toride et al. 1993), solute reactions with aquifer materials (Svensson and Dreybrodt 1992), or multiple flow paths.

Currently, the ADM and the two-region non-equilibrium model (2RNE) are two of the most popular models used for simulating solute transport in solution conduits (Toride et al., 1993; Field and Pinsky, 2000; Birk et al., 2005; Göppert and Goldscheider, 2008; Goldscheider, 2008). The 2RNE is advantageous in that excessive BTC skewness can be well simulated, but has the disadvantage of requiring additional parameters that lead to mathematical complications and possible errors in parameterization if local minima (as opposed to a global minimum) create a condition of non-uniqueness during inverse analysis (see, for example, Moré and Wright, 1993). The likelihood of a local minimum being encountered increases as the number of model parameters increases, especially if the initial value for one or more of the varying parameters is far from the real value.

The currently favored ADM is actually the solution for the boundary-value problem in which a zero initial condition is assumed such that the solute source is a selected boundary condition. In other words, it is the boundary condition that drives the BTCs, and that is most applicable to tracing experiments. In this paper, we first describe a complete solution that considers the contribution of the initial condition (similar to that of Toride et al., 1995, pp. 4–6). Second, we use a conductance-fitting method to obtain the input history of a dye tracing experiment.

* Corresponding Author
[1] U.S. Environmental Protection Agency, National Center for Environmental Assessment (8623P), 1200 Pennsylvania, Ave., N.W., Washington, D.C. 20460, USA, field.malcolm@epa.gov
Disclaimer: The views expressed in this paper are solely those of the authors and do not necessarily reflect the views or policies of the U.S. Environmental Protection Agency.
[2] Department of Geophysics, Yunnan University, 2 North Green Lake Rd., Kunming, Yunnan 650091, P. R. China, guangquanli74@gmail.com

Finally, we discuss the difference of the ADM and the 2RNE in modeling transport in solution conduits.

Advection-Dispersion Modeling in Solution Conduits

Problem Formulation

The essential features of solute transport in a solution conduit may be described using a one-dimensional advection-dispersion equation (Taylor, 1954), which arises from mass conservation of the solute, but water exchange between the solution conduit and the surrounding rock matrix is neglected. The governing equation of the general ADM is given as

$$\frac{\partial C}{\partial t} + W\frac{\partial C}{\partial z} = D\frac{\partial^2 C}{\partial z^2}. \quad (1)$$

Solute concentration is denoted as C. The dispersion coefficient D can be parameterized with the conduit radius, a, and solute velocity W as follows (Li et al., 2008),

$$D = \beta a W, \quad (2)$$

where the dimensionless dispersion coefficient β is used to quantify the strength of dispersion. We note that βa is often referred to as dispersivity.

Because the length of the conduit is invariably finite, there is an initial condition within the solution conduit ($0 \le z \le L$, where L is the downstream position of the spring),

$$C(z,0) = C_{\mathrm{I}}(z), \quad (3)$$

and a boundary condition at the sinkhole ($z = 0$)

$$C(0,t) = C_{\mathrm{B}}(t). \quad (4)$$

The general problem consists of Equation (1) subject to conditions shown in Equations (3) and (4). Because the mathematical problem is linear with respect to concentration, we can decompose this general problem of the ADM into two problems; a boundary-value problem (BVP) and an initial-value problem (IVP) (Fig. 1). The solution is the superposition of the two solutions for these two problems.

Solution for the Boundary-Value Problem

The boundary-value problem consists of Equations (1) and (4), with a zero concentration initial condition, $C_{\mathrm{I}}(z) = 0$. The Green's function for this problem can be obtained by the Laplace transform, and the solution is

$$C_{\mathrm{BVP}}(z,t) = \int_0^t C_{\mathrm{B}}(\tau)\frac{z}{\sqrt{4\pi D(t-\tau)^3}} \exp\left\{-\frac{[z - W(t-\tau)]^2}{4D(t-\tau)}\right\} d\tau, \quad (5)$$

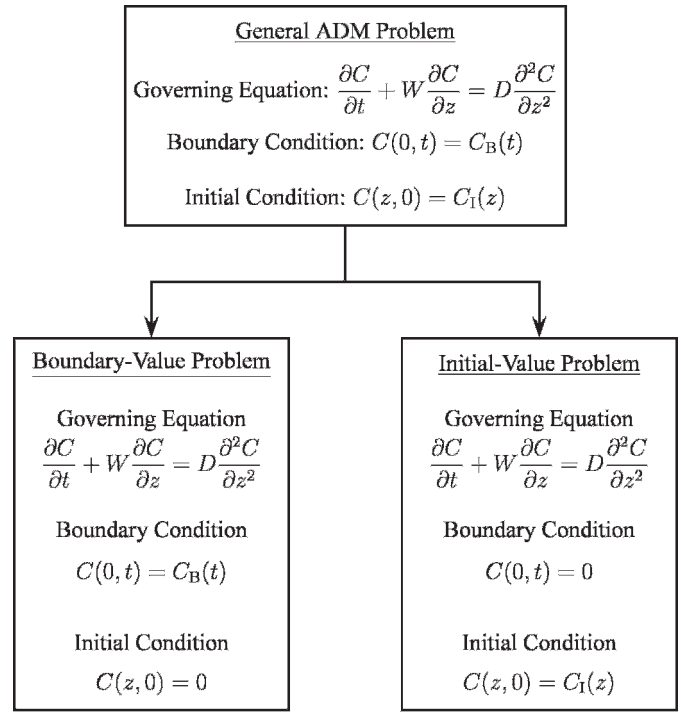

Figure 1. The schematic decomposition of the general problem of the ADM. The complete solution is a superposition of the solutions for each subproblem.

which is equivalent to the solution listed in Table 2 of Kreft and Zuber (1978) and Table 2.2 of Toride et al. (1995). Here, τ represents the past time, i.e., the time earlier than t.

Solution for the Initial-Value Problem

The solution for the initial-value problem is a convolution of the initial condition with the associated Green's function:

$$C_{\mathrm{IVP}}(z,t) = \int_0^L C_{\mathrm{I}}(\zeta)\left\{\frac{1}{\sqrt{4\pi Dt}}\exp\left[\frac{-(z - Wt - \zeta)^2}{4Dt}\right] - \int_0^t \frac{1}{\sqrt{4\pi D\tau}}\exp\left[\frac{-(W\tau + \zeta)^2}{4D\tau}\right]\frac{z}{\sqrt{4\pi D(t-\tau)^3}} \times \exp\left(\frac{-[z - W(t-\tau)]^2}{4D(t-\tau)}\right) d\tau\right\} d\zeta. \quad (6)$$

Note that the term inside the big bracket is the Green's function for the initial-value problem. Here, ζ is a variable denoting the spatial coordinate of the solute-concentration distribution at $t = 0$.

The Green's function for the initial-value problem in infinite space can be obtained from the Fourier transform, which is the first term inside the big bracket. However, this term causes a positive value at the boundary $z = 0$. The initial-value problem requires a zero value at this location.

Table 1. The parameters of the simulation example.

Parameter	Value	Units
Conduit radius, a	2.44	m
Conduit length, L	8.0	km
Flow velocity, W	0.095	m s^{-1}
Dimensionless dispersion coeff., β	7.0	…
Total mass of dye, M	476	gram
Dye concentration at sinkhole, C_0	420	μg L^{-1}
Input duration at sinkhole, T_{ST}	10	min
Time sampling interval	1	min

For this reason, a negative value must be prescribed at this boundary and the contribution of this negative boundary value must be included, which is the second term inside the big bracket. This Green's function (i.e., the term inside the big bracket) is equivalent to that listed in Table 2.2 of Toride et al. (1995).

The Complete Solution

The complete solution of Equation (1), subject to the initial and boundary conditions imposed by Equations (3) and (4), respectively is a superposition of solutions (5) and (6) that is given as

$$C(z,t) = C_{\mathrm{BVP}}(z,t) + C_{\mathrm{IVP}}(z,t). \tag{7}$$

Application

This section applies Equation (5) for the boundary-value problem to a tracer experiment conducted at the Lost River Cave System located in Bowling Green, Kentucky. Formed in the Ste. Genevieve and St. Louis Limestones of Middle to Late Mississippian age and developed on top of the Lost River Chert, the Lost River Cave System begins with the Lost River flowing directly into the cave entrance. Lost River then traverses the cave to eventually reemerge 8 km downstream.

Flow along the length of the cave is relatively uniform along much of its length, but older, higher passages can be inundated by flood-flow conditions (Crawford, 1986, p. 7). Blocks of the Lost River Chert routinely detach from cave walls and line the cave floor as the limestone dissolves away. The detached chert blocks create minor detention backwaters containing immobile-flow regions. Undercut benches and recirculation with scalloped walls also serve as minor immobile flow regions.

The tracer input is modeled using a typical step-like function with time. By fitting the theoretical BTC against the measured BTC, the parameters of the solution conduit and solute transport, as well as the input history of tracer, are inverted (Table 1). In our inversion process, the total mass of dye provides a constraint as follows:

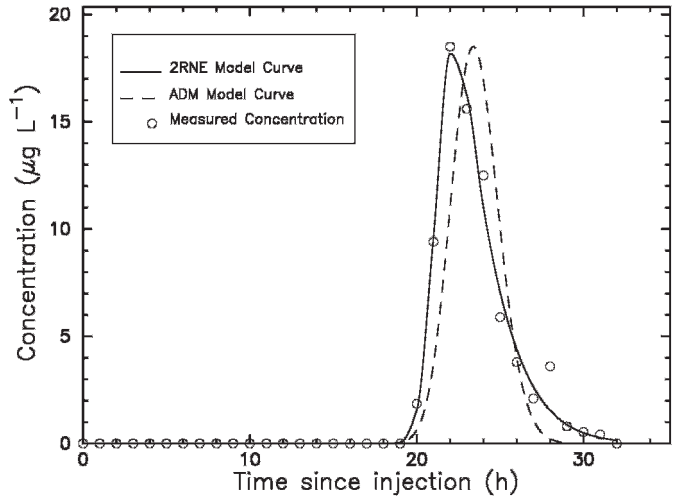

Figure 2. The theoretical breakthrough curves versus the measured curve. The initial condition is zero, and for the ADM, the boundary condition at the sinkhole is assumed to be a step-like function with time.

$$T_{ST} = \frac{M}{QC_0}, \tag{8}$$

where M is the total mass of dye (476 gram), T_{ST} is the duration of dye input at the sinkhole, C_0 is the amplitude of dye concentration at the tracer release point, and $Q = \pi a^2 W$ is the spring discharge (1.78 m^3/s). For the ADM, the boundary condition at the input point is assumed to be a step function with time (constrained by Equation (8)).

The 2RNE is also used to simulate the measured BTC. Both models (ADM and 2RNE) achieve a good fit against the measured BTC, as depicted in Fig. 2. The peak of the BTC modeled from ADM has an error of 2 hours (Fig. 2) because the ADM cannot adequately simulate the skewness of the measured BTC. The 2RNE visually appears to a better fit than the ADM in simulating the falling skewed limb.

Often, the dye release is assumed to be instantaneous (a Dirac-δ source). This assumption is reasonable as a first-order approximation. However, this assumption mathematically implies an infinite solute-concentration at the injection moment. To overcome this physical problem, we include the input history into the ADM, and obtain a reasonable history of about 10 minutes. This result should be regarded as the second-order of approximation. Actually, because this duration is much shorter than the width of the measured BTC and the amplitude of solute concentration at the tracer release point C_0 (420 μg L^{-1}) is much larger than the maximum amplitude of the measured BTC at the spring (18.5 μg L^{-1}), the continuous input could be regarded as a Dirac-δ source. For this reason a Dirac-δ source assumption often works well. Nevertheless,

the continuous input is physically more reasonable, because concentration can never be infinitely large.

Discussion

For the inversion procedure, we use conductance-fitting, which is an indirect inversion method. Direct inversion may be thought of as using a negative velocity and a negative dispersion coefficient to infer the input history directly from the measured BTC. However, the Green's function for a Dirac-δ input at the spring does not exist. In a physical sense, a point source at the spring would be restored to an input history that never exists. Mathematically, this can be shown by rewriting Equation (5) to

$$C_{\mathrm{BVP}}(z,t) = C_{\mathrm{B}}(t) * G_{\mathrm{B}}(z,t), \tag{9}$$

where * represents convolution. Performing the Laplace transform with respect to time on Equation (9) yields

$$C_{\mathrm{B}}(p) = \frac{C_{\mathrm{BVP}}(z,p)}{G_{\mathrm{B}}(z,p)}, \tag{10}$$

and applying an inverse Laplacian transform and convolution on Equation (10) yields

$$C_{\mathrm{B}}(t) = C_{\mathrm{BVP}}(z,t) * LT^{-1}\left[\frac{1}{G_{\mathrm{B}}(z,p)}\right], \tag{11}$$

where LT^{-1} denotes inverse Laplacian transform. The inverse Laplacian transform of the reciprocal of $G_{\mathrm{B}}(z,p)$ doesn't exist. Therefore, we cannot invert for the input history $C_{\mathrm{B}}(t)$ directly from the spring BTC $C_{\mathrm{BVP}}(z,t)$, and the conductance-fitting must be used.

The ADM is often applied to tracer experiments in karstic aquifers for which the initial condition is zero, but the boundary condition (history of the tracer solute) at the input point is not zero. Besides tracing experiments, the ADM is also applicable to the simulation of transport in which the boundary condition is zero, but the initial condition is not zero. Such a situation may be encountered when water entering a sinkhole or similar input point is tracer free, but water rich in dissolved solutes (e.g., calcium carbonate) preexists inside the conduit. Because the initial condition is often unknown and not measurable, the distribution of solutes in the solution conduit must be assumed *a priori*.

Toride et al. (1993) proposed a 2RNE model, to describe nonequilibrium solute transport with first-order decay and zero-order production. The ADM model could be seen as a simplification of their model. The Toride et al. model dealt with the case in which there is a strong solute interaction between mobile- and immobile-flow regions or aquifer kinetic reactions, while our model focuses on the case in which aquifer kinetic reactions and solute interaction between mobile- and immobile-flow regions are negligible. Our solution to the ADM may be regarded as more robust, because it requires fewer parameters, which is similar to the findings of Göppert and Goldscheider (2008). In this sense, our model may be more suitable to the relatively rapid transport conditions that typically occur in solution conduits, because when solutes are rapidly flushed and entrained through the solution conduit, only a small portion of the solute will likely be sequestered in an immobile-flow region (Li et al., 2008) and probably only for a very short time. Therefore, the solute interaction between the mobile- and immobile-flow regions should be very limited, and our model should behave very well as a first-order approximation. Nevertheless, the 2RNE model provides a more accurate tool, because it considers temporary solute detention in immobile-flow regions. For this reason, the 2RNE is better for simulating BTCs that exhibit significant skewness and long tailing phenomena (see Birk et al., 2005), while the ADM is suitable for simulating the primary large signals that arrive earlier.

Summary and Conclusion

Transport in a solution conduit is often described by the advection-dispersion model that is subjected to various initial and boundary conditions. The general problem is a superposition of two solutions: one is for the problem consisting of a boundary condition and a zero initial condition (Equation (5)), and the other is for the problem consisting of an initial condition and a zero boundary condition (Equation (6)).

We used Equation (5) and the breakthrough curve measured from a dye tracing experiment to invert for the history of dye injection at the input point. The inverted parameters are reasonable, which illustrates that the BTCs can be used to obtain the history of solute injection at input points. From Figure 2, the breakthrough curve of the boundary-value problem still exhibits some skewness. In this sense, the 2RNE is a better model that better replicates the typically strong skewness and tailing observed in measured BTCs. It is our contention that the ADM will have important and profound applications in modeling transport of solutes that preexist in solution conduits (e.g., dissolved carbonates).

Acknowledgements

This research was financially supported in part by the University Fund of Yunnan University under contract KL090020. The authors are deeply grateful to the Associate Editor, Prof. Gregory S. Springer for his insightful comments and constructive suggestions.

NOTATION

a	conduit radius (m)
C, $C(z,t)$	solute concentration in conduit (g L^{-1})
C_0	concentration of dye at sinkhole (g L^{-1})
$C_B(t)$	boundary condition at sinkhole (g L^{-1})
$C_{BVP}(z,t)$	solute concentration for the boundary-value problem (g L^{-1})
$C_I(t)$	initial condition within conduit (g L^{-1})
$C_{IVP}(z,t)$	solute concentration for the initial-value problem (g L^{-1})
D	dispersion coefficient (m^2 s^{-1})
$G_B(z,t)$	Green's function for the boundary-value problem with source fixed at $t = 0$ (s^{-1})
L	conduit length (m)
M	total mass of dye (gram)
p	Laplacian transform variable (s^{-1})
Q	water discharge (m^3 s^{-1})
t	time (s)
T_{ST}	input duration of dye at sinkhole,
W	flow velocity in conduit (m s^{-1})
z	conduit downstream location starting from sinkhole (m)
β	dimensionless dispersion coefficient

REFERENCES

Birk, S., Geyer, T., Liedl, R., and Sauter, M., 2005, Process-based interpretation of tracer tests in carbonate aquifers: Ground Water, v. 43, no. 3, p. 381–388, doi: 10.1111/j.1745-6584.2005.0033.x.

Crawford, N.C., 1986, Karst hydrologic problems associated with urban development: ground water contamination, hazardous fumes, sinkhole flooding, and sinkhole collapse in the Bowling Green area, Kentucky, Guide Book to Field Trip B: Environmental Problems in Karst Terranes and Their Solutions Conference (Bowling Green): National Water Well Association, Dublin, Ohio, 85 p.

Field, M.S., and Pinsky, P.F., 2000, A two-region nonequilibrium model for solute transport in solution conduits in karstic aquifers: Journal of Contaminant Hydrology, v. 44, no. 3–4, p. 329–351.

Goldscheider, N., 2008, A new quantitative interpretation of the long-tail and plateau-like breakthrough curves from tracer tests in the artesian karst aquifer of Stuttgart, Germany: Hydrogeology Journal, v. 16, p. 1311–1317, doi: 10.1007/s10040-008-0307-0.

Göppert, N., and Goldscheider, N., 2008, Solute and Colloid Transport in Karst Conduits under Low- and High-Flow Conditions: Ground Water, v. 46, no. 1, p. 61–68, doi: 10.1111/j.1745-6584.2007.00373.x.

Kreft, A., and Zuber, A., 1978, On the physical meaning of dispersion equation and its solution for different initial and boundary conditions: Chemical Engineering Science, v. 33, no. 11, p. 1471–1480.

Li, G., Loper, D.E., and Kung, R., 2008, Contaminant sequestration in karstic aquifers: Experiments and quantification: Water Resources Research, v. 44, W02429, doi: 10.1029/2006WR005797.

Moré, J.J., and Wright, S.J., 1993, Optimization software guide: Philadelphia, Society for Industrial and Applied Mathematics, 154 p.

Svensson, U., and Dreybrodt, W., 1992, Dissolution kinetics of natural calcite minerals in CO_2-water systems approaching calcite equilibrium: Chemical Geology, v. 100, no. 1–2, p. 129–145.

Taylor, G.I., 1954, The dispersion of matter in turbulent flow through a pipe: Proceedings of the Royal Society London, Ser. A, v. 223, p. 446–468, doi: 10.1098/rspa.1954.0130.

Toride, N., Leij, F.J., and van Genuchten, M.T., 1993, A comprehensive set of analytical solutions for nonequilibrium solute transport with first-order decay and zero-order production: Water Resources Research, v. 29, no. 7, p. 2167–2182, doi: 10.1029/93WR00496.

Toride, N., Leij, F.J., and van Genuchten, M.T., 1995, The CXTFIT code for estimating transport parameters from the laboratory or field tracer experiments; version 2.0: US Salinity Laboratory Research Report 137, 121 p.

J.W. Dixon – The role of small caves as bat hibernacula in Iowa. *Journal of Cave and Karst Studies,* v. 73, no. 1, p. 21–27. DOI: 10.4311/jcks2010lsc0145

THE ROLE OF SMALL CAVES AS BAT HIBERNACULA IN IOWA

JOSEPH W. DIXON
Iowa Grotto of the National Speleological Society, P.O. Box 228, Iowa City, IA 52244, joedixon@mchsi.com

Abstract: Small caves provide habitat for a variety of species, including bats. Past research on cave bats in Iowa has focused on a few large caves. Large caves are uncommon and represent only a portion of the known caves in the state. Since few hibernacula are protected in Iowa and no assessment of small caves has been done, bat census data were compared to cave morphology to determine the significance of small caves as hibernacula. Twelve years of census data (1998–2009) were reviewed for small caves (≤ 50.0 m in length) where hibernating bats had been documented. Four morphological features were compared against the data: entrance aspect, entrance size, cave length, and internal surface area. Student's t-test and Spearman rank correlation were used to test for relationships between the presence and abundance of each species and each of the four morphological features. The eastern pipistrelle occurred in 68% of the caves, and the little brown bat in 24%. Student's t-test showed a significant correlation with cave length for eastern pipistrelles. Spearman rank correlation showed a significant negative correlation with entrance aspect and significant positive correlations for cave length and internal surface area for eastern pipistrelles. The results are different from previous studies on larger Iowa caves, which showed big brown bats and little brown bats as the most abundant species. Eastern pipistrelles preferred larger caves with vertical entrances. However, large is a subjective term, and the results indicate that small caves are an important source of hibernacula for the eastern pipistrelle.

INTRODUCTION

Small caves often receive little notice from researchers, cavers, and the general public. Larger and more complex caves receive more attention in the form of exploration, study, or recreational caving (Kastning, 2006). This bias is often the result of anthropocentric criteria, such as cave length, which is usually arbitrarily determined (Curl, 1966). For example, among state cave surveys in the Untied States, a minimum length is often established to filter out those caves deemed less important; caves that fall below this discretionary length are simply not included in the survey (Mylroie, 2007). Such discriminatory practices towards small caves are unfortunate, since small caves can occasionally be geologically, historically, or archaeologically significant (Kastning, 2006). In addition, small caves may also be biologically significant, since they have been known to provide habitat for a variety of temperate vertebrate trogloxenic species, such as snakes (Drda, 1968), salamanders (Briggler and Prather, 2006; Camp and Jensen, 2007), and frogs (Blair, 1951; Prather and Briggler, 2001).

The biological significance of small caves may be applicable to bats as well. The fact that larger caves support both greater numbers (Raesley and Gates, 1987; Briggler and Prather, 2003) and greater diversity of bats (Arita, 1996; Fuszara et al., 1996; Brunet and Medellín, 2001; Nui et al., 2007) has been well documented, but small caves have also been observed as a source of hibernacula for some species. For example, Ozark big-eared bats (*Corynorhinus townsendii ingens*) (Prather and Briggler, 2002) and eastern pipistrelles[1] (*Perimyotis subflavus*) (Briggler and Prather, 2003) both utilize small caves as hibernacula. Prather and Briggler (2002) observed that the endangered Ozark big-eared bat used small caves to such an extant that they recommended those in their study area be protected and further surveys for Ozark big-eared bats be conducted in additional small caves.

The lack of interest in small caves could potentially result in the unintentional exclusion of pertinent data. Caves are known to provide some of the most important hibernacula sites for bats (Pierson, 1998), and bat communities in small hibernacula can differ dramatically from those utilizing large hibernacula (Lesiński et al., 2004). Numerous species of cave-hibernating bats exhibit considerable fidelity to hibernacula (Harvey, 1992). For many species of temperate bats, appropriate hibernacula are essential for their survival, and a greater understanding of hibernacula is necessary to make appropriate conservation and management decisions (Brack, 2007).

The state of Iowa has not been an exception to this pattern. Previous research on bats in Iowa caves has been irregular (Bowles et al., 1998) and focused on larger caves, averaging several hundred meters, and occasionally over a thousand meters, in length (see Muir and Polder, 1960; Kunz and Schlitter, 1968; Pruszko and Bowles, 1986; and

[1] Editor's Note: The eastern pipistrelle is now more properly called the tri-colored bat. (http://www.batcon.org/news2/scripts/article.asp?articleID=128).

Clark et al., 1987, for names of caves surveyed and Lace and Ohms, 1992; Lace, 1997; Lace and Klausner, 2001; and Lace and Klausner, 2004, for cave lengths). Caves of this size are uncommon and represent only a fraction of the caves found within the state. Of the approximately 1,300 caves documented by the Iowa Grotto of the National Speleological Society (Kambesis and Lace, 2009), it is estimated that as many as 90% are 50 m or less in length (Dixon, 2009). Although previous research provided valuable information on the status and distribution of the state's bat populations, these data may not represent a completely accurate assessment because they did not include the typical small caves that dominate Iowa's karst landscape.

Of the eleven species of bats recorded in Iowa (Laubach et al., 1994; Bowles et al., 1998), five have been documented roosting in caves within the state: the big brown bat (*Eptesicus fuscus*), the eastern pipistrelle, the Indiana bat (*Myotis sodalis*), the little brown bat (*Myotis lucifugus*), and the northern myotis (*Myotis septentrionalis*) (Muir and Polder, 1960; Kunz and Schlitter, 1968; Pruszko and Bowles, 1986; Clark et al., 1987; Iowa Department of Natural Resources, unpublished data; Iowa Grotto, unpublished data). All five are considered regular cave-using species (Harvey, 1992), and of the five, all but the Indiana bat regularly hibernate in caves in eastern Iowa (Laubach et al., 1994). Two of the remaining four species, the little brown bat and the eastern pipistrelle, may even hibernate exclusively in caves in some regions (Tuttle, 2003).

Since the majority of the caves in Iowa are considerably smaller than those that have been surveyed for bats in the past, and few major hibernacula are protected in the state (Bowles et al., 1998), data collected by the Iowa Grotto were examined and compared with attributes of cave morphology using published cave maps to determine what, if any, role small caves played in providing bat hibernacula in Iowa and which of the four commonly occurring cave species utilized these hibernacula on a regular basis. Cave morphology was selected as the limiting factor to be tested, because exterior habitat appears to have little to no relationship with the selection of a cave as a hibernaculum (Raesley and Gates, 1987; Briggler and Prather, 2003), while the interior climate that results from morphological features has been known to influence roost selection (Arita and Vargas, 1995; Rodriquez-Duran, 1998).

METHODS

In 1987, the Iowa Grotto began the Iowa Small Caves Survey Project (ISCSP) with the goal to systematically survey all the caves in the state without bias. In 1998, bat censuses were added as a component of the ISCSP. Surveys were conducted for both summer roosting and hibernating bats using either the direct count or surface area estimate methods as described by Thomas and LaVal (1988). For direct counts, each individual bat was counted and identified to species. For surface area estimates, species were identified, but numbers of bats were estimated. In situations where species identification was not possible (e.g., a high roosting position), only numbers of bats were recorded. All bat censuses were conducted using visual observations only. No bats were handled or molested during sampling procedures.

Twelve years of bat census data collected by the Iowa Grotto were reviewed for caves that met four pre-established criteria: (1) the total surveyed cave length was 50 m or less, (2) the census date was during hibernation, (3) if bats were present, the direct count method was used, and (4) any observed bats were identified to species. A maximum length of 50 m was chosen as the limit above which a cave would be considered too large for this study because, as stated previously, many of the historical bat surveys were conducted in caves larger than this and caves longer than 50 m in length are uncommon in Iowa. Any census conducted during September through mid-May was considered an observation of hibernating individuals. Of the five species of bats that roost in Iowa caves, the eastern pipistrelle is typically the first to enter hibernacula and the last to leave, usually entering in mid-October and departing in mid-April (Schwartz and Schwartz, 2001, p. 80–83). However, they have been known to enter caves for hibernation as early as September and remain as late as mid-May to the end of May (Whitaker and Rissler, 1992; Vincent and Whitaker, 2007). Therefore, the hibernation period for this study was expanded to September through mid-May in order to ensure that early-arriving and late-departing bats were included in the sample.

Four morphological features were selected for comparison against the bat census data: entrance aspect (compass direction), entrance size, cave length, and internal surface area. Published cave maps (Lace, 1997; Lace and Klausner, 2001; Lace and Klausner, 2004) were used to quantify morphological features. All caves had been surveyed and mapped using standard cartographic techniques described by Dasher (1994). Entrance aspects were measured in degrees of azimuth using a Suunto A1000 compass. The compass was oriented to magnetic north on each map and azimuth bearings were taken on the centerline of the cave entrance that was perpendicular to the plane of the entrance. For caves that had a vertical entrance (i.e., a sinkhole) an aspect of −90 degrees was arbitrarily assigned to represent the nadir since an azimuth bearing did not exist.

Entrance size was determined by measuring the cave entrance at the widest (plan) and highest (profile) points using a Staedtler Engineer's Scale calibrated to the map scale in meters. These values were then used to calculate the approximate size of the entrance in square meters. Cave lengths were taken directly from maps as this feature is a standard component of cave maps published by the Iowa Grotto. Although cave length is a standard for measuring

cave size, it has been criticized for being potentially inaccurate (Mylroie, 2007). To compensate for this, internal surface area was selected as an alternative means of measuring cave size and was defined as the surface area available for roosting inside each cave and included the walls and ceilings of every surveyed passage. Caves were divided into sections based on profile views. The height, width, and length of each section was then measured using the same Staedtler Engineer's Scale calibrated to the map scale. These values were then used to calculate the surface area in square meters and the results of each section summed to determine the total internal surface area for each cave.

Relationships to cave morphology were determined by comparing the presence and abundance of each species of bat to each of the four morphological features for the caves in which they were documented. Students t-tests were used to test for differences between caves that had a species present versus those that did not for each of aspect, entrance size, length, and internal surface area. Spearman rank correlation (r_s) was used to determine if there were any correlations between each morphological feature and the number of bats from each species. All statistical tests were done at 95% significance ($P < 0.05$).

Results

A total of twenty-five caves met the sampling criteria; all caves were solutional caves with a single entrance. Caves were located in seven different counties in northeastern Iowa (Fig. 1). The number of caves per county ranged from 1 to 10 with an average of 3.6 (± 3.4 SD). The average aspect for all caves combined was 97.4 degrees (± 169.8 degrees SD). However, 32% (8/25) of the caves had a vertical entrance and were therefore assigned a value of −90 degrees since they did not have a geographic aspect. The remaining 17 caves had horizontal entrances. These caves had aspects ranging from 0 to 352 degrees with a mean of 185.5 degrees (± 132.1 degrees SD). Cave entrances ranged from 0.2 to 27.1 m^2 and had a mean of 4.8 m^2 (± 6.4 m^2 SD). Cave length ranged from 6.4 to 34.9 m, with an average length of 18.7 m (± 9.9 m SD). The internal surface area had a range of 15.5 to 383.8 m^2, the mean internal surface area was 125.3 m^2 (± 103.7 m^2 SD).

Three species of bats were documented from 23 of the 25 caves. The eastern pipistrelle was the most common species and was found in 68% (17/25) of the caves. The number of eastern pipistrelles ranged from 0 to 7 with an average of 1.20 (± 1.47 SD) bats per cave. The little brown bat was the second most common species, though it occurred much less frequently than the eastern pipistrelle. Little brown bats were found in only 24% (6/25) of the caves sampled. The number of little brown bats per cave ranged from 0 to 6 with an average of 0.76 (± 1.67 SD). Eastern pipistrelles and little brown bats did not occur together in any of the caves in the sample. Lastly, a single big brown bat was found in one cave along with several little brown bats.

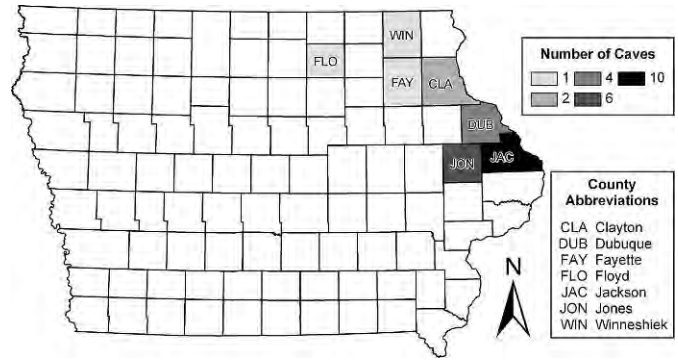

Figure 1. Map of Iowa depicting counties, with numbers of caves included in this study.

The Student's t-test indicated a marginally significant difference for cave length between caves occupied by eastern pipistrelles and those that were unoccupied ($t = 2.09$, $df = 23$, $P = 0.048$). The Student's t-tests did not indicate a significant difference for the remaining morphological features, nor did it indicate any significant differences for any of the caves selected by little brown bats (all $P \geq 0.237$). Spearman rank correlation indicated that caves selected as hibernacula by eastern pipistrelles had a significant, moderately negative correlation with entrance aspect ($r_s = -0.408$, $P = 0.043$). There was no discernible relationship between entrance size and hibernacula selection ($P = 0.289$). There was however a very significant, moderate positive correlation for cave length ($r_s = 0.506$, $P = 0.010$) and a significant, moderate positive correlation for internal surface area ($r_s = 0.455$, $P = 0.022$) for caves selected by eastern pipistrelles as hibernacula. No significant correlations for little brown bats were detected for any of the four morphological features (all $P \geq 0.388$). No statistical analysis was completed for big brown bats since the single individual did not represent a sufficient sample.

Discussion

With only 25 caves meeting the pre-established criteria, it appears that the criteria were perhaps too restrictive. However, since the focus of this study was on small caves and their use as hibernacula, modifying the criteria to include larger caves or those that contained observations outside of the hibernation period would have invalidated any results. Also, the small percentage of caves without bats is probably the result of sampling error. Some of the surveyed caves were not recorded if bats were not present, according to Ed Klausner (personal communication). An additional limitation would be the failure to include cave-like features or exceptionally small caves. Like other state cave surveys, Iowa utilizes a minimum cave length, in this

case 15 ft (about 4.5 m), and no bat surveys have been undertaken below this limit. The wide range in sampling dates (1998 to 2009) may also introduce temporal variation in distribution and abundance that could potentially bias these results. Due to these limitations, it may be inappropriate to infer that these results are broadly applicable. However, several significant relationships were present and merit discussion.

The results contradict previous surveys that found the big brown bat (Muir and Polder, 1960; Pruszko and Bowles, 1986; Clark et al. 1987) and little brown bat (Iowa Department of Natural Resources, unpublished data) to be the most abundant species in Iowa caves. This is likely due to the history of focusing on large caves within the state. Best et al. (1992) observed that the eastern pipistrelle was the most common species hibernating in small caves (< 65 m long) surveyed in southern Alabama. Prior to their study, the species was thought to be uncommon in that part of the state. The eastern pipistrelle is not considered uncommon in eastern Iowa (Laubach et al., 1994; Bowles et al., 1998), and these results are supported by Brack et al. (2004), who observed that eastern pipistrelles are usually the only species found in small caves.

Only a single cave harbored more than one species (little brown bats and the single big brown bat). Although caves are known to provide shelter for multiple species (Kunz, 1982), smaller caves and smaller hibernacula, in general, usually have less diverse bat populations (Arita, 1996; Fuszara et al., 1996; Brunet and Medellín, 2001; Lesiński et al., 2004; Nui et al., 2007). The results of this study fit that pattern. The observed segregation of little brown bats and eastern pipistrelles was unexpected, however, since both species are known to hibernate in the same larger caves within Iowa (Laubach et al., 1994). Little brown bats are usually more abundant in large, complex caves (Gates et al., 1984), so the few individuals encountered in these small caves was not surprising. However, there appears to be wide array of morphological features for the surveyed caves that were selected as hibernacula by little brown bats.

Indeed, the caves utilized by little brown bats fell within the range of characteristics of those utilized by eastern pipistrelles and, with the exception of cave length, there was not a significant difference between the caves selected by each species. Due to the small sample size for little brown bats, this segregation may simply be the result of chance. However, it could be the result of previously undocumented interspecific competition, since a smaller cave would be a more limited resource (i.e., less space available for roosting). Previous surveys in the state would not have observed this competition because they were conducted in larger caves. Future research efforts in small caves should include little brown bats to further clarify this behavior.

The low numbers of eastern pipistrelles matched previously documented behavior for this species. Eastern pipistrelles hibernate in small numbers as solitary individuals (Fujita and Kunz, 1984; Vincent and Whitaker, 2007), and their numbers in caves can vary considerably during hibernation (Brack et al., 2003). The lack of a relationship with cave entrance size matched expected behavior as well. As with this study, Briggler and Prather (2003) found no significant relationship with entrance size of caves used by eastern pipistrelles. Briggler and Prather (2003) also observed that longer caves supported greater numbers, as indicated in this study by both the Student's t-test and the Spearman rank correlation. This relationship with cave length is most certainly the result of the pipistrelles' preference for hibernating in thermally stable environments (Rabinowitz, 1981; Fujita and Kunz, 1984; Briggler and Prather, 2003; Brack, 2007; Vincent and Whitaker, 2007), since the longer the cave, the greater the thermal stability (Tuttle and Stevenson, 1978; Fernández-Cortéz et al., 2006). Future studies in small caves should incorporate climate monitoring.

Internal surface area was selected as one of the morphological features to be tested not only as an alternative means of measuring cave size, but also because it has also been positively correlated with bat-species richness (Brunet and Medellín, 2001). There was no evidence from this study to support this relationship in small caves. A positive correlation with eastern pipistrelles and internal surface area is supported by Raesley and Gates (1987), who found that larger caves supported greater numbers of hibernating bats in general. This would appear to be similar to cave length, since cave volume is also known to influence cave temperature (Tuttle and Stevenson, 1978). However, an extremely significant, strong correlation was noticed between cave length and internal surface area ($r_s = 0.877$, $P < 0.001$). That is, longer caves in this study had correspondingly larger internal surface areas. Therefore, these results can not say with any certainty if the preference exhibited by eastern pipistrelles was the result of cave length, internal surface area, or a combination of both interrelated spatial parameters.

The negative correlation between entrance aspect and eastern pipistrelle hibernacula would seem to indicate a preference for sinkhole entrance caves since approximately one-third of the caves in the sample (32%) were caves with the arbitrarily assigned −90 degree aspect. Greater numbers of eastern pipistrelles were found in caves with vertical entrances. Sinkhole-entrance caves had an average of 2.13 (± 2.23 SD) eastern pipistrelles per cave, while horizontal-entrance caves averaged 0.76 (± 0.66 SD) per cave. Briggler and Prather (2003) found larger caves with east-facing aspects were preferred by eastern pipistrelles over other morphologies. They noted however that the majority of the east-facing caves they examined were sinkhole-entrance caves on comparatively flat ground. In this study as well, sinkhole-entrance caves were typically longer and larger, having greater internal surface area.

The average length and internal surface area of horizontal entrance caves in this study was 15.6 m (± 8.8 m SD) and 82.3 m^2 (± 53.1 m^2 SD), respectively. The average length and internal surface area of vertical entrance caves was 25.2 m (± 9.3 m SD) and 216.5 m^2 (± 128.2 m^2 SD). Briggler and Prather (2003) hypothesized that the preference they observed for sinkhole entrance caves was due to the size of the caves and not the result of entrance aspect. However, considering the previously mentioned preference for thermally stable hibernacula, this may be evidence of a preferred morphological feature when selecting a hibernaculum, since vertical entrance caves are more thermally stable than those with horizontal entrances (Daan and Wichers, 1968; Tuttle and Stevenson, 1978). This behavior has been observed in other species as well, such as the Ozark big-eared bat, which also has a preference for hibernating in caves with sinkhole entrances (Clark et al., 1996; Prather and Briggler, 2002). Like cave length and internal surface area, these results are still uncertain due to the association between entrance aspect and cave size. Based on these data, there is no way to determine if this correlation is a result of entrance aspect alone.

Despite the previously listed limitations, the results of this study and the cited works of others demonstrate that eastern pipistrelles select larger caves as hibernacula. This is supported not only by the positive Spearman rank correlations, but also by the Student's t-test that found a significant difference for caves selected by eastern pipistrelles based on cave length. This preference is most likely due to more stable temperatures present in larger caves. However, it is apparent from these data that ''large'' is an extremely subjective term since the largest caves in this study were only around 34 m in length with approximately 300 m^2 of internal surface area. Based on these results, I can only conclude that even though they were small, the caves in this sample were still of sufficient size to exhibit sufficient stability of temperature that eastern pipistrelles tolerate. Although the sample size was modest and the sampling dates spread out over a twelve-year period, these results should not be discounted. Trombulak et al. (2001) used similar irregular census data spanning several decades from only twenty-three hibernacula caves to document population trends in Vermont.

This study also demonstrates that local grottos of the National Speleological Society can be a valuable source of data and play a key role in monitoring and studying local bat populations. Knowledge of hibernacula roosting habits is an indispensable tool in understanding the biogenic and anthropogenic impacts on populations (O'Shea et al., 2003; Tuttle, 2003). Accurate conservation decisions can only be made with a full understanding of hibernacula requirements (Brack, 2007), and given the threat that many species face today (e.g., white-nose syndrome, destruction of habitat, etc.), this knowledge is perhaps more important now than ever. More detailed and organized survey efforts by the Iowa Grotto, and other grottos around the country, is both encouraged and recommended.

Conclusions

Gates et al. (1984) stated that eastern pipistrelles were generalists when it came to cave selection. This is supported by Harvey (1992) and Brack et al. (2003), who noted that in the eastern United States they are known to utilize more caves as hibernacula than any other species. However, eastern pipistrelles have also been known to express a pronounced fidelity to particular hibernacula (Fujita and Kunz, 1984). In their study of underground cellars in Poland, Lesiński et al. (2004) stated that small, well-distributed hibernacula are most likely to be used by local bat communities, as this would increase their chance of survival as opposed to a long migration to a larger hibernacula site. Since hibernacula for eastern pipistrelles are presumed to be within 100 km of summer roosting sites (Vincent and Whitaker, 2007) and comparatively permanent roosts such as caves are able to support stable bat populations and annual use patterns (Agosta et al., 2005), it is apparent that small caves are an important source of hibernacula for the eastern pipistrelle.

Further research on the role of small caves as hibernacula is needed. First, the preferred morphology of sinkhole entrances by eastern pipistrelles evident in this study and noted by Briggler and Prather (2003) needs to be validated or refuted. At the present time, there is no way of discerning whether this is an actual preferred feature or whether this was merely a coincidental occurrence with larger caves. Second, additional data are needed in order to determine whether the presence of some species hibernating in small caves, such as the little brown bats observed in this study, are anomalies or whether these species also utilize small caves on a regular basis. Specific knowledge of hibernacula is necessary to adequately meet conservation needs (O'Shea et al., 2003; Tuttle, 2003; Brack, 2007), even for common species that are considered abundant (Agosta, 2002). A more complete understanding of roosting habitats is essential since the destruction of more significant hibernacula may result in less important sites (such as small caves) emerging as major hibernacula (Gates at al., 1984).

Acknowledgments

I would like to thank Ed Klausner and Mike Lace for reviewing this manuscript. I would also like to thank the following fellow members of the Iowa Grotto for their diligent work in recording bat observations in Iowa caves; without them this paper would not have been possible: Ed Klausner, Elizabeth Miller, Mike Lace, Chris Beck, Gary Engh, Jim Roberts, Rich Feltes, Phil LaRue, and Ray Finn.

REFERENCES

Agosta, S.J., 2002, Habitat use, diet and roost selection by the big brown bat (*Eptesicus fuscus*) in North America: A case for conserving an abundant species: Mammal Review, v. 32, p. 79–198, doi:10.1046/j.1365-2907.2002.00103.x.

Agosta, S.J., Morton, D., Marsh, B.D., and Kuhn, K.M., 2005, Nightly, seasonal, and yearly patterns of bat activity at night roosts in the central Appalachians: Journal of Mammalogy, v. 86, p. 1210–1219, doi: 10.1644/05-MAMM-A-012R1.1.

Arita, H.T., 1996, The conservation of cave-roosting bats in Yucatan, Mexico: Biological Conservation, v. 76, p. 117–185.

Arita, H.T., and Vargas, J.A., 1995, Natural history, interspecific association, and incidence of the cave bats of Yucatan, Mexico: Southwestern Naturalist, v. 40, p. 29–37.

Best, T.L., Carey, S.D., Caesar, K.G., and Henry, T.H., 1992, Distribution and abundance of bats (Mammalia: Chiroptera) in coastal plain caves of southern Alabama: NSS Bulletin, v. 54, p. 61–65.

Blair, A.P., 1951, Winter activity in Oklahoma frogs: Copeia, v. 2, 178 p.

Bowles, J.B., Howell, D.L., Lampe, R.P., and Whidden, H.P., 1998, Mammals of Iowa: Holocene to the end of the 20th century: Journal of the Iowa Academy of Science, v. 105, p. 123–132.

Brack, V. Jr., Johnson, S.A., and Dunlap, R.K., 2003, Wintering populations of bats in Indiana, with emphasis on the endangered Indiana myotis, *Myotis sodalis*: Proceedings of the Indiana Academy of Science, v. 112, p. 61–74, (www.indianaacademyofscience.org/media/attachments/IAS_v112_n1_p61-74.pdf).

Brack, V. Jr., 2007, Temperatures and locations used by hibernating bats, including *Myotis sodalis* (Indiana bat), in a limestone mine: Implications for conservation and management: Environmental Management, v. 40, p. 739–746, doi: 10.1007/s00267-006-0274-y.

Brack, V. Jr., Whitaker, J.O. Jr., and Pruitt, S.E., 2004, Bats of Hoosier National Forest: Proceedings of the Indiana Academy of Science, v. 113, p. 76–86, (www.indianaacademyofscience.org/media/attachments/PIAS_v113_n1_p76-86.pdf).

Briggler, J.T., and Prather, J.W., 2003, Seasonal use and selection of caves by the eastern pipistrelle bat (*Pipistrellus subflavus*): American Midland Naturalist, v. 149, p. 406–412, doi: 10.1674/0003-0031(2003)149[0406:SUASOC]2.0.CO;2.

Briggler, J.T., and Prather, J.W., 2006, Seasonal use and selection of caves by plethodontid salamanders in a karst area of Arkansas: American Midland Naturalist, v. 155, p. 136–148, doi: 10.1674/0003-0031(2006)155[0136:SUASOC]2.0.CO;2.

Brunet, A.K., and Medellín, R.A., 2001, The species-area relationship in bat assemblages of tropical caves: Journal of Mammalogy, v. 82, p. 1114–1122, doi: 10.1644/1545-1542(2001)082<1114:TSARIB>2.0.CO;2.

Camp, C.D., and Jensen, J.B., 2007, Use of twilight zones of caves by plethodontid salamanders: Copeia, v. 3, p. 594–604, doi: 10.1643/0045-8511(2007)2007[594:UOTZOC]2.0.CO;2.

Clark, B.S., Bowles, J.B., and Clark, B.K., 1987, Summer occurrences of the Indiana bat, Keen's myotis, evening bat, silver-haired bat, and eastern pipistrelle in Iowa: Proceedings of the Iowa Academy of Science, v. 94, p. 89–93.

Clark, B.K., Clark, B.S., Leslie, D.M. Jr., and Gregory, M.S., 1996, Characteristics of caves used by the endangered Ozark big-eared bat: Wildlife Society Bulletin, v. 24, p. 8–14.

Curl, R.L., 1966, Caves as a measure of karst: Journal of Geology, v. 74, p. 798–830.

Daan, S., and Wichers, H.J., 1968, Habitat selection of bats hibernating in a limestone cave: Zeitschrift fur Saugetierkunde, v. 33, p. 262–287.

Dasher, G.R., 1994, On Station: A Complete Handbook for Surveying and Mapping Caves: Huntsville, Alabama, National Speleological Society, 242 p.

Dixon, J.W., 2009, Cave size in Iowa: How long is the average Iowa cave?: Intercom, published semi-spasmodically by the Iowa Grotto of the National Speleological Society, v. 45, p. 17–22.

Drda, W.J., 1968, A study of snakes wintering in a small cave: Journal of Herpetology, v. 1, p. 64–70.

Fernández-Cortéz, A., Calaforra, J.M., Jiménez-Espinosa, R., and Sánchez-Martos, F., 2006, Geostatistical spatiotemporal analysis of air temperature as an aid to delineating thermal stability zones in a potential show cave: Implications for environmental management: Journal of Environmental Management, v. 81, p. 371–383, doi: 10.1016/j.jenvman.2005.11.011.

Fujita, M.S., and Kunz, T.H., 1984, *Pipistrellus subflavus*: Mammalian Species, v. 228, p. 1–6.

Fuszara, E., Kowalski, M., Lesiński, G., and Cygan, J.P., 1996, Hibernation of bats in underground shelters of central and northeastern Poland: Bonner zoologische Beitrage, v. 46, p. 349–358.

Gates, J.E., Feldhamer, G.A., Griffith, L.A., and Raesly, R.L., 1984, Status of cave-dwelling bats in Maryland: Importance of marginal habitats: Wildlife Society Bulletin, v. 12, p. 162–169.

Harvey, M.J., 1992, Bats of the Eastern United States: Little Rock, Arkansas, Arkansas Game and Fish Commission, 46 p.

Kambesis, P., and Lace, M., 2009, Iowa, *in* Palmer, A.N., and Palmer, M.V., eds., Caves and Karst of the USA: Huntsville, Alabama, National Speleological Society, p. 151–154.

Kastning, E.H., 2006, Very small eclectic caves: conservation and management issues, *in* Rea, G.T., ed., Proceedings of the 17th National Cave and Karst Management Symposium: Albany, New York, NCKMS Steering Committee, p. 92–101.

Kunz, T.H., 1982, Roosting ecology of bats, *in* Kunz, T.H., ed., Ecology of Bats: New York, New York, Plenum Press, p. 1–55.

Kunz, T.H., and Schlitter, D.A., 1968, An annotated checklist of bats from Iowa: Transactions of the Kansas Academy of Science, v. 71, p. 166–175, (www.bu.edu/cecb/files/2009/08/iowachecklist.pdf).

Lace, M.J., ed., 1997, The Iowa Cave Map Book, Volume II: Iowa City, Iowa, Iowa Grotto of the National Speleological Society, 210 p.

Lace, M.J., and Klausner, E., eds., 2001, The Iowa Cave Map Book, Volume III: Iowa City, Iowa, Iowa Grotto of the National Speleological Society, 223 p.

Lace, M.J., and Klausner, E., eds., 2004, The Iowa Cave Map Book, Volume IV: Iowa City, Iowa, Iowa Grotto of the National Speleological Society, 183 p.

Lace, M.J., and Ohms, M., eds., 1992, The Iowa Cave Map Book, Volume I: Iowa City, Iowa, Iowa Grotto of the National Speleological Society, 151 p.

Laubach, C.M., Bowles, J.B., and Laubach, R., 1994, A Guide to the Bats of Iowa: Des Moines, Iowa, Iowa Department of Natural Resources, Nongame Technical Series No. 2, 18 p.

Lesiński, G., Kowalski, M., Domański, J., Dzięciołowski, R., Laskowska-Dzięciołowska, K., and Dzięgielewska, M., 2004, The importance of small cellars to bat hibernation in Poland: Mammalia, v. 68, p. 345–352.

Muir, T.J., and Polder, E., 1960, Notes on hibernating bats in Dubuque County caves: Proceedings of the Iowa Academy of Science, v. 67, p. 602–606.

Mylroie, J., 2007, Cave surveys, cave size, and flank margin caves: Compass & Tape, v. 17, no. 4, p. 8–16, (www.caves.org/section/sacs/rr/cavelenth.pdf).

Nui, H., Wang, N., Zhao, L., and Lui, J., 2007, Distribution and underground habitats of cave-dwelling bats in China: Animal Conservation, v. 10, p. 470–477, doi: 10.1111/j.1469-1795.2007.00136.x.

O'Shea, T.J., Bogan, M.A., and Ellison, L.E., 2003, Monitoring trends in bat populations of the United States and territories: Status of the science and recommendations for the future: Wildlife Society Bulletin, v. 31, p. 16–29, (www.fort.usgs.gov/Products/Publications/21045/21045.pdf).

Pierson, E.D., 1998, Tall trees, deep holes, and scarred landscapes: Conservation biology of North American bats, *in* Kunz, T.H., and Racey, P.A., eds., Bat Biology and Conservation: Washington, D.C., Smithsonian Institution Press, p. 309–325.

Prather, J.W., and Briggler, J.T., 2001, Use of small caves by anurans during a drought period in the Arkansas Ozarks: Journal of Herpetology, v. 35, p. 675–678.

Prather, J.W., and Briggler, J.T., 2002, Use of small caves by Ozark big-eared bats (*Corynorhinus townsendii ingens*) in Arkansas: American Midland Naturalist, v. 148, p. 193–197, doi: 10.1674/0003-0031(2002)148[0193:UOSCBO]2.0.CO;2.

Pruszko, R., and Bowles, J.B., 1986, Survey of some eastern Iowa caves for wintering bats: Proceedings of the Iowa Academy of Science, v. 93, p. 41–43, (137.227.227.130/BPD/BPD_bib_viewObs.asp?BibID=1300).

Rabinowitz, A., 1981, Thermal preference of the eastern pipistrelle bat (*Pipistrellus subflavus*) during hibernation: Journal of the Tennessee Academy of Science, v. 56, p. 113–114.

Raesly, R.L., and Gates, J.E., 1987, Winter habitat selection by north temperate cave bats: American Midland Naturalist, v. 118, p. 15–31.

Rodríguez-Durán, A., 1998, Nonrandom aggregations and distributions of cave-dwelling bats in Puerto Rico: Journal of Mammalogy, v. 79, p. 141–146.

Schwartz, C.W., and Schwartz, E.R., 2001, The Wild Mammals of Missouri: Columbia, Missouri, University of Missouri Press, 392 p.

Thomas, D.W., and LaVal, R.K., 1988, Survey and Census Methods, *in* Kunz, T.H., ed., Ecological and Behavioral Methods for the Study of Bats: Washington, D.C., Smithsonian Institution Press, p. 77–89.

Trombulak, S.C., Higuera, P.E., and DesMeules, M., 2001, Population trends of wintering bats in Vermont: Northeastern Naturalist, v. 8, p. 51–62, doi: 10.1656/1092-6194(2001)008[0051:PTOWBI]2.0.CO;2.

Tuttle, M.D., 2003, Estimating population sizes of hibernating bats in caves and mines, *in* O'Shea, T.J., and Bogan, M.A., eds., Monitoring Trends in Bat Populations of the United States and Territories: Problems and Prospects: U.S. Geological Survey, Biological Resources Discipline, Information and Technology Report USGS/BRD/ITR-2003-0003. p. 31–39.

Tuttle, M.D., and Stevenson, D.E., 1978, Variation in the cave environment and its biological implications, *in* Zuber, R., Chester, J., Gilbert, S., and Rhodes, D., eds., Proceedings of the 1977 National Cave Management Symposium: Albuquerque, New Mexico, Adobe Press, p. 108–121.

Vincent, E.A., and Whitaker, J.O. Jr., 2007, Hibernation of the eastern pipistrelle, *Perimyotis subflavus*, in an abandoned mine in Vermillion County, Indiana, with some information on *Myotis lucifugus*: Proceedings of the Indiana Academy of Science, v. 116, p. 58–65, (www.indianaacademyofscience.org/media/attachments/Proc_v116_1_2007_pp58-65.pdf).

Whitaker, J.O. Jr., and Rissler, L.J., 1992, Seasonal activity of bats at Copperhead Cave: Proceedings the Indiana Academy of Science, v. 101, p. 127–134.

R. Djanashvili and S. Barjadze – A new species of the genus *Plutomurus* Yosii, 1956 (Collembola, Tomoceridae) from Georgian caves. *Journal of Cave and Karst Studies,* v. 73, no. 1, p. 28–30. DOI: 10.4311/jcks2010lsc0147

A NEW SPECIES OF THE GENUS *PLUTOMURUS* YOSII, 1956 (COLLEMBOLA, TOMOCERIDAE) FROM GEORGIAN CAVES

Revaz Djanashvili and Shalva Barjadze
Entomology and Biocontrol Research Centre, Ilia State University, Chavchavadze av. 31, 0179, Tbilisi, Georgia, shalva1980@yahoo.com

Abstract: A new species, *Plutomurus birsteini* sp. n., from Georgian caves is described and illustrated. It is similar to *Plutomurus baschkiricus* (Skorikow, 1899). Differences between the species are discussed. A key to the genus *Plutomurus* species found in the Caucasus is provided.

Introduction

The genus *Plutomurus* Yosii, 1956 is represented by twenty-three species worldwide (Kniss and Thibaud, 1999; Bellinger et al., 1996–2010). The species belonging to this genus are distributed in North America, Europe, and Asia and live in caves or soils (Yosii, 1956, 1966, 1967, 1991; Chrisitiansen, 1964, 1980; Gruia, 1965; Martynova, 1969, 1977; Rusek and Weiner, 1977; Kniss and Thibaud, 1999).

Before now, four species, *Plutomurus abchasicus* Martynova, 1969 (Georgia, in soils), *P. jeleznovodski* Kniss and Thibaud, 1999 (north Caucasus, in cave), *P. kelasuricus* Martynova, 1969 (north and south Caucasus, in caves) and *P. sorosi* Kniss and Thibaud, 1999 (north Caucasus, in cave) have been recorded in the Caucasus (Martynova, 1969; Kniss and Thibaud, 1999; Barjadze and Djanashvili, 2008).

Re-examination of the springtails collected by Dr. R. Djanashvili in Georgian caves during 1966–1970 led us to describe here a new species.

Diagnosis of the Genus *Plutomurus* Yossi, 1956

Eyes from 6 + 6 to 0 + 0. Prelabial setae from 2 + 2 to 4 + 4. This genus is easily distinguished by the presence of large spine-like setae at the external bases of the dens combined with a well developed multisetaceous trochateral organs on the trochanter and on the base of the femur. There are four or fewer intermediate teeth on the mucro, and there is only a single small mucronal lamella, usually on the basal tooth. Most have some pigment, but eyes are often reduced. Sexual dimorphism absent. The genus is Holarctic but does not occur in arctic regions. It often is found in alpine areas. Within the Holarctic region, they are limited to eastern Asia, western Europe, the Caucasian region, and western North America. Although 60% are found in caves and many of these have not been found elsewhere, they show very little troglomorphy.

Material Examined

Holotype ♂ from Sakishore Cave, 06.VII.1969, leg. R. Djanashvili and 21 paratypes are on the slides. Specimens from the same locality are mounted on the same slide. Paratypes: three specimens, Chuneshi Cave, 21.IX.1968, leg. R. Djanashvili; one specimen, Sataplia IV Cave, 10.X.1966, leg. R. Djanashvili; one specimen, Tvishi Cave, 12.IX.1968, leg. R. Djanashvili; one specimen, Magara Cave, 18.VIII.1967, leg. R. Djanashvili; three specimens, Tsakhi Cave, 31.VIII.1966, leg. R. Djanashvili; one specimen, Sharaula II Cave, 20.VII.1970, leg. R. Djanashvili; four specimens, Nikortsminda Cave, 03.VII.1969, leg. R. Djanashvili; one specimen, Sakishore Cave, 06.VII.1969, leg. R. Djanashvili; two specimens, Bnelaklde Cave, 18.IX.1967, leg. R. Djanashvili; one specimen, Taroklde Cave, 15.IX.1967, leg. R. Djanashvili; three specimens, Khvedelidze Cave, 29.VI.1969., leg. R. Djanashvili. Holotype and paratypes are deposited in the Entomology and Biocontrol Research Centre of Ilia State University, Tbilisi, Georgia.

Description of *Plutomurus birsteini* Djanashvili and Barjadze sp. n.

Body length 1.0 to 3.3 mm. Body light yellowish-gray; anterior part of head and III and IV antennal segments a little darker. Antenna c. 1.5 times shorter than body. Eye patch small, black with 6 eyes (Fig. 1 A). Prelabial setae 2+2, labrum with 5, 5, 4 setae and 4 curved setae on the distal part of labrum. Trochanteral organ well developed on trochanter and femur, composed of large number of short setae (more than 40) and several long setae. All parts of ventral tube with many setae. Spine-like setae on tibiotarsus I, II, and III: 0, 0, 1. Tenent hairs weakly to moderately clavate. Ratio of unguis, unguiculus, and tenent hair in holotype 16:9:11. Unguis with well developed pseudonychia, 0.38 to 0.56 times as long as inner part of unguis. Unguis of prolegs with 2 to 4 inner teeth. Unguis of meso and metalegs with 2 to 3 inner teeth (Fig. 1 B). Unguiculus of all legs always without inner teeth. Tenaculum with 4+4 teeth and 1 heavy seta on corpus (Fig. 1 C). Ratio of manubrium/dens/mucro in holotype 6.3:9.8:1. Ventral side of manubrium with numerous relatively thick and large setae. Outer margins of dens with 4 thick and large spine-like setae. Mucro with 2 basal

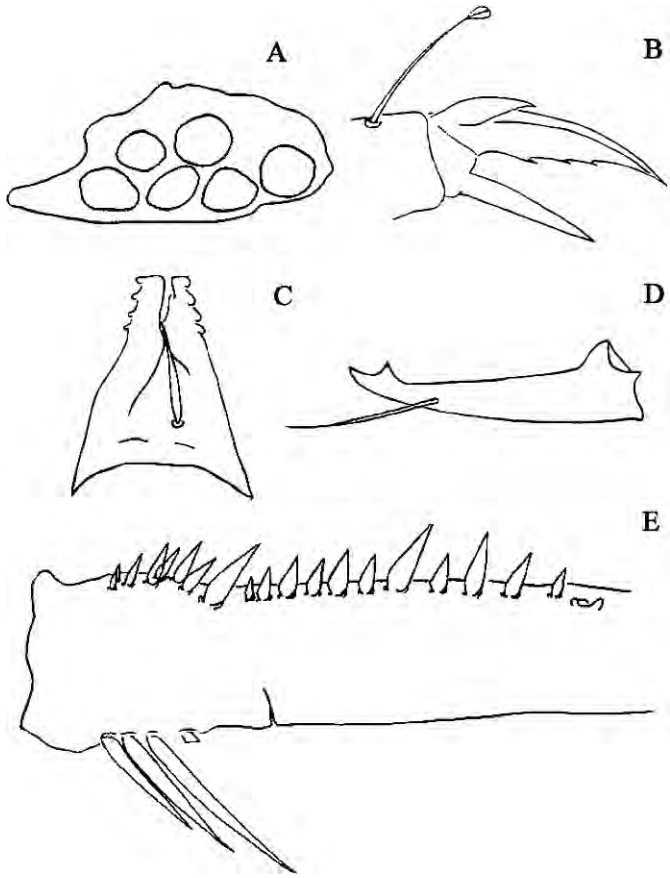

Figure 1. *Plutomurus birsteini* sp. n.: (A) eye patch; (B) claw III; (C) tenaculum; (D) mucro; (E) dens.

denticles, without subapical denticles and 1 seta projecting prominently beyond apex (Fig. 1 D). Dental formula variable: 5-15 *1-2* / 2-9 *1* 0-3 *0-1* 0-3 *0-1* 0-3 *0-1* 0-2 *0-1* 0-2 *0-1* (Fig. 1 E).

Etymology

The specific name is chosen in honor of the Russian biospeleologist Dr. J.A. Birstein, who was a supervisor of the first author.

Discussion

The lack of troglomorphic modifications makes it likely that this is a troglophile species and will be found outside of caves. This species is a very similar to *Plutomurus baschkiricus*, which differs from *P. birsteini* by: **1.** Larger number of setae on the trochanteral organ (more than 40 short setae) and several long setae in *P. birsteini*, while there are 18 to 40 short setae and 2 to 4 large ones in *P. baschkiricus*; **2.** Spine-like setae on tibiotarsus I, II, and III are 0, 0, 1 in *P. birsteini*, while 0, 0, 2 in *P. baschkiricus*; **3.** Unguiculus of all legs always without minute inner teeth in *P. birsteini*, while 2 to 3 inner teeth are on each unguiculus of *P. baschkiricus*; **4.** Dental formula: 5-15 *1-2* / 2-9 *1* 0-3 *0-1* 0-3 *0-1* 0-3 *0-1* 0-2 *0-1* 0-2 *0-1* in *P. birsteini*, while 6-8 *1* / 9-13 *1* in *P. baschkiricus*. A key to the genus *Plutomurus* Yosii, 1956 species distributed in the Caucasus is provided in Table 1.

Acknowledgements

We would like to thank to Dr. Kenneth A. Christiansen, Grinnell College, USA, for the valuable comments on the species description.

Table 1. A key to the genus *Plutomurus* Yosii, 1956 species distributed in the Caucasus.

1.	Tenent hairs weakly to moderately clavate	2
	Tenent hairs acuminate	4
2.	Eye patch always with 6 eyes. Mucro without subapical small denticles	3
	Eye patch with 4 or 5 eyes. Mucro with 3 subapical denticles	*P. sorosi* Kniss and Thibaud, 1999
3.	Trochanteral organ with more than 40 setae. Unguiculus of all legs always without minute inner teeth. Dental formula: 5-15 1-2 / 2-9 1 0-3 0-1 0-3 0-1 0-3 0-1 0-2 0-1 0-2 0-1	*P. birsteini* sp.n.
	Trochanteral organ with less than 40 setae. Unguiculus of all legs always with a few minute inner teeth. Dental formula: 4-5 1 / 6 1 3 1	*P. jeleznovozski* Kniss and Thibaud, 1999
4.	Spine-like setae on tibiotarsus I, II, and III 0, 0, 1. Prelabial setae 3+3	*P. kelasuricus* Martynova, 1969
	Spine-like setae on tibiotarsus I, II, and III 0, 0, 2. Prelabial setae 2+2	*P. abchasicus* Martynova, 1969

REFERENCES

Barjadze, Sh., and Djanashvili, R., 2008, Checklist of the springtails (Colembola) of Georgia: Caucasian Entomological Bulletin, v. 4, no. 2, p. 187–193.

Bellinger, P.F., Christiansen, K.A., and Janssens, F., 1996–2010, Checklist of the Collembola of the World. http://collembola.org [accessed April 27, 2010]

Christiansen, K., 1964, A revision of the nearctic members of the genus *Tomocerus*: Revue d'Écologie et de Biologie du Sol, v. 1, p. 639–678.

Christiansen, K., 1980, A new nearctic species of the genus *Tomocerus* (Collembola: Entomobryidae): Proceedings of the Iowa Academy of Sciences, v. 87, p. 121–123.

Gruia, M., 1965, Contributii la studiul collembolelor din România: Lucrarile Institutului de Speologie "Emil Rakovita", v. 4, p. 191–202.

Kniss, V., and Thibaud, J., 1999, Le genre Plutomurus en Russie et en Georgie (Collembola, Tomoceridae): Revue française d' Entomologie (N.S.), v. 21, no. 2, 57_64 p.

Martynova, E., 1969, Springtails of the family Tomoceridae (Collembola) from the fauna of the USSR: Entomological Review, v. 43, p. 299–314 (in Russian).

Martynova, E., 1977, Springtails of the family Tomoceridae (Collembola) from the fauna of the Far East: Insect Fauna of the Far East, v. 46, no. 149, p. 3–16 (in Russian).

Rusek, J., and Weiner, W.M., 1977, *Plutomurus carpaticus* sp. n. (Collembola: Tomoceridae) from the Carpathian Mountains: Bulletin de l'Académie Polonaise des Sciences, v. 25, p. 741–747.

Yosii, R., 1956, Monographie zur Höhlencollembolen Japans: Contribution from the Biological Laboratory Kyoto University 3, 109 p.

Yosii, R., 1966, Results of the speleological survey of South Korea 1966, IV cave Collembola: Bulletin of the National Science Museum Tokyo, v. 9, p. 541–561.

Yosii, R., 1967, Studies on the collembolan family Tomoceridae with special reference to Japanese forms: Contribution from the Biological Laboratory Kyoto University 20, 54 p.

Yosii, R., 1991, A new species of Tomocerid Collembola from the cave of the Pref. Iwata: Annals of the Speleological Research Institute of Japan, v. 9, p. 1–2.

R.Ø. Skoglund and S.-E. Lauritzen – Subglacial maze origin in low-dip marble stripe karst: examples from Norway. *Journal of Cave and Karst Studies,* v. 73, no. 1, p. 31–43. DOI: 10.4311/jcks2009ES0108

SUBGLACIAL MAZE ORIGIN IN LOW-DIP MARBLE STRIPE KARST: EXAMPLES FROM NORWAY

Rannveig Øvrevik Skoglund[1] and Stein-Erik Lauritzen[1,2]

Abstract: Maze caves or network caves are enigmatic in their evolution, as they form flow nets rather than more efficient, direct point-to-point flow routes. Network caves are often characterized by uniform passage dimensions in several directions, which indicates simultaneous dissolution of most available fractures. Nonshauggrotta in Gildeskål, northern Norway, is formed in low-dip marble strata and situated as a relict in a topographical and hydrological hanging position, thus lacking a modern drainage area. The cave displays a reticulate network geometry dictated by two orthogonal fracture sets. Passage morphology and paleocurrent marks in the cave walls (scallops) demonstrate that the cave evolved under water-filled conditions (phreatic) and that the relatively slow flow was directed uphill towards the confining aquiclude and the cliff face. In that sense, it has some resemblance to hypogene caves. However, we propose that the cave is a result of ice-contact speleogenesis, as it developed in the lee side of the Nonshaugen ridge under topographically directed glacier flow and seems independent of the otherwise variable flow regimes characteristic of the glacial environment.

Introduction

Karst caves in limestone are formed by dissolution when water aggressive with respect to calcium carbonate flows through integrated openings in the rock. This fundamental process results in a wide variety of cave geometries, controlled by the original porosity in the rock and hydraulic boundary conditions (Palmer, 1991). Maze caves are more enigmatic in their origin than meteoric or ''common'' caves (Ford and Williams, 2007), because maze caves consist of flow nets, in contrast to efficient point-to-point flow routes, as in linear and branchwork caves. Mazes evolve by simultaneous dissolution of all available fractures at similar rates, so conduits in these caves tend to be of equal dimensions. In accordance with this observation, two alternative mechanisms of maze origin are proposed (White, 1969; Palmer, 1975, 1991; Ford and Williams, 2007). Mazes can originate through diffuse, slow inter-formational recharge (transverse speleogenesis) (Klimchouk, 2009) or by recharge through repeated flooding in a variable fluvial regime. Diffuse recharge supplies all available fractures with solutionally aggressive water from an overlying or underlying unit, generally a sandstone, so that all fractures are dissolved and enlarged simultaneously and at similar rates. A similar effect occurs if there are short flow paths from where water enters the rock, causing all fractures except for the tightest to enlarge simultaneously at similar rates, as in epikarst (Palmer, 2002).

Flooding causes temporal variation in discharge and steepening of the hydraulic gradient, forcing aggressive water into available fractures, which accordingly dissolve at similar rates (Palmer, 2001). High discharge and high hydraulic gradient may occur in hydraulic regimes with great variability, as in the epiphreatic or flood-water zone of river caves. A particularly efficient situation occurs when a trunk passage is choked due to collapse. Here, the damming effect of the constriction increases the hydraulic head and amplifies the effect of floods, which will force water into all available fractures (Palmer, 2002).

Maze caves are loci of extreme karst porosity that, like large chambers, are possible precursors to breccia zones in paleokarst (see for instance mechanisms suggested by Loucks, 1999). Areas of moderate to high karst porosity are of major importance for the capacity and yield of groundwater aquifers, for mineralization, and for petroleum migration in carbonate reservoirs. This is part of the motivation for understanding the speleogenetic mechanisms for maze caves.

Maze Caves in Stripe Karst

Maze caves are quite common in the stripe karst of central Scandinavia. Stripe karst occurs in thin layers of marble interbedded with layers of impermeable bedrock, mainly mica schist (Horn, 1937; Lauritzen, 2001). Stripe karst often has great lateral extent and intersects the land surface at an angle. The insoluble aquicludes provide both geometric and hydrologic constraint to cave development. Accordingly, the caves in stripe karst are essentially two-dimensional. Metamorphic alteration has removed all original porosity in the rock, so that all pre-karst water circulation, and thus speleogenetic inception, is restricted to fractures, faults, and lithological contacts developed

[1] Department of Earth Science, University of Bergen, Allégaten 41, N-5007 Bergen, Norway. rannveig.ovrevik@geo.uib.no
[2] Department of Plant and Environmental Sciences, The Norwegian University of Life Sciences, 1532 Ås, Norway. Stein.Lauritzen@geo.uib.no

under post-metamorphic, brittle regimes. This gives predictable boundary conditions and makes caves in stripe karst favorable for analysis and modeling.

During the Quaternary, repeated glaciations of variable duration and extension (e.g., Sejrup et al., 2000) shaped the landscape of western Scandinavia, and thus, the stripe karst. The karst hydrological regime has varied according to the climatic conditions between the extremes of fluvial, during interglacials similar to the present, and subglacial, during glaciations with thick continental ice-sheets.

The orientations and dips of fractures and lithological contacts and the connectivity between fractures and interfaces are the most important passive factors for speleogenesis in a given rock mass. Their intersections with the surface define input and output boundaries for the karst. Water recharge and water chemistry are active factors. Lauritzen (2001, p. 75) examined how passive factors constrain cave patterns in stripe karst and found that "the various morphotypes show systematic dependence on stratal dip of the allogenic stripe contacts, of the type of contacts, and to a lesser extent, the fracture patterns," where type of contact means aquifer type (i.e., confined, unconfined, or perched). However, there is considerable overlap between the occurrence of maze caves and other cave patterns with respect to these parameters. In other words, a stripe karst setting does not give a complete explanation of maze evolution. Of the presently accepted mechanisms of maze origin, diffuse recharge seems quite improbable in the metamorphic stripe karst, with its impermeable wall rocks. Since many such mazes are situated in hanging positions in glacial valleys or at summits, isolated from any present-day fluvial drainage, the flood-water model is also not a satisfactory explanation of maze morphology in glacial stripe karst. Our hypothesis is that, in this geological setting, aspects of the subglacial or ice-contact regime may have been responsible for maze-cave evolution.

Paleocurrents in and speleogenesis of a tiered maze cave in strata dipping steeply more than 60° (Lauritzen, 2001), Pikhåggrottene in Rana, northern Norway, were previously described and analyzed by Lauritzen (1982). In the present work, we have examined a group of maze caves in stripe karst with lower dips of less than 30° (Lauritzen, 2001), Nonshauggrotta and adjacent caves in Gildeskål, Nordland. The caves are relict and have a hanging topographic position, displaying a quite uniform passage geometry and morphology. This in turn suggests that the cave passages may have a correspondingly uniform history. Through detailed study of cave's geometry, passage morphology, flow function, and structural template, we aim at a closer understanding of both passive and, more important, the active factors of subglacial maze origin. These issues are further explored by survey and examination of Lønngangen, a small cave a few kilometers away, and two other small caves in Nonshaugen ridge.

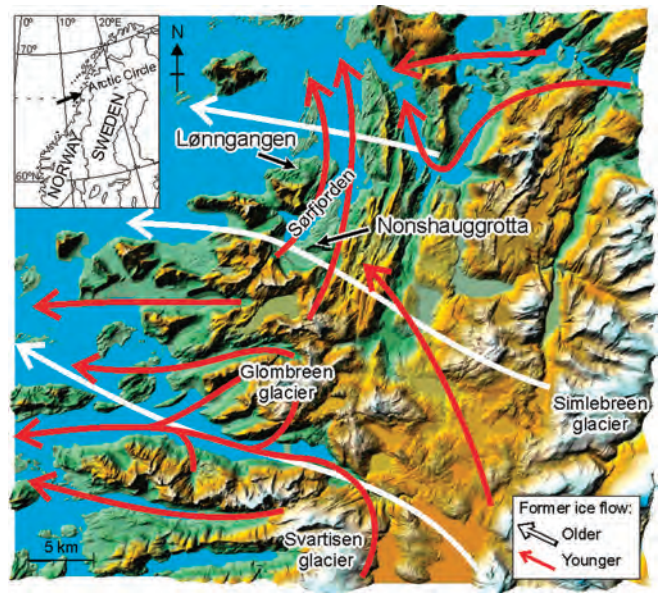

Figure 1. The area north of Svartisen glacier with location of Nonshauggrotta and Lønngangen. White arrows show the direction of ice flow during maximum glaciation. Red arrows show the direction of glacier movement during the last deglaciation. Glacier flows from Rasmussen (1981).

BACKGROUND

GEOMORPHOLOGICAL AND GEOLOGICAL SETTING

Nonshauggrotta (66°57′N 13°58′E) is located near the coast northwest of Svartisen glacier, northern Norway (Fig. 1). The area is characterized by glacially incised fjords and valleys, surrounded by mountains with alpine peaks reaching elevations of 800 to 1100 m. Nonshauggrotta is situated on the northern side of Nonshaugen, a small, 300 m ridge at the end of Sørfjorden fjord. Nonshaugen has the shape of a glacial whaleback, with a steep lee side to the north and a more gently dipping stoss side to the south.

The cavernous carbonate essentially consists of calcite marble that was folded in several phases during the Caledonian orogeny (Gustavson, 1985; Stephens et al., 1985; Gustavson and Solli, 1989). The rocks of Nonshaugen contain a recumbent fold, the Nonshaugen fold, that is overturned to the north with a predominantly east-west trend (Wells and Bradshaw, 1970). During the last phase, the rock sequence was folded to form an open antiform trending north-south, the Sørfjorden fold (Wells and Bradshaw, 1970), so that the Nonshaugen fold plunges to the east and west from the top of the hill (Fig. 2). The marble-schist interface in Nonshauggrotta dips gently southward (082°/25°). Although inclined stripe karst of this type may be considered covered karst, the exposure in the Nonshaugen wall is nevertheless a stripe karst.

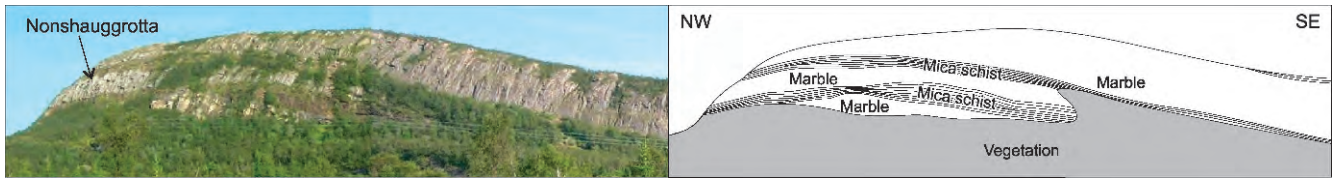

Figure 2. Low-dip stripe karst. Along the northern cliff face of Nonshaugen the low-dip marble-schist sequence crops out and makes the open Sørfjorden antiform visible.

Glacial History

In coastal areas, glaciation was not a continuous period of glacial cover, but rather a sequence of glacial advances of various durations and extents (e.g., Sejrup et al., 2000; Mangerud, 2004). According to Olsen (1997), the periods of ice growth and ice recession had durations of only a few thousand years during the period 15–40 ka BP. During maximum glaciation, ice flow in Gildeskål was westward (Rasmussen, 1981) (Fig. 1). The ice sheet was thick, so that flow was essentially independent of bed topography. During deglaciation, the ice thickness was reduced and ice flow was directed by the highest peaks and partly diverted into the main fjords and valleys. During the latest stages of glaciation, valley and fjord glaciers flowed from local ice masses at Svartisen and Glombreen (Rasmussen, 1981). Observations of glacial striations on the top and eastern side of Nonshaugen indicate an ice flow toward the northwest (302 to 316°), corresponding to a young, topographically directed ice flow. The rapid ice retreat after the maximum ice extent at about 18 ka BP probably occurred partly through ice shelf break up and massive iceberg formation after a rapid global sea-level rise starting at about 15 ka BP (Linge et al., 2007). Sørfjorden, and thus Nonshauggrotta, have been ice-free since Early Allerød time (13.7 ka BP) (Rasmussen, 1981).

Methods

Nonshauggrotta was first surveyed by Corbel (1957) and later by Holbye and Trones (unpublished plan map), and Lønngangen was surveyed by Eikeland (1986). However, our study required more complete and accurate three-dimensional cave maps with detailed geological information. Both caves were therefore resurveyed to BCRA grade 5C (Day, 2002), using passage-centerline polygons, where walls, ceiling, and floor are defined by their distance from each survey station. From survey data, 3-D models of the caves were obtained by using the Grottolf cave survey program (Lauritzen, 2004). During the survey process, the passage morphology was thoroughly examined, sketched, and photographed. The distribution and approximate grain size of surface sediments along the passage floor were also recorded. Guiding fractures (i.e., those fractures that had been widened into cave conduits by dissolutional enlargement) were logged, in addition to the marble-schist interface, foliations, and surface fractures. Some of the surface fracture were observed in the overlying mica-schist and in a stratigraphically higher marble layer.

Passage morphology reflects the hydrological conditions when they formed (e.g., Lauritzen and Lundberg, 2000). Under phreatic (water-filled) conditions, conduits form by corrosion in all directions outward from the passage center. This results in circular, elliptical, or lenticular passage cross-sections. Geological structures act as passive constraints on the passage shape. Under open-channel (vadose) conditions, corrosion and erosion only attack the floor, forming an incised canyon. A transition from phreatic to vadose conditions normally results in the keyhole shaped, two-stage cross-section.

Scallops are corrosional flow marks in the cave walls (Curl, 1974). They are imprints of the last active stage that lasted long enough for water to erase any previous scallop patterns. Scallop analyses were performed in accordance with the protocol described in Lauritzen (1982) and in Lauritzen and Lundberg (2000). From scallop symmetry and wavelength, paleocurrent direction was defined. Fluid velocity and, in turn, discharge can then be calculated from an estimate of water temperature (+1 °C) and passage dimensions. For statistical confidence, populations of at least 30 well-shaped scallops from the same area must be measured for discharge determination. However, flow direction can be deduced from a single well-developed scallop or a small group.

Variation in marble carbonate content was examined by loss-on-ignition (LOI) and acid-insoluble-residue tests of rock samples throughout the marble layer, and LOI was measured on two samples of mica schist from the confining beds. During the LOI tests at 800 °C, CO_2 is expelled from calcite ($CaCO_3$) and dolomite ($CaMg(CO_3)_2$) in the rock, forming the corresponding oxides. Theoretical weight loss in pure calcite is 44% and in pure dolomite 48%. Carbonates dissolve completely in 1 M hydrochloric acid, and the residual is a measure of insoluble impurities present in the marble.

Speleometric Characterization

The cave survey program Grottolf provides several geometrical parameters of the void that can be used for its characterization. Cave length is the total length including all surveyed passage segments. Cave depth is the vertical difference between the highest and lowest elevated passage.

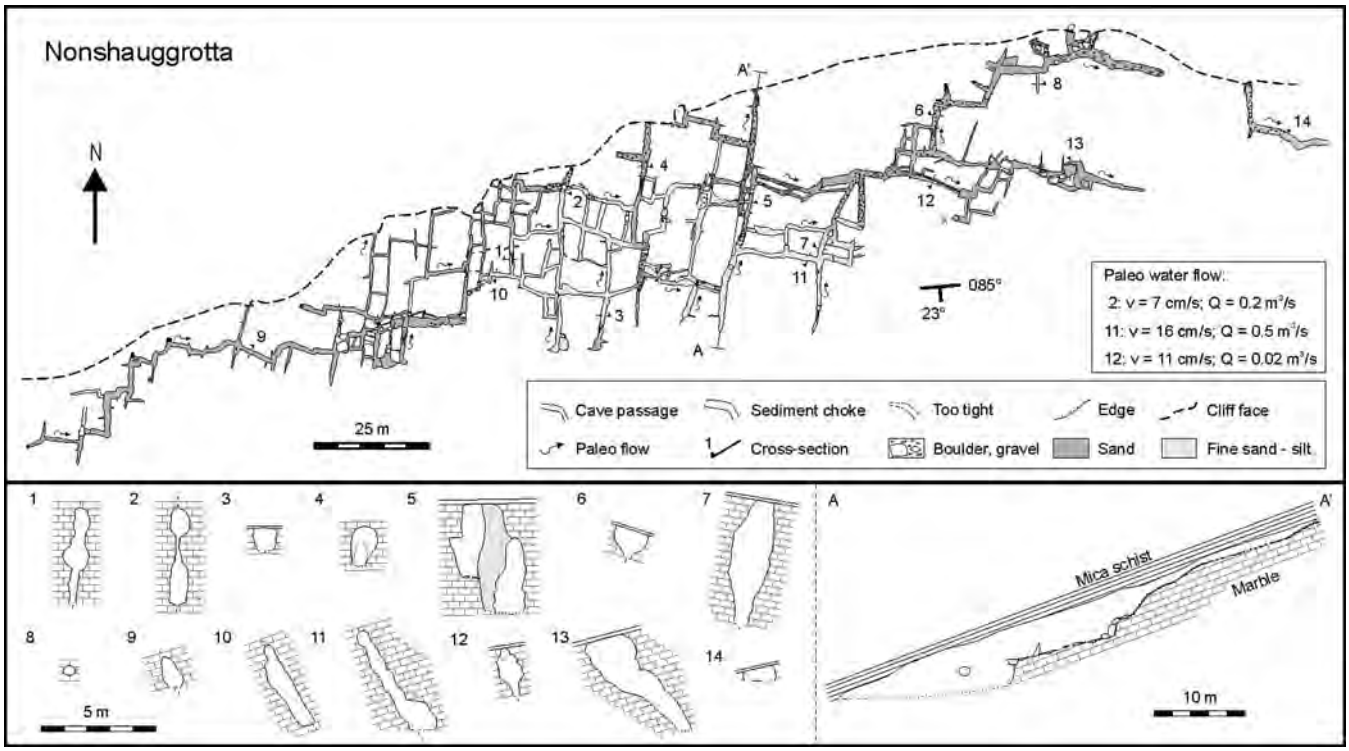

Figure 3. Plan map of Nonshauggrotta with passage cross-sections (5× exaggeration). A-A′: Longitudinal (vertical) profile of a N-S passage (2× exaggeration). ×: Circular shaft. Site of scallops analysis refers to cross-section number. v: calculated paleocurrent velocity. Q: calculated paleo discharge.

Cave area is the total horizontal plan area of the passage outline. Cave volume is the total volume of all cave passages based on elliptical cross-sections. The rock area that encloses the cave is estimated as its convex hull, a polygon of only convex angles enclosing all cave passages in plan view. The rock volume that holds all cave conduits is here calculated as the convex hull area multiplied by the maximum passage height. From these data the following speleometric parameters can be calculated. Mean passage cross-sectional area (cave volume divided by cave length). Passage density (cave length divided by convex hull area). Areal coverage (cave area divided by the convex hull area expressed as percent). Cave porosity (cave volume divided by rock volume expressed as percent).

As a measure of how completely the cave fills a plane of projection, we use the fractal dimension or box dimension, determined by standard box-counting (Feder, 1988). The box dimension, D, of the cave can be calculated as (Simanca and Sutherland, 2002)

$$D = -\lim_{\varepsilon \to \infty} \frac{\log N_\varepsilon(S)}{\log \varepsilon}, \qquad (1)$$

where $N_\varepsilon(S)$ is the minimum number of two-dimensional squares of side-length ε needed to cover the filled outline of the cave (S). Accordingly, D is the slope of the log-log plot of $N_\varepsilon(S)$ versus ε. This approach differs from the volumetric, modular method of Curl (1986), but serves our purpose best, because the cave is essentially two-dimensional due to the stripe geometry, and it permits comparison with other caves where volumetric passage details are not available.

RESULTS

CAVE DESCRIPTION OF NONSHAUGGROTTA

Nonshauggrotta was surveyed to a total passage length of 1.5 km, at elevations between 231 and 260 m (Fig. 3). The highest passages are located in the northeast and along the cliff face. The passage density is quite high, 148 km/km^2, as is the plane-filling fractal dimension, D = 1.5 (Table 1). Explorable cave conduits penetrate less than 50 m down-dip from the cliff face, but extend nearly 300 m along it. The surveyed passages compose only a minimum estimate of the actual cave extent. Almost all south-trending conduits terminate in sand chokes; those that are open continue beyond explorable dimensions. Essentially all north-trending conduits end as openings in the cliff face, and were apparently truncated either by glacier plucking or by gravitational retreat of the cliff face. Therefore, the absolute boundary of cave passages cannot be established unambiguously, although our observations suggest that many passages taper out to small dimensions down-dip to

Table 1. Speleometric data.

Parameter	Nonshauggrotta	Lønngangen	Upper Nonshauggrotta
Length, 10^3 m	1.5	0.30	0.23
Depth, m	29	12	36
Cave area, 10^3 m^2	1.6	0.4	0.3
Cave volume, 10^3 m^3	2.3	0.8	0.4
Convex hull, 10^3 m^2	10.2	4.2	0.9
Rock volume, 10^3 m^3	92	25	6
Mean passage cross-sectional area, m^2	1.5	2.8	1.9
Passage density, km/km^2	148	70	256
Areal coverage, %	16	9	36
Cave porosity, %	2.5	3.2	7.0
Fractal dimension	1.5	1.2	1.1

the south when followed deeper into the rock mass. So the density of cave voids appears to decrease in the down-dip direction.

Structural Speleology

The cave system displays a reticulated network architecture (Fig. 3). Cave conduits are oriented parallel with the strike and dip of the marble-schist interface (082°/25°), thus intersecting at nearly right angles. The predominate set of guiding fractures is steeply dipping, striking south-southwest (190°/79) (Fig. 4). The other set of guiding fractures has a moderate dip and strikes west-northwest (282°/49°). Only the predominate fracture set could be detected on the land surface above the cave (Fig. 4). We have not been able to detect any displacement along fractures or found other brittle kinematic indicators. At several locations, the west-northwest fractures terminate at the south-southwest fractures, though this relationship was not established unambiguously. However, if so, it implies that the south-southwest-trending fractures are older than the west-northwest-trending fractures. If not, the two fracture sets might have been formed simultaneously.

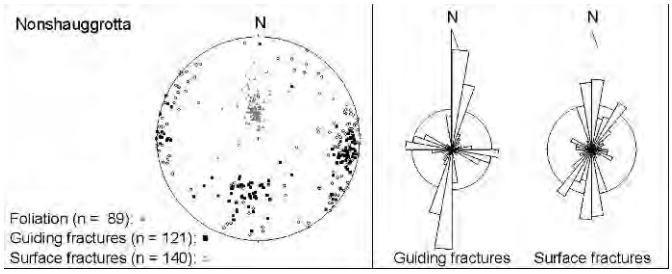

Figure 4. Left: Stereographic projection (equal area, lower hemisphere, magnetic north) of poles to foliation and fractures at Nonshaugen. Right: Rose diagrams (equal area, magnetic north) of trend of surface fractures and guiding fractures. Circle: 10%.

Morphology

The passage cross-sections are high and narrow, with elliptical or irregular rift shapes reflecting the guiding fractures (Fig. 3). The passage cross-sections are related to the slope of the guiding fractures; south trending passages have vertical cross-sections, whereas west-trending passages have slanting cross-sections (Fig. 5). Mean passage cross-sectional area, approximated as ellipses, is estimated as about 1.5 m^2. The largest measured cross-sectional area is about 16 m^2 and is a result of breakdown modification. Dead end, tight fissures are common, while narrow vadose channel incisions are rare and, even when apparent, ambiguous. Where passages terminate in the cliff face and their entire cross-section is visible, they lack vadose incisions. In sum, the cave appears essentially phreatic, with negligible, if any, vadose modification. One of the southern conduits ends in a circular shaft 2 m deep plugged with sand and micaceous silt (Fig. 3).

Mica-Schist Cap Rock

The mica-schist ceiling forms a hydrological constraint that renders the cave system essentially two-dimensional. Passages were developed along and just below the upper marble-schist contact (i.e., in hydraulically confined settings) (Fig. 3).

Corrosional drip-pits in the marble underlying the schist ceiling demonstrate that seepage from the schist is occasionally acidic. Substantial efflorescence of gypsum on cave walls and rusty weathering of the mica schist reveal that iron oxides and sulfides are present in the mica schist, the sulfides having produced sulphuric acid by oxidation.

Lithology

The results from the loss-on-ignition and acid-insoluble-residue tests are inversely proportional ($r = -0.99$), and consistent. The insoluble residuals were in the range 1 to 21% (Fig. 6), which indicate that the purity of the marble is variable, with between 79 and 99% $CaCO_3$ and $CaMg(CO_3)_2$. However, the composition of the upper,

Figure 5. Passages of Nonshauggrotta with distinct guiding fractures. Left: south-trending passage with subvertical guiding fracture. Right: west-trending passage with moderately dipping guiding fracture, mica schist ceiling, efflorescences of gypsum and hydromagnesite, rusty coloring, and fine sediments on lower wall and floor.

cavernous part of the marble layer, where cave conduits occur, does not differ from the rest of the marble layer either in loss-on-ignition (t-test, $t_{17} = -0.67$, $p = 0.51$) or acid insoluble residual (t-test, $t_{17} = 0.55$, $p = 0.59$). Consequently, variation in marble purity fails to explain the stratigraphic position of the cave conduits adjacent to the confining strata in the sequence. The absolute content of insoluble residue is quite high, but has not choked off speleogenesis, probably because mica and quartz do not swell in contact with water.

Sediments

The passage floor consists essentially of fine to coarse sand (Fig. 3). Mica is abundant and seems to dominate the coarser sand fractions. Some of the northern passages contain pebbles and cobbles. Angular breakdown occurs in a few of the largest passages. Some of the north-trending passages are plugged by breakdown and scree material that penetrated from the cliff face. No varved, clayey sediments have yet been found in the cave, and the layers of sand and gravel are probably a fluvial lag.

Paleohydrology

Nonshauggrotta is relict and dry and lacks a modern drainage area due to its topographic position in the northern cliff face of Nonshaugen, in the lee side of the glacial whaleback. Scallops in conduit walls and ceiling display a consistent flow pattern, eastward in east-west trending passages and northward in north-south trending passages (Fig. 3). Accordingly, water flow was upward, artesian, and the hydraulic gradient was directed toward the northeast. Hence the network had an effluent flow under phreatic conditions; it represented the discharge boundary of the karst aquifer. The Sauter mean of scallop length, L_{32}, was deduced from scallop populations in three different sites (Fig. 3), 32 cm at one site and 20 cm at two other sites. Calculated paleoflow velocities were in the range of 7 to 16 cm s^{-1}, while paleodischarges were in the range of 0.02 to 0.5 m^3 s^{-1}. Although only a few sites were suitable for statistical analysis of scallops, numerous other observations indicate that scallop lengths throughout the network are within the same size range. We were unable to detect any variation in mean scallop length with height above the passage floor.

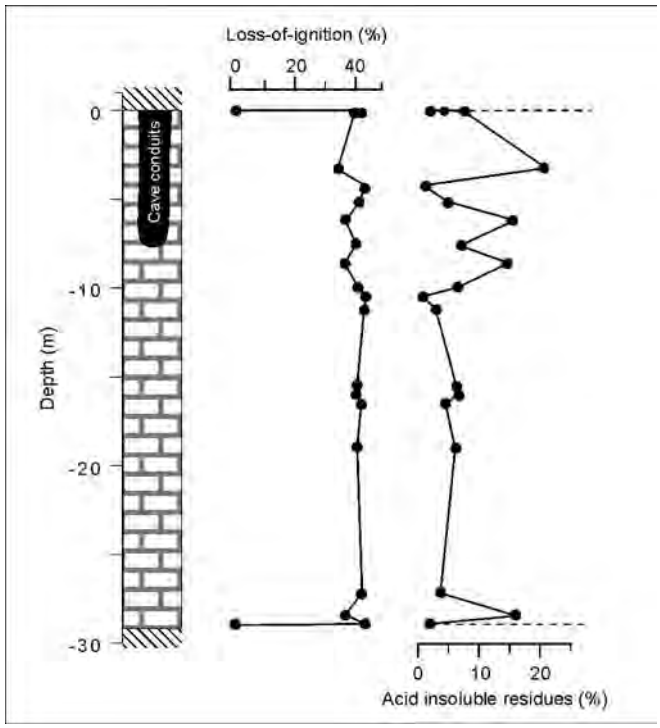

Figure 6. Loss-on-ignition and acid-insoluble-residue from 19 marble samples and 2 mica-schist samples (only LOI) from the marble layer in which Nonshauggrotta is situated (cave position marked in black).

Other Caves and Karst Features in Nonshaugen

Upper Nonshauggrotta is situated about 100 m south of Nonshauggrotta in a stratigraphically higher marble layer at an elevation of about 285 m, but in a similar position below an upper marble-schist interface (Fig. 7). The cave was surveyed to a length of 175 m and a depth of 36 m. The lower part of the cave is a shaft slanting downward at about 36° and trending south, ending in a breakdown choke at the bottom of a 3 m vertical drop (Fig. 7). In its upper part, the cave consists of two stories and some branches and loops. Morphology and scallops indicate that paleoflow was slow and uphill.

A small cave is situated at the southern side of Nonshaugen, at an elevation of approximately 140 m, here termed Small Cave (Fig. 7). The cave is a single passage trending north and plugged by sediments after about 30 m. This passage is mainly in schist with an angular and irregular cross-section, indicating that it has migrated upward by breakdown from the dissolutional conduit in the underlying marble unit.

Four dolines were noted in the upper marble layer at the top of the western side of Nonshaugen ridge (Fig. 7). Three small dolines (2 to 5 m^2 in cross-sectional area and 0.6 to 1.2 m deep) are situated in a row oriented east-west. South of these dolines lies a single larger doline, about 8 m in diameter and 3.7 m deep.

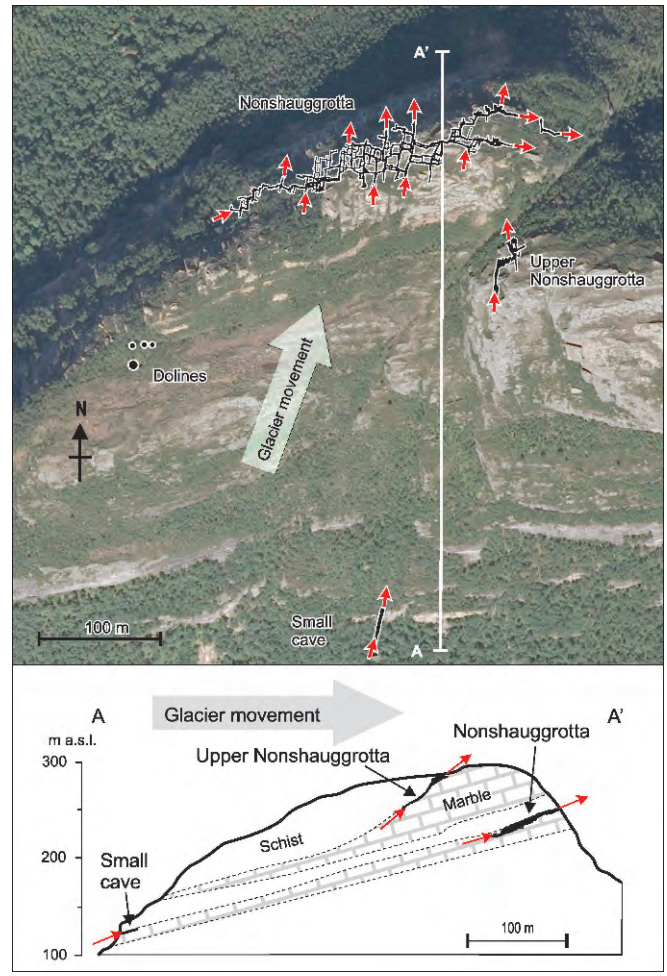

Figure 7. Upper: Aerial photograph of Nonshaugen with caves. A-A′: Line of cross-section. Lower: Vertical cross-section of Nonshaugen. Marble-schist contacts in the middle of the ridge are hypothesized. Red arrows: paleoflow direction from scallops. Grey arrows: Topographically directed ice flow (in accordance with Rasmussen 1981).

Lønngangen

Lønngangen (67°00′N 13°57′E) is situated on the peninsula west of Sørfjorden (Fig. 1). The cave is located on the western limb of the Sørfjorden fold. Accordingly, the marble-schist interface dips gently toward the west-southwest (154°/11°).

Lønngangen was surveyed to a length of about 300 m. The cave has four openings in a cliff face less than 10 m high, at elevations between 60 and 70 m. In plan view, the cave has an angular pattern (Fig. 8). Compared to Nonshauggrotta, the cave has a low passage density of 70 km/km^2 and a low fractal dimension of 1.2 (Table 1). The passage morphology and geometry are dictated by two orthogonal sets of steeply dipping guiding fractures. The guiding fractures strike southwest (216°/75°) and northwest (315°/74°) (Fig. 9). Passages are essentially high and narrow rifts with a mean cross-sectional area of 2.8 m^2 in

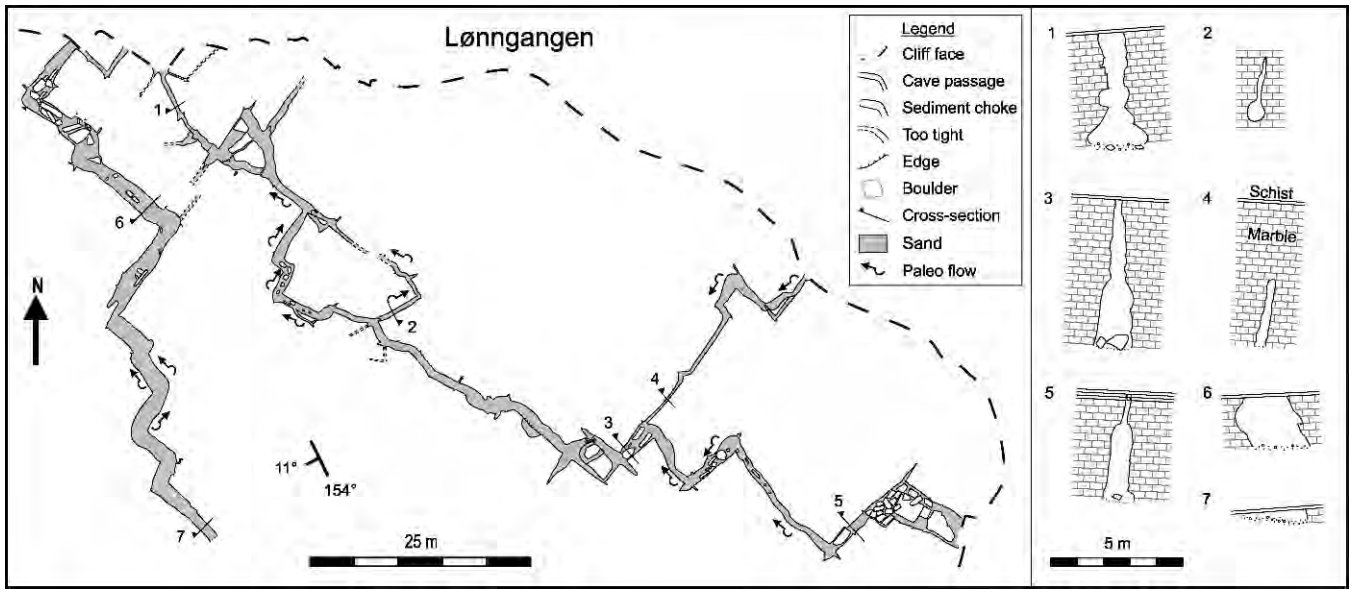

Figure 8. Plan map of Lønngangen with passage cross-sections (3× exaggeration).

elliptical approximation (Fig. 8). A few small, sub-circular side conduits intersect the main passage and form closed loops. Negligible vadose modification is seen, and marble breakdown occurs in only a few places, most prominently by the eastern entrance. Sandy sediments compose the passage floor, and shell sand plugs the innermost conduit. Sub-rounded gravel occurs in a few places (Fig. 8). The mica-schist cap rock frequently forms the ceiling of the passages (Fig. 8). Corrosional drip-pits are found on marble boulders below mica-schist exposures.

The paleoflow direction deduced from scallops is from east to northwest (Fig. 8). The eastern entrances conveyed water into the rock, while water emerged from the northwestern entrances (Fig. 10). Accordingly, the cave contains a complete flow route between input and output boundaries at the topographic surface.

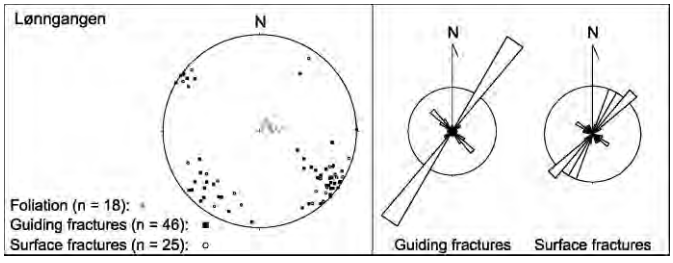

Figure 9. Left: Stereographic projection (equal area, lower hemisphere, magnetic north) of poles to foliation and fractures from Lønngangen. Right: Rose diagrams (equal area, magnetic north) of trend of surface fractures and guiding fractures. Circle: 20%.

DISCUSSION

STRUCTURAL GUIDING

Nonshauggrotta and Lønngangen are each guided by orthogonal fracture sets. However, the fracture sets of the two caves have different orientations.

In the map of tectonic lineaments of Norway (Gabrielsen et al., 2002), the regional trends of Nordland and Troms are northeast-southwest and northwest-southeast. On the map, lineaments trending north-northeast–south-southwest and west-northwest–east-southeast are abundant in the Gildeskål area, whereas lineaments trending north-south, east-west, and northeast-southwest are present but sparse. North to north-northeast is also the regional Caledonian strike direction and the axial trend of the Sørfjorden antiform.

The two sets of guiding fractures of Nonshauggrotta are parallel to the pronounced trends of tectonic lineaments in the Gildeskål area. In Nonshaugen, the south- to south-southwest-striking fracture set is dominant. This fracture set guides the passage trends in the Nonshaugen caves and is the single pronounced fracture set on the surface above the cave. The west-northwest-striking fractures were only detected within Nonshauggrotta. We assume that by logging surface fractures in the vicinity of the cave, the true fracture distribution is identified. However, here the attitude of the west-northwest-striking fracture set may have made it less pronounced in surface outcrops.

The southwest- and northwest-striking guiding fractures in Lønngangen are consistent with surface fractures (Fig. 9), local lineaments determined from aerial photos (Fig. 10), and the regional lineament trends in Nordland and Troms (Gabrielsen et al., 2002). On the other hand, they differ from the south-southwest and west-northwest

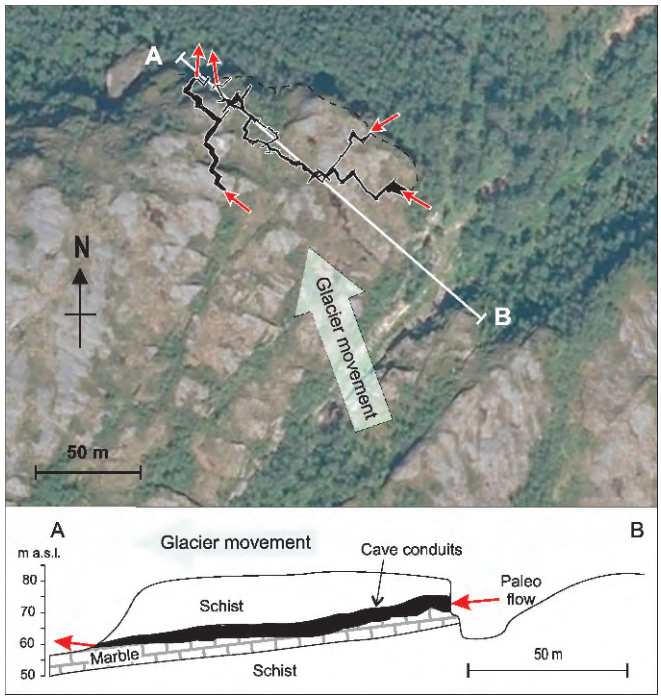

Figure 10. Upper: Aerial photograph of the area around Lønngangen. A-B: Line of cross-section. Lower: Vertical cross-section of Lønngangen with topography. Black: cave passages. Red arrows: paleowater flow direction from scallops. Grey arrows: Topographically directed ice flow (in accordance with Rasmussen, 1981).

strike of guiding fractures found in Nonshauggrotta. This pronounced difference in fracture sets may be related to the location of Lønngangen at the limb of the fold of the Sørfjorden antiform, whereas Nonshaugen is situated in the hinge of the fold.

The fractures predate the speleogenesis in the metacarbonates. Otherwise, there is no unequivocal evidence of chronological relationships between the fracture sets. Since the Devonian, the regional tectonic stress field has varied significantly (Bergh et al., 2007), and it does not seem prudent, on the basis of this locality, to associate the local fractures with specific phases of the regional geological history.

Stratigraphic Cave Position

The lack of correlation between marble purity and concentration of cave voids in Nonshauggrotta suggests that the stratigraphic position of the cave is controlled by hydrological factors rather than the distribution of solubility. It is conceivable that the position of the cave is a result of artesian flow towards a low-dip confining contact.

Occurrence of iron oxides and pyrite in the mica schist suggests that cave inception may have been aided by sulfuric-acid speleogenesis at the marble-schist interface.

Paleohydraulic Function

Flow Direction and Flow Components

All interpretations of paleocurrents are based on scallop morphometry and surface sediments at the passage floor, all of which are remnants of the last active stage. Our interpretations, therefore, primarily concern the last stages of evolution.

In Nonshauggrotta, the passage cross-sections indicate symmetrical dissolution outward from the guiding fractures under phreatic conditions. Artesian water flow, deduced from scallops, is consistent with evolution under confined settings. In accordance with the paleocurrent direction, the southern vertical conduit (Fig. 3) is interpreted as a phreatic artesian feeder. Since several passages seem to taper out southwards into the rock mass, we suggest that only a few riser tubes fed the system from below. Upper Nonshauggrotta displays the same flow function and conduit pattern as Nonshauggrotta, feeder tubes and distributary networks, although more fragmentary due to its smaller size (Fig. 8). This supports the interpretation of artesian water flow from the south through an effluent flow network. The low-dip, confining aquiclude may have caused a spreading and slight retardation of the flow, and thus, enhanced maze formation. The rudimentary network evolution in Upper Nonshauggrotta may be partly attributed to the steeper dip of the marble-schist interface except in the upper, outermost part.

The stratigraphic position of Small Cave at the southern side of Nonshaugen may align with either Nonshauggrotta or Upper Nonshauggrotta. It might therefore be an example of an influx conduit feeding the cave network from the southern, stoss side of the glacial whaleback.

The deduced hydraulic gradient direction toward the northeast and the consistent flow direction towards the east in the western part of the cave and in east-west passages together imply that there might have been additional recharge from the western or southwestern side of the ridge, giving a flow component sub-parallel with the cliff face. This may be considered as a sort of flank margin subglacial pattern of genesis or perhaps flank margin adaptation of a covered or confined network of conduits. However, there is no sign of solution sculpture by flow into or out of the cave in the northern cliff-face.

Slow Paleocurrent

As scallop lengths seem to be quite consistent throughout Nonshauggrotta, the mean paleoflow velocity in the cave system as a whole is similar to the spot observations of calculated velocities (a few tens of cm s^{-1}). Slow flow conditions were also observed in Upper Nonshauggrotta. Low flow velocities are also consistent with the widespread deposits of fine-grained sediments. According to the Hjulstrøm diagram (Sundborg, 1956), fine sand is deposited at velocities of less than 20 cm s^{-1}, while coarse sand is

deposited at velocities less than 40 cm sec^{-1}. Discharge determined from scallops has been shown to represent discharges within the highest 2 to 15% of the annual flows (Lauritzen, 1989; Lauritzen and Lundberg, 2000). The conspicuous lack of coarse fluvial lag material further supports the impression that low velocities have dominated the network flow.

SPELEOGENETIC SETTING

Based on the cave geometry, passage morphology, hydraulic function, and topographically and hydrologically hanging position, several different origins of Nonshauggrotta may be considered: (1) hypogene origin, where the aquifer is fed from below and without relation to surface drainage, (2) post-glacial or late interglacial origin, in a topographical position similar to the present, (3) pre-glacial or early interglacial origin, as a flood-water maze in the bottom of a fluvial valley; and (4) subglacial origin, in a topographical position similar to the present and in contact with a glacial aquifer as part of a subglacial drainage network.

The network geometry and the effluent flow function are suggestive of caves of hypogene origin (Klimchouk, 2003, 2009). However, this sort of hypogene speleogenesis is characterized by water injection from a porous aquifer below or above the soluble strata, and the presence of impermeable strata in stripe karst makes a hypogene origin implausible. In contrast to isolated maze caves, which are typically formed in confined aquifers by a locally generated boost of the groundwater aggressivity (Frumkin and Fischhendler, 2005), the network of Nonshauggrotta is an integrated cave system that was formed by water that was already aggressive when injected into the marble.

Pyrite or sulfide oxidation could have been a source of locally generated aggressiveness when ascending groundwater mixed with oxygenated surface water. For pyrite, the total reaction is

$$4FeS_2 + 16CaCO_3 + 15O_2 + 14H_2O = 16Ca^{2+} + 16HCO_3^- + 8SO_4^{2-} + 4Fe(OH)_3. \quad (2)$$

One formula weight unit of pyrite can dissolve four formula weights of calcite, or by volume 1 mm^3 pyrite would dissolve 6.4 mm^3 marble and leave a considerable amount of insoluble hydrated iron oxide. The iron hydroxide will act as a surface inhibitor. If speleogenesis was based on pyrite oxidation alone, the dissolution of the marble would have required 16% of its volume in pyrite. Therefore, it is evident that the modest sulfide concentration (no pyrite grains have been directly observed) in the upper mica-schist layer is not enough to account for the total volume of the cave, so that the sulfuric-acid mechanism could only have been important at the cave-inception stage. It is, however, quite conceivable that oxygenated water, either directly from the surface or from the glacier environment, combined with some sulfide, might have been crucial in establishing integrated flow at the very commencement of speleogenesis.

Phreatic formation of the caves in Nonshaugen requires that the water table was above the top of the caves. Two different settings have provided high water tables in the past: bedrock, before the valley was entrenched, and glaciers, when they filled the valley and raised the water table in the adjacent rocks. The caves of Nonshaugen and Lønngangen lacked a surface drainage area during past and present interglacials due to their hanging position in the cliff face. Consequently, post-glacial or late interglacial origin of the caves is rejected.

In previous works, valley erosion rates by glaciers have been estimated to range from 15 to 55 m per 100 ka (Lauritzen, 1990, and references therein; Nesje and Sulebak, 1994). This implies a minimum of 500 ka since Nonshauggrotta may have been situated below the valley floor. Small passage cross-sectional areas indicate a short evolution time because "after a passage reaches the maximum annual enlargement rate, its size depends mainly of the length of time it contains flowing water" (Palmer, 1991, p.10). Under subglacial settings the cave conduits tend to be water-filled, and active water circulation, and thus dissolutional widening, occurs at least occasionally (Ford, 1977; Lauritzen, 2006). Small passage dimensions are inconsistent with evolution in a valley bottom during fluvial regimes and repeated subglacial conditions, and pre-glacial or early interglacial evolution of Nonshauggrotta as a floodwater maze in the valley bottom is rather improbable.

The most probable setting for artesian conditions in this topographic and geological environment is subglacial. Subglacial and englacial water drainage is controlled by the surface slope of the glacier and is essentially independent of bed topography. Water flow toward the northeast in Nonshauggrotta and toward the north in Upper Nonshauggrotta is consistent with observed glacial striations toward the northwest on the eastern side of the ridge and with younger, topographically directed glacier flow (Rasmussen, 1981) (Fig. 7). When directed by the topography, the glacier would flow over the summit and around Nonshaugen, so that both the southern and western side of the ridge have been subject to high pressure. Effluent flow is consistent with the network occurring at the lee side of the ridge. The consistently slow flow rates observed in the Nonshaugen caves may be due either to great glacier thickness with a gentle surface slope or something else that damped the strong fluctuations of glacial flow.

The observed flow direction in the caves is perpendicular to the direction of glacier movement during full glaciation. A gentle glacier surface slope parallel with the observed direction of water flow is therefore more likely to correspond to early periods of deglaciation, when the mountains in the west started to control the glacier flow and turned it northward. During deglaciation it can be assumed that high flow rates occurred during the melting

season. The lack of signs or remnants of high flow rates or flushing, such as coarse-grained lag, suggest that the cave was not exposed to the natural fluctuations of meltwater discharge. Accordingly, we suggest that some control of the flow occurred in the karst system or in the contact between the karst system and the glacier. A glacier is a dynamic aquifer with an ephemeral drainage pattern and discharge, and the maze was established in the lee side of the hill. Accordingly, we suggest that restricted outflow towards the ice contact has caused network evolution in the outflow zone. Modeling experiments by Skoglund et al. (2010) support this interpretation.

Speleogenesis of Lønngangen

The underlying cave pattern of Lønngangen cannot be decided unequivocally due to its small size and fragmentary form. We suggest that it is a rudimentary or degenerated network cave; it either never developed into a proper network or has been truncated and partly destroyed by glaciers. Water flow in Lønngangen was parallel to the cliff face and the cap-rock contact, not toward them (Fig. 10). This contrasts with the setting of Nonshaugen, and the lack of outflow restriction is a possible explanation of the rudimentary network pattern.

The passage morphology in Lønngangen also indicates symmetrical dissolution around steeply dipping guiding fractures under phreatic conditions. Lønngangen was situated below sea level for about 4 ka after the last deglaciation (ML 89 m a.s.l., Rasmussen, 1981), since sea level did not drop below the cave level until the Boreal. However, the phreatic passage morphology, the small passage cross-sections, and the cave's location in the sea-facing cliff indicate that the cave is quite young and, in accordance with the previous discussion of Nonshauggrotta, has probably developed under subglacial conditions. The paleocurrent direction deduced from scallops in Lønngangen is not compatible with submarine or shoreline erosion. Paleocurrent direction is consistent with glacier flow during both full glaciation and deglaciation (Figs. 1 and 10). However, it is conceivable that there was less water available below the glacier during full glaciation, and accordingly, that water circulation and dissolution were more efficient during glacial retreat and advance.

Conditions of Subglacial Speleogenesis

The homogeneous character and lack of modifications of the passage morphology in Nonshauggrotta suggest that evolution either has been continuous or the cave evolved through a series of stages with a quite similar hydrological regime. Glaciations are characterized by strong fluctuations in hydrology, both on a short time scale (annually) and on a long time scale (glacial/interglacial cycles). Accordingly, active subglacial solutional widening of karst aquifers is most likely disrupted by periods of stagnation, possible silting up, and drained periods during interstadials and interglacials (Ford, 1977).

We may estimate the age of Nonshauggrotta by considering the time required to form the passages under different wall-retreat rates. In an allogenic stream in a cave south of Svartisen glacier, the dissolution rate is estimated at 0.2 mm/a in an unpublished study by Lauritzen, so a scallop relief of about 2 cm would require about 100 years under interglacial conditions to be established or replace a previous pattern. From corrosion of an interglacial speleothem, Lauritzen (1990) reported a total subglacial solutional wall retreat rate of 5 to 10 cm/100 ka, corresponding to an average rate of about 0.001 mm/a. At this rate it would take 20 ka to form the scallop, which is a gross overestimate, as the corrosion was most likely discontinuous.

If Nonshauggrotta was widened from the proto-cave stage (>1 cm, Ford and Williams, 2007) to the present conduit size (mean width = 1.2 m, max dissolved width ≈ 2.0 m) during the last glaciation, this would have required a mean subglacial wall-retreat rate between 0.006 and 0.01 mm/a. This is about 10 times higher than the subglacial rate measured by direct radiometric dating. Based on this estimate, no unequivocal statement can be made on whether the cave evolved during the last or several of the latest glaciations. Evolution of the cave during the about 4 ka of the last deglaciation, when large amounts of water were available, would have required a wall-retreat rate of about 0.2 mm/a. This rate is equal to the present wall retreat rate by an allogenic stream and 200 times higher than the subglacial rate of Lauritzen (1990). That would be an improbable dissolution rate for subglacial water, which is characterized by low aggressiveness (Tranter et al., 1993), in the moderate quantities permitted by the slow flow velocity observed. Accordingly, we may state that the cave is certainly older than the last deglaciation.

Conclusions

Nonshauggrotta is a network cave situated in a topographically and hydrologically hanging position. It was developed under artesian water flow towards the confining mica-schist cap rock. Its stratigraphic position just below the confining cap-rock was controlled by the contact, as there is no correlation between purity of the marble and the location of the passages.

Nonshauggrotta and Lønngangen are both developed along orthogonal fracture sets. We suggest that the different orientations of the guiding fractures in the two caves is a result of local structure; Nonshaugen is located in the hinge area and Lønngangen in the fold limb of the Sørfjorden antiform.

The network of Nonshaugen ridge had an effluent flow function, and we suggest that the network was fed from the south by a few feeder tubes. This is supported by the caves' architecture and the paleoflow pattern of Upper Nonshauggrotta. However, the consistent flow direction toward the northeast in Nonshauggrotta indicates an

additional flow component along the cliff face. Accordingly, the network was probably fed from the southwestern or western side of the ridge as well.

Lønngangen is a short cave with an angular passage pattern and seems to have developed by phreatic water flow parallel to the cliff face. The cave does not display a proper maze pattern.

The flow functions of Upper Nonshauggrotta and Lønngangen may serve to demonstrate the two suggested recharge components of Nonshauggrotta separately. Upper Nonshauggrotta displays a single north-trending artesian feeder tube with a rudimentary labyrinth structure towards the cliff face that was developed in a confined setting. Lønngangen displays a rudimentary network developed along an escarpment with both recharge conduits and outflow conduits, but few closed loops. We may speculate that a combination of two flow components might have created the elaborate labyrinth of Nonshauggrotta.

All observations support the hypothesis that the maze caves were developed under subglacial conditions related to wet-based, topographically directed glacier flow. The consistently slow water flow in the Nonshaugen caves implied by scallop morphometry and sediment distribution makes us suggest that the ice-surface slope was very gentle, that the ice contact restricted outflow, or both.

ACKNOWLEDGEMENTS

The work of this paper was funded by the Research Council of Norway, grant No. 160232/V30 "Porosity development in marble stripe karst." David St. Pierre, Helge Skoglund, Terje Solbakk, and Arnfinn Jonsen are thanked for their assistance during cave surveys. Elsa Norum is thanked for her hospitality during field work. Walter Wheeler and Derek Ford are thanked for constructive comments that improved the manuscript. Statens Kartverk provided the aerial photos in Fig. 7 and 10.

REFERENCES

Bergh, S.G., Eig, K., Kløvjan, O.S., Henningsen, T., Olesen, O., and Hansen, J.-A., 2007, The Lofoten-Vesterålen continental margin: a multiphase Mesozoic-Palaeogene rifted shelf as shown by offshore-onshore brittle fault-fracture analysis: Norwegian Journal of Geology, v. 87, p. 29–58.

Corbel, J., 1957, Les karsts du nord-ouest de l'Europe et de quelques régions de comparaison: Institut des études rhodaniennes de l'Universite de Lyon, Mémoires et Documents 12, 541 p.

Curl, R.L., 1974, Deducing flow velocity in cave conduits from scallops: NSS Bulletin, v. 36, no. 2, p. 1–5.

Curl, R.L., 1986, Fractal dimensions and geometries of caves: Mathematical Geology, v. 18, p. 765–783.

Day, A., 2002, Cave Surveying: Buxton, British Cave Research Association, Cave Studies Series 11, 40 p.

Eikeland, R., 1986, Lønngangen: Norsk Grotteblad, v. 16, p. 25–26.

Feder, J., 1988, Fractals: New York, Plenum Press, Physics of Solids and Liquids series, 283 p.

Ford, D.C., 1977, Karst and glaciation in Canada, *in* Proceedings, 7th International Speleological Congress: Sheffield, British Cave Research Association, p. 188–189.

Ford, D.C., and Williams, P., 2007, Karst hydrogeology and geomorphology, 2nd edition: Chichester, John Wiley and Sons Ltd, 562 p.

Frumkin, A., and Fischhendler, I., 2005, Morphometry and distribution of isolated caves as a guide for phreatic and confined paleohydrological conditions: Geomorphology, v. 67, p. 457–471.

Gabrielsen, R.H., Braathen, A., Dehls, J., and Roberts, D., 2002, Tectonic lineaments of Norway: Norwegian Journal of Geology, v. 82, no. 3, p. 153–174.

Gustavson, M., 1985, Glomfjord, foreløpig berggrunnsgeologisk kart: Norges Geologiske Undersøkelse, 1928 I, 1:50 000.

Gustavson, M., and Solli, A., 1989, Berggrunnskart Gildeskål: Norges Geologiske Undersøkelse, 1929 II, 1:50 000.

Horn, G., 1937, Über einige Karsthöhlen in Norwegen: Mitteilungen für Höhlen und Karstforschung, p. 1–15.

Klimchouk, A.B., 2003, Conceptualisation of speleogenesis in multi-storey artesian systems: a model of transverse speleogenesis: Speleogenesis and Evolution of Karst Aquifers, v. 1, no. 2, 18 p. [Available at http://speleogenesis.info/pdf/SG2/SG2_artId24.pdf.]

Klimchouk, A.B., 2009, Principal features of hypogene speleogenesis, *in* Klimchouk, A.B., and Ford, D.C., eds., Hypogene Speleogenesis and Karst Hydrogeology of Artesian Basins: Simferopol, Ukrainian Institute of Speleology and Karstology Special Paper 1, p. 7–16.

Lauritzen, S.E., 1982, The paleocurrents and morphology of Pikhåggrottene, Svartisen, North Norway: Norsk Geografisk Tidsskrift, v. 36, p. 183–209.

Lauritzen, S.E., 1989, Scallop dominant discharge, *in* Proceedings, 10th International Speleological Congress, v. 1: Budapest, Hungarian Speleological Society, p. 123–124.

Lauritzen, S.E., 1990, Tertiary caves in Norway: a matter of relief and size: Cave Science, v. 17, no. 1, p. 31–37.

Lauritzen, S.E., 2001, Marble stripe karst of the Scandinavian Caledonides: An end-member in the contact karst spectrum: Acta Carsologica, v. 30, no. 2, p. 47–79.

Lauritzen, S.E., 2004, Grottolf Program for processing, plotting and analysis of cave survey data, University of Bergen.

Lauritzen, S.E., 2006, Caves and speleogenesis at Blomstrandsøya, Kongsfjord, W. Spitsbergen: International Journal of Speleology, v. 35, no. 1, p. 37–58.

Lauritzen, S.E., and Lundberg, J., 2000, Solutional and erosional morphology of caves, *in* Klimchouk, A.B., Ford, D.C., Palmer, A.N., and Dreybrodt, W., eds., Speleogenesis: Evolution of Karst Aquifers: Huntsville, Alabama, National Speleological Society, p. 406–426.

Linge, H., Olsen, L., Brook, E.J., Darter, J.R., Mickelson, D.M., Raisbeck, G.M., and Yiou, F., 2007, Cosmogenic nuclide surface exposure ages from Nordland, northern Norway: implications for deglaciation in a coast to inland transect: Norwegian Journal of Geology, v. 87, p. 269–280.

Loucks, R.G., 1999, Paleocave carbonate reservoirs: Origins, burial-depth modifications, spatial complexity, and reservoir implications: American Association of Petroleum Geologists Bulletin, v. 83, p. 1795–1834.

Mangerud, J., 2004, Ice sheet limits on Norway and the Norwegian continental shelf, *in* Ehlers, J., and Gibbard, P., eds., Quaternary Glaciations - Extent and Chronology: Part 1 Europe: Amsterdam, Elsevier, Developments in Quaternary Science series 2, p. 271–294.

Nesje, A., and Sulebak, J.R., 1994, Quantification of late Cenozoic erosion and denudation in the Sognefjord drainage basin, western Norway: Norsk Geografisk Tidsskrift, v. 48, p. 85–92.

Olsen, L., 1997, Rapid shifts in glacial extension characterize a new conceptual model for glacial variations during the Mid and Late Weichelian in Norway: Norges Geologiske Undersøkelse Bulletin, no. 433, p. 54–55.

Palmer, A.N., 1975, The origin of maze caves: National Speleological Society Bulletin, v. 37, no. 3, p. 56–76.

Palmer, A.N., 1991, Origin and morphology of limestone caves: Geological Society of American Bulletin, v. 103, p. 1–21.

Palmer, A.N., 2001, Dynamics of cave development by allogenic water: Acta Carsologica, v. 30, no. 2, p. 13–32.

Palmer, A.N., 2002, Speleogenesis in carbonate rocks, *in* Gabrovšek, F., ed., Evolution of Karst: From Prekarst to Cessation: Ljubljana, Inštitut za raziskovanje krasa, ZRC SAZU, p. 43–59.

Rasmussen, A., 1981, The deglaciation of the coastal area NW of Svartisen, Northern Norway: Norges Geologiske Undersøkelse Bulletin, no. 369, p. 1–31.

Sejrup, H.P., Larsen, E., Landvik, J., King, E.L., Haflidason, H., and Nesje, A., 2000, Quaternary glaciations in southern Fennoscandia: evidence from southwestern Norway and the northern North Sea region: Quaternary Science Reviews, v. 19, p. 667–685.

Simanca, S.R., and Sutherland, S., 2002, Fractal Dimension, *in* Mathematical Problem Solving with Computers, coarse notes for MAT 331 at University of Stony Brook, http://www.math.sunysb.edu/~scott/Book331/Fractal_Dimension.html, [accessed July 5, 2009].

Skoglund, R.Ø., Lauritzen, S.E., and Gabrovšek, F., 2010, The impact of glacier ice-contact and subglacial hydrochemistry on evolution of maze caves: a modeling approach. Journal of Hydrology, (in press; posted online 2010).

Stephens, M.B., Gustavson, M., Ramberg, I.B., and Zachrisson, E., 1985, The Caledonides of central-north Scandinavia - a tectonostratigraphic overview, *in* Gee, D.G., and Sturt, B.A., eds., The Caledonide Orogen - Scandinavia and Related Areas, Part 1: Chichester, U.K., John Wiley and Sons Ltd., p. 135–162.

Sundborg, Å., 1956, The river Klarälven, a study of fluvial processes: Geografiska Annaler, v. 38, p. 125–237.

Tranter, M., Brown, G., Raiswell, R., Sharp, M., and Gurnell, A., 1993, A conceptual model of solute acquisition by Alpine glacial meltwaters: Journal of Glaciology, v. 39, p. 573–580.

Wells, M.K., and Bradshaw, R., 1970, Multiple folding in the Sørfinnset area of Northern Nordland: Norges Geologiske Undersøkelse Bulletin, no. 262, 89 p.

White, W.B., 1969, Conceptual models of carbonate aquifers: Groundwater, v. 7, p. 15–21.

BOOK REVIEW

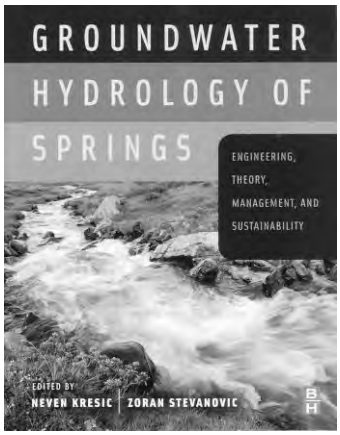

Groundwater Hydrology of Springs: Theory, Management, and Sustainability

Neven Kresic and Zoran Stevanovich (eds.), 2010. Burlington, Mass., Butterworth-Heinemann (imprint of Elsevier), 573 p., 7⅝ × 9½ inches, ISBN 978-1-85617-502-9, hardbound, $130.00.

Spring flow and quality are important groundwater issues, particularly in karst. Many textbooks address groundwater hydrology, but to my knowledge this is the first book that specifically addresses the hydrology of springs. All kinds of springs and in all kinds of terranes are considered, as well as their relation to surface hydrology. Karst receives special attention, however, because spring-flow is such an important aspect of karst aquifers, and karst is the main specialty of the editors and the majority of the authors. Authors were selected by the editors based on recognized expertise and geographic distribution. The editors also contributed material to the book.

The book includes a general discussion of springs, technical aspects and methods, and specific examples. The discussion begins with a chapter on the sustainability and management of springs that incorporates large excerpts from previous reports. It is a good general discussion of the use and management of springs and covers much material on hydraulic systems (man-made structures) at springs in the U.S. and in foreign countries. Chapter 2 is a discussion of spring types and their classification, both karstic and non-karstic (it even briefly mentions geysers and fumaroles). Many photos are provided for clarification.

Chapter 3 begins the technical section of the book with a discussion of recharge to springs. Basic principles are introduced, as well as methods for quantifying recharge (e.g., via artificial and environmental tracers). Mathematical and chemical principles are mentioned, but, as is appropriate for a book of this type, not in great detail, as this is already available in textbooks. Chapter 4 provides a fairly comprehensive discussion of spring-hydrograph analysis. Quantitative techniques are presented in a style that is relatively easy, useful, and clear. It is possible to obtain much of this information from books on surface-water hydrology, but these rarely discuss spring flow.

Chapters 5 and 6 address hydrologic modeling and geochemistry. They are clear and informative summaries of vast topics, and those who wish further information can consult specialized textbooks. It would have been handy if these chapters included references and links to relevant software.

Chapter 7 concerns water-quality treatment of springs to acceptable drinking-water standards. It includes several case studies that fit better here than in a separate chapter of their own. Chapter 8 describes the delineation of spring-recharge zones and strategies for protection. This concept has recently received much attention in Europe, but less so in the U.S. It is a brief discussion of a subject that is continually being revised within individual European countries and includes recommendations in the research of Ravbar (2007). Many useful references are included.

Chapter 9 addresses the utilization and regulation of spring flow. The historical development of capturing and protecting spring waters is described, and several case studies are provided. This topic is rarely considered in the U.S., but it probably should be. This chapter could provide guidance.

Chapter 10 is a collection of case studies. This is the longest chapter in the book (176 pages) and consists of ten sections. Included are detailed descriptions of springs used for water supply in southeastern Europe, Austria, Romania, Turkey, Iran, Texas (Edwards Aquifer), and China. Topics include geology, hydrogeology, water quality, exploitation, protection, and regional distribution of springs. Again, this chapter may be especially useful in the U.S. if communities begin to utilize spring waters more than they currently do.

This book is worth purchasing by any groundwater hydrologist who works with spring waters. It is not cheap, but its large amount of material and good-quality back-and-white figures make the price reasonable. There are inevitably a few typographic and formatting errors, but these are minor (except for some faulty references). The topics flow smoothly from chapter to chapter, reflecting the care in preparation and editing. I might have recommended including a chapter on spring biota (e.g., that in Gibert et al., 1994), which, among other things, can be a measure of the long-term health of the spring and its water source. I expect to keep this book close at hand as a guide to my own work.

References

Gibert, J., Danielopol, D.L., and Stanford, J.A., eds., 1994, Groundwater ecology: San Diego, Academic Press, 571 p.

Ravbar, N., 2007, The protection of karst waters: A comprehensive Slovene approach to vulnerability and contamination risk mapping: Ljubljana, Slovenia, Založba ZRC (ZRC Publishing), 256 p.

Reviewed by Malcolm Field, National Center for Environmental Assessment (8623P), Office of Research and Development, U.S. Environmental Protection Agency, 1200 Pennsylvania Ave., NW, Washington, DC 20460-0001 (field.malcolm@epa.gov).

DOI: 10.4311/jcks2010br0135

BOOK REVIEW

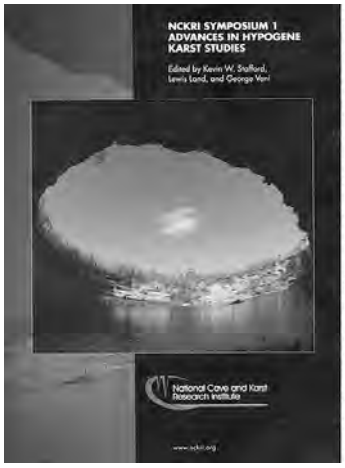

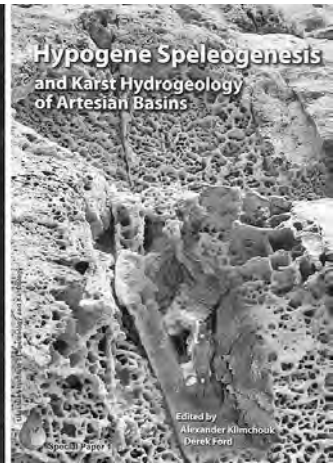

Advances in Hypogene Karst Studies

Kevin W. Stafford, Lewis Land, and George Veni (eds.), 2009. Carlsbad, New Mexico, National Cave and Karst Research Institute Symposium 1, 182 p., 8.5 × 11 inches, $50 plus shipping from sales@nckri.org. ISBN 978-0-9795422-4-4

Hypogene Speleogenesis and Karst Hydrogeology of Artesian Basins

Alexander Klimchouk and Derek Ford (eds.), 2009. Simferopol, Ukraine, Ukrainian Institute of Speleology and Karstology Special Paper 1, 292 p., 8.2 × 11.7 inches, $50 plus shipping from nssbookstore.org. ISBN 978-966-2178-38-8

For most of the past several centuries, students of caves and karst were satisfied with a single, underlying conceptual model. Meteoric water interacted with soluble bedrock, usually limestone or dolomite, sometimes gypsum, and occasionally salt. Differential dissolution on exposed land surfaces produced the characteristic karst landforms: closed depressions, sculptured bedrock, and residual hills of unusual shape. Infiltration of meteoric water through closed depressions and sinking streams developed caves with great varieties of lengths and patterns. The inlet points and their sources, combined with the outlet points at springs, allowed the identification of karst drainage basins and the underlying karst aquifers. Karst systems took on a tremendous variety of detail, depending on local climate and geologic setting, but the underlying processes were the same—a single concept.

This concept was challenged in the later decades of the 20th century. Studies of caves such as those in the Guadalupe Mountains of New Mexico and the Black Hills of South Dakota, as well as the giant maze caves of Ukraine, have revealed other processes involving upward migrating fluids, some of them at high temperatures or carrying sulfuric acid in addition to carbonic acid. The concept of deep-seated or hypogenetic speleogenesis had been born. These ideas were summarized in Alexander Klimchouk's *Hypogene Speleogenesis* (reviewed by John Mylroie in the *Journal of Cave and Karst Studies* 70, 129–131, 2008). The hypogene concept has now received enough attention to warrant two symposia, the proceedings of which are the volumes reviewed here.

The Stafford et al. book consists of fourteen papers that describe the influence of deep groundwater flow on the origin of caves and related features. It is based on presentations at a special session at the 2008 national meeting of the Geological Society of America. This volume represents a North American point of view, as twelve of the fourteen papers are by US and Canadian authors. The book is very nicely produced, with color photographs and illustrations throughout.

In the first chapter, Alexander Klimchouk describes hypogene cave origin, with special attention to the rise of water across stratal boundaries in the distal portions of regional and intermediate-scale groundwater systems. A suite of characteristic cave features is described, including floor slots, wall grooves, ceiling channels, and cupolas, all of which he attributes to rising groundwater. In the next chapter, however, John and Joan Mylroie urge caution in ascribing these features solely to rising groundwater. They cite examples of sea-coast caves in poorly lithified limestones that contain most or all of the features described in the previous chapter, but which have never been in confined settings or exposed to rising groundwater. Short-term flooding by epigenic processes also produces many such features.

Marcus Gary and John Sharp document several deep Mexican springs that are fed by rising groundwater, with CO_2, H_2S, and mild heat supplied by volcanic sources. They introduce the term *volcanogenic karst* for features originating in this way. Their type example is El Zacatón, a 319 m water-filled shaft that is one of the deepest known in the world. Philippe Audra and coauthors describe cave folia, which consist of arrays of sub-horizontal fungus-like calcite growths. They attribute these deposits to hypogene degassing of CO_2 on the basis of morphological features such as bubble-trails inscribed in the cave walls by the escaping gas.

A collection of field examples follows, each documenting a specific aspect of hypogene processes. Kelton Barr and Calvin Alexander describe depressions in Minnesota where water rises into valleys buried by glacial deposits and causes collapse at the outlets, a topic of growing concern to engineers and land-use managers. Paul Burger examines structural and facies control of caves in the Guadalupe Mountains of New Mexico. These are sulfuric acid caves

DOI: 10.4311/jcks2010br0155

formed by the oxidation of rising H_2S. He demonstrates, for example, that maze patterns in the caves strongly correlate with paleokarst and early tectonic breccias.

George Veni and Lynn Heizler use Robber Baron Cave, in Cretaceous limestone of south-central Texas, as an example of cave origin by rising groundwater. Ceiling cupolas and residual bedrock bridges across passages are cited as representative byproducts. Van Brahana et al. describe an unusual cave in Arkansas in which epigenic passageways have intersected much older rooms lined with calcite spar crystals up to 1.9 m long. Isotopic signatures indicate that the calcite was of hypogene origin with temperatures greater than 100 °C. Relationships to dolomitization, brecciation, and Mississippi-Valley-type ore deposits are discussed.

Three chapters concern hypogene processes and features in Permian gypsum in southeastern New Mexico and western Texas. This area is one of the least-studied karst regions of the USA. Ray Nance and Kevin Stafford describe caves and surface karst features with hypogenic characteristics, such as calcitization of evaporites, sulfur deposits, and solution breccias. These are attributed to the influence of hydrocarbons carried by rising water. Kevin Stafford et al. describe regional flow patterns related to the Pecos River. The river has long served as a target for groundwater rising under semi-confined conditions. Hypogene dissolution has produced multi-story caves, oil-field porosity, and surface depressions. Lewis Land discusses the impact of deep-seated processes on the water resources of the area. Karstic artesian basins supply nearly all of the water necessary to sustain a level of population growth and agricultural development that would otherwise be impossible in this semi-arid region.

Three chapters concern the application of hypogene karst processes to economic geology and regional tectonic history. Harvey DuChene provides field evidence that oil fields north and west of the Guadalupe Mountains supplied the hydrogen sulfide that formed the local caves (e.g., Carlsbad Cavern). He relates the changes in oil-field character, groundwater patterns, and cave development to block faulting in the Rio Grande Rift zone to the west. Derek Ford interprets the paragenesis of carbonate-hosted sulfide ores in the Nanisivik mining area of Baffin Island, northern Canada. He interprets the ore as having formed along the interface between saline water and gas or oil about 1600 m below the surface, with simultaneous carbonate dissolution and ore deposition. Langhorne Smith describes hydrothermal petroleum reservoirs in Ordovician rocks of eastern North America that formed in dolomitized zones around basement-rooted trans-tensional faults. Dissolution and mineralization along the faults was accomplished mainly by rising thermal fluids. Natural gas is abundant in and around elongate fault-bounded structural lows (interpreted to be negative flower structures). This timely chapter transcends the usual boundaries of karst studies by concentrating on deep-seated tectonic and geochemical processes, as well as their application to petroleum geology.

The Klimchouk and Ford volume contains the thirty-nine papers presented at the International Conference on Hypogene Speleogenesis held at Chernivtsi, Ukraine, in May 2009. Thirty-six of the papers are in English and three are in Russian. Contributions are from Europe, Russia, Australia, Brazil, the US, and Canada. Once identified, it appears that hypogene caves are everywhere.

The opening paper by Alexander Klimchouk and the two following papers by Philippe Audra and his colleagues set out to identify the characteristic morphological forms that result from hypogene speleogenesis: cave patterns with elaborate three-dimensional structure, cupolas, half-tubes, and the planated surfaces associated with condensation-corrosion. Morphological forms can be subject to multiple interpretations. More solid evidence is provided by mineral deposits, especially the isotopic composition of coarsely crystalline calcite. Dublyansky and Spötl describe oxygen isotope ratios in the calcite coating of cavities in a cave in the Austrian Alps that identify the temperature of waters that moved through the cave.

Microbial processes are known to be important catalysts in the geochemical reactions of hypogene speleogenesis. P.J. Boston and her colleagues give an overview and an assessment of their importance.

Modeling of hypogene systems is extremely difficult because there are few hard data on the sources, early flow paths, and chemistry of the fluids. Three attempts are made to at least describe the mechanics of fluid flow. Rehrl, Birk, and Klimchouk offer a generic model showing how fracture systems might be expected to evolve. Dreybrodt, Romanov, and Kaufmann describe a quantitative model for mixing-corrosion that can be applied to coastal karst with freshwater-saltwater mixing zones. It should also be applicable to deep-seated upwelling fluids. Another approach to modeling of mixing zone karst is described by Antoine Lafare and his colleagues and applied to the Mediterranean karst.

As might be expected, most of the papers describe specific hypogene caves that the authors think they have identified, or to caves where hypogenetic processes are thought to have played an important role. There is an amazing diversity of sites. There are the Obruks, giant collapse shafts in Turkey (Bayari and colleagues). There is the endokarst of Mallorca (Ginés and colleagues). There are the hypogene caves of the Italian Apennines (Sandro Galdenzi), which include the important Frasassi Caves, in which much microbiology research is now underway. Beyond these, there are examples of hypogene caves from Austria, Slovenia, Israel, the Crimea, Brazil, Poland, Romania, Greece, Norway, Russia, Jordan, and Saudi Arabia, to name only the main localities.

In this collection of papers from both symposia, there is some impressive progress and at least one serious gap. As to progress, caves of hypogenetic origin have been

identified from many regions and in many environments. Additionally, many caves, clearly remnants of the development of contemporary watersheds, also have an initial hypogenic component. The gap is the absence of any detailed geochemical model for a dissolution process where rising groundwater alone is responsible for cave origin. Fluids percolating up from depth are rarely seen and are difficult to analyze.

These books illustrate that karst processes can extend to considerable depth and involve chemical processes that are seldom observed at the surface. Readers who wish to apply the methods discussed here should keep in mind that interpretations must be compatible with regional groundwater flow rates, chemical environments, and the geologic time frame and that many relict geomorphic features can be attributed to more than a single process. These important books show the wide range of these interpretations and applications.

Reviewed by Arthur N. Palmer, Dept. of Earth Sciences, State University of New York, Oneonta, NY 13820-4015 (palmeran@oneonta.edu), and William B. White, Materials Research Laboratory, Pennsylvania State University, University Park, PA 16802-4801 (wbw2@psu.edu).

GUIDE TO AUTHORS

The *Journal of Cave and Karst Studies* is a multidisciplinary journal devoted to cave and karst research. The *Journal* is seeking original, unpublished manuscripts concerning the scientific study of caves or other karst features. Authors do not need to be members of the National Speleological Society, but preference is given to manuscripts of importance to North American speleology.

LANGUAGES: The *Journal of Cave and Karst Studies* uses American-style English as its standard language and spelling style, with the exception of allowing a second abstract in another language when room allows. In the case of proper names, the *Journal* tries to accommodate other spellings and punctuation styles. In cases where the Editor-in-Chief finds it appropriate to use non-English words outside of proper names (generally where no equivalent English word exists), the *Journal* italicizes them. However, the common abbreviations i.e., e.g., et al., and etc. should appear in roman text. Authors are encouraged to write for our combined professional and amateur readerships.

CONTENT: Each paper will contain a title with the authors' names and addresses, an abstract, and the text of the paper, including a summary or conclusions section. Acknowledgments and references follow the text.

ABSTRACTS: An abstract stating the essential points and results must accompany all articles. An abstract is a summary, not a promise of what topics are covered in the paper.

STYLE: The *Journal* consults The Chicago Manual of Style on most general style issues.

REFERENCES: In the text, references to previously published work should be followed by the relevant author's name and date (and page number, when appropriate) in parentheses. All cited references are alphabetical at the end of the manuscript with senior author's last name first, followed by date of publication, title, publisher, volume, and page numbers. Geological Society of America format should be used (see http://www.geosociety.org/pubs/geoguid5.htm). Please do not abbreviate periodical titles. Web references are acceptable when deemed appropriate. The references should follow the style of: Author (or publisher), year, Webpage title: Publisher (if a specific author is available), full URL (e.g., http://www.usgs.gov/citguide.html) and date when the web site was accessed in brackets; for example [accessed July 16, 2002]. If there are specific authors given, use their name and list the responsible organization as publisher. Because of the ephemeral nature of websites, please provide the specific date. Citations within the text should read: (Author, Year).

SUBMISSION: Effective July 2007, all manuscripts are to be submitted via AllenTrack, a web-based system for online submission. The web address is http://jcks.allentrack2.net. Instructions are provided at that address. At your first visit, you will be prompted to establish a login and password, after which you will enter information about your manuscript (e.g., authors and addresses, manuscript title, abstract, etc.). You will then enter your manuscript, tables, and figure files separately or all together as part of the manuscript. Manuscript files can be uploaded as DOC, WPD, RTF, TXT, or LaTeX. A DOC template with additional manuscript specifications may be downloaded. (Note: LaTeX files should not use any unusual style files; a LaTeX template and BiBTeX file for the *Journal* may be downloaded or obtained from the Editor-in-Chief.) Table files can be uploaded as DOC, WPD, RTF, TXT, or LaTeX files, and figure files can be uploaded as TIFF, EPS, AI, or CDR files. Alternatively, authors may submit manuscripts as PDF or HTML files, but if the manuscript is accepted for publication, the manuscript will need to be submitted as one of the accepted file types listed above. Manuscripts must be typed, double spaced, and single-sided. Manuscripts should be no longer than 6,000 words plus tables and figures, but exceptions are permitted on a case-by-case basis. Authors of accepted papers exceeding this limit may have to pay a current page charge for the extra pages unless decided otherwise by the Editor-in-Chief. Extensive supporting data will be placed on the *Journal*'s website with a paper copy placed in the NSS archives and library. The data that are used within a paper must be made available. Authors may be required to provide supporting data in a fundamental format, such as ASCII for text data or comma-delimited ASCII for tabular data.

DISCUSSIONS: Critical discussions of papers previously published in the *Journal* are welcome. Authors will be given an opportunity to reply. Discussions and replies must be limited to a maximum of 1000 words and discussions will be subject to review before publication. Discussions must be within 6 months after the original article appears.

MEASUREMENTS: All measurements will be in Systeme Internationale (metric) except when quoting historical references. Other units will be allowed where necessary if placed in parentheses and following the SI units.

FIGURES: Figures and lettering must be neat and legible. Figure captions should be on a separate sheet of paper and not within the figure. Figures should be numbered in sequence and referred to in the text by inserting (Fig. x). Most figures will be reduced, hence the lettering should be large. Photographs must be sharp and high contrast. Color will generally only be printed at author's expense.

TABLES: See http://www.caves.org/pub/journal/PDF/Tables.pdf to get guidelines for table layout.

COPYRIGHT AND AUTHOR'S RESPONSIBILITIES: It is the author's responsibility to clear any copyright or acknowledgement matters concerning text, tables, or figures used. Authors should also ensure adequate attention to sensitive or legal issues such as land owner and land manager concerns or policies.

PROCESS: All submitted manuscripts are sent out to at least two experts in the field. Reviewed manuscripts are then returned to the author for consideration of the referees' remarks and revision, where appropriate. Revised manuscripts are returned to the appropriate Associate Editor who then recommends acceptance or rejection. The Editor-in-Chief makes final decisions regarding publication. Upon acceptance, the senior author will be sent one set of PDF proofs for review. Examine the current issue for more information about the format used.

ELECTRONIC FILES: The *Journal* is printed at high resolution. Illustrations must be a minimum of 300 dpi for acceptance.

Journal of Cave and Karst Studies

Volume 73 Number 1 April 2011